THE EFFICACY OF SURFACE HAPTICS AND FORCE FEEDBACK IN EDUCATION

By

Jenna Lynn Gorlewicz

Dissertation

Submitted to the Faculty of the

Graduate School of Vanderbilt University

in partial fullfillment of the requirements

for the degree of

DOCTOR OF PHILOSOPHY

in

Mechanical Engineering

May, 2013

Nashville, Tennessee

Approved:

Robert Webster III

Michael Goldfarb

Stacy Klein-Gardner

Nilanjan Sarkar

Thomas Withrow

To Matt, the love of my life,

whose enduring love has made this dissertation possible.

Acknowledgments

Where better to begin thanksgiving, than to start with God, the source from whom all life and blessings flow. For with Him, nothing is impossible and through Him, all good things come. It is my hope that this dissertation and all future work that comes from it, is done in service to Him.

I would also like to express my deepest gratitude to my advisor, Bob Webster, who has selflessly supported and encouraged me throughout my graduate career and is the perfect example of what it means to be a good mentor. Bob's positive attitude and genuine care for his students have made a tremendous impact on me. Had it not been for him, I would likely not have completed this dissertation. He not only allowed me to spend time searching for what my passions were, but he encouraged me to do so and was always willing to go above and beyond to help me pursue these. He was also very good at putting things into perspective. I will never forget what Bob told me during one of my "I don't know if this graduate school thing is for me!" conversations. He said, "Jenna, always remember the big picture. It's God, family, and then work, in that order. If ever you find yourself in a situation where this is not true, then change it. If it is true, then it's probably ok." This had a resounding effect on me, and it is something that I will always use to put things into perspective. Bob has served as an excellent role model, both in and out of academics, and there are many things I have learned from him that extend far beyond a research lab.

I would also like to thank my dissertation committee members: Bob Webster, Michael Goldfarb, Stacy Klein-Gardner, Nilanjan Sarkar, and Thomas Withrow, who, through their own research and teaching, have also inspired me in several ways. Your time and efforts in reading this work and offering valuable feedback are greatly appreciated.

The work in this dissertation reflects contributions from a number of individuals. First, I would like to thank Tom Withrow, who I have shared numerous conversations with covering all facets of this dissertation. Tom was always willing to provide input, brainstorm ideas, and give valuable feedback, while also sharing his expertise in being a great teacher. I am also very grateful to Stacy Klein-Gardner, who has served as a source of inspiration for me in the engineering education field, and has graciously shared many discussions with me on being an effective teacher, assessing student learning, and doing K-12 outreach, all of which served as motivation for this dissertation and my future career path. I also thank the following individuals for their contributions to this dissertation: Louis Kratchman, Caleb Rucker, and all of the former teaching assistants of the System Dynamics Lab, who have made the work in Chapter 2 possible; Jessica Burgner, (who was simply irreplacable and had made my graduate career that much more enjoyable and successful, particularly through her encouragement and mentoring and her expertise in software development), and Ann Smith, Kim Mountjoy, Doug Conley, and all of the educators of the visually impaired in the Metropolitan Nashville Public School (MNPS) System, for their contributions to Chapter 3; Dr. Kenneth Frampton, Sam Malanoski, and Syed Muhsin Syed Abdul Hamid for their efforts in the work presented in Chapter 4. I would also like to thank all of the individuals who were a part of the user studies described in Chapters 2 and 3, and I would particularly like to acknowledge the three visually impaired students who I had the privelege of working with and who were a large source of inspiration in this work. I also acknowledge Rob Labadie, Mike Fitzpatrick, Ramya Balachandran, Andrei Danilchenko, Benjamin Munske, Pietro Valdastri, Byron Smith, Gastone Cuiti, Giuseppe Tortora, and Massimiliano Simi, all of whom I have had the privelege of working with on various side

projects.

In addition to those mentioned above, I would like to thank all of my other colleagues in the MED Lab: Diana Cardona, Hunter Gilbert, Richard Hendrick, Ray Lathrop, Caleb Rucker, and Phil Swaney, as well as all of the undergraduates that have worked in the lab. The MED lab has evolved into a vibrant, dynamic, and friendly work environment, and I was honored to be a part of it. I greatly appreciate and will always remember the friendships and fun times that I had there.

A big thank you also goes out to the Mechanical Engineering Administrative staff, including Suzanne Weiss, Jean Miller, and Myrtle Daniels, who keep the ME department running, are always willing to assist with any matter (including orders, registrations, reimbursements, etc.), and have shared many conversations and laughs with me that I greatly appreciated. I also thank Rachel Ruffin, who helped me with the logistics of my IBM Fellowship.

I would like to thank the National Science Foundation and the MathWorks Inc., which have supported me throughout graduate school and have enabled me to explore and pursue interesting ideas that may otherwise not have been possible. I also acknowledge the MNPS Institutional Review Board (IRB) and the Vanderbilt IRB for permitting me to complete the user studies in this dissertation.

There are no words quite fitting to describe the gratitude I have for my family. First, I thank my parents, Mike and Brenda Toennies, and my sister, Kayla, who have encouraged me in all of my endeavors, have inspired me in their own successes, and have given me unwavering support and love that I forever cherish. I also thank my extended family and the family I was lucky enough to marry into, who have provided support and friendship,

no matter how far away I was from “home.” Finally, I thank my husband, Matt, who in addition to all of the above, has selflessly shared this journey with me from the beginning and was always there for me to lean on. Having him to come home to at the end of each work day, makes every day worthwhile.

Abstract

This dissertation bridges the fields of haptics, engineering, and education to realize some of the potential benefits haptic devices may have in Science, Technology, Engineering, and Math (STEM) education. Specifically, this dissertation demonstrates the development, implementation, and assessment of two haptic devices in engineering and math education and then describes the modeling of a new class of tactile touchscreens. These force feedback and tactile devices provide robust, engaging interfaces to enhance student learning in the classroom.

First, we explore the potential of a force feedback device in teaching a core mechanical engineering undergraduate course. The haptic paddle, a one degree of freedom force feedback joystick, has been adopted at several universities for teaching system dynamics and controls in engineering education. Through design, hardware, and software improvements, we have enhanced the ease of use of the haptic paddle and have lowered its cost to less than $100 including all components but a laptop. We have performed the first formal assessment of the learning benefits of the haptic paddle laboratories in System Dynamics through a multi-year study evaluating both what concepts students are learning and when they are learning them. Our results show significant increases in student learning after having completed the haptic paddle laboratories.

Next, we explore the potential of commercially available tactile touchscreens for teaching graphical mathematics to blind students. Tactile (vibratory) touchscreens are specifically designed for portability and robustness, are commercially available, and share a small number of common software platforms, providing a unique opportunity for quick adoption

and implementation within an educational setting. User studies with sighted and blind individuals demonstrate that users can perceive basic graphical mathematics concepts using surface vibrations and auditory feedback.

Toward enhancing the realism of current tactile feedback provided in touchscreens and toward providing a more engaging user experience, we then explore the modeling of a new class of variable friction touchscreens. These touchscreens use ultrasonic vibrations to create changes in perceived friction on flat surfaces, enabling users to feel sensations resembling textures and other surface properties. We model and simulate these plate vibrations under varying conditions, including number and location of actuators and plate properties. We experimentally validate our model under various cases and show its effectiveness in serving as a design tool for variable friction touchscreens.

Haptic devices, to date, have had only minimal exposure to educational settings, largely due to their high costs and unquantified evidence of enhanced learning experiences. The research in this dissertation is motivated by providing higher fidelity haptic interactions via new technologies, facilitating the adoption of haptic devices in educational settings, enhancing active learning environments through these devices, and assessing the benefits haptic devices have in student learning. However, the methods and devices presented in this work are broadly applicable in other domains where force feedback or surface haptics can facilitate enhanced human-machine interfaces.

Contents

List of Figures

List of Tables

Chapter 1

Introduction

1.1 Background and Motivation

Technological advancements over the last two decades have revolutionized the way humans access information and have enabled users to interact with virtual or remote objects through new user interfaces (UI). These new UIs have enabled users to interact with such objects using several sensory modalities, including vision, aural, and more recently, touch. Further, robotic teleoperated systems, where a slave device mimics the motion of a master controlling another device, now provides users with the ability to operate machinery in unsafe environments or perform a surgery in remote locations, all from a counsole stationed within a safe environment. These innovations are due to a number of advancements, including the development of smaller, more efficient actuators, sensor technologies, and computational platforms, etc. [66]. Though the mechanisms, control, and applications of these devices may differ, they all have a commonality in that they rely on the user's sense of touch to manipulate objects.

Until recently, most UIs were touch input devices, relying only on the user's touch position to perform a task [49]. Any feedback the user received was often through other sensory channels, such as visual or aural. Recently, however, technology has advanced to the level that enables us to mimic physical touch interactions with virtual or remote objects. This technology is known as haptic feedback. Haptics, which comes from the Greek word *haptesthai*, pertains to the sense of touch. Haptic feedback is essentially force

or tactile feedback that enables a user to "feel" virtual objects in a computer simulation, or physical objects in remote locations [66]. It allows simulated objects to be perceived as having actual physical properties, including mass, stiffness, and texture. It is a means for humans to communicate bidirectionally via their sense of touch with machine or computer interfaces [49]. This birectional flow of information (sensing and manipulating) is what makes haptics, or touch, unique compared to our other senses [76]. In fact, touch is one of the most informative senses that humans possess and provide users with vital information about their environment [66].

A haptic interface typically consists of three components (see Figure 1.1): the device itself which couples the user to a virtual or remote environment, a controller which ensures the appropriate feedback is provided, and a virtual or remote haptic environment [66]. The hardware of the haptic interface includes the mechanical components of the device, the sensors which track the position of the device, and the actuators, which generate forces to the user through the device. The controller typically follows one of two architectures. The first, impedance control, relies on motion input from the device and generates corresponding forces according to a system model. The alternate approach is admittance control, which is the opposite of impendance control in that forces are measured and corresponding device motions are commanded to move the device accordingly. The haptic environment, which is defined via a mathematical model implemented in software, completes the haptic interface and describes the system the user is interacting with [66]. The purpose of this environment is to provide appropriate haptic rendering, or the methods used to generate feedback, to the user [49].

While there are several classifications for haptic devices, we will follow the broad divi-

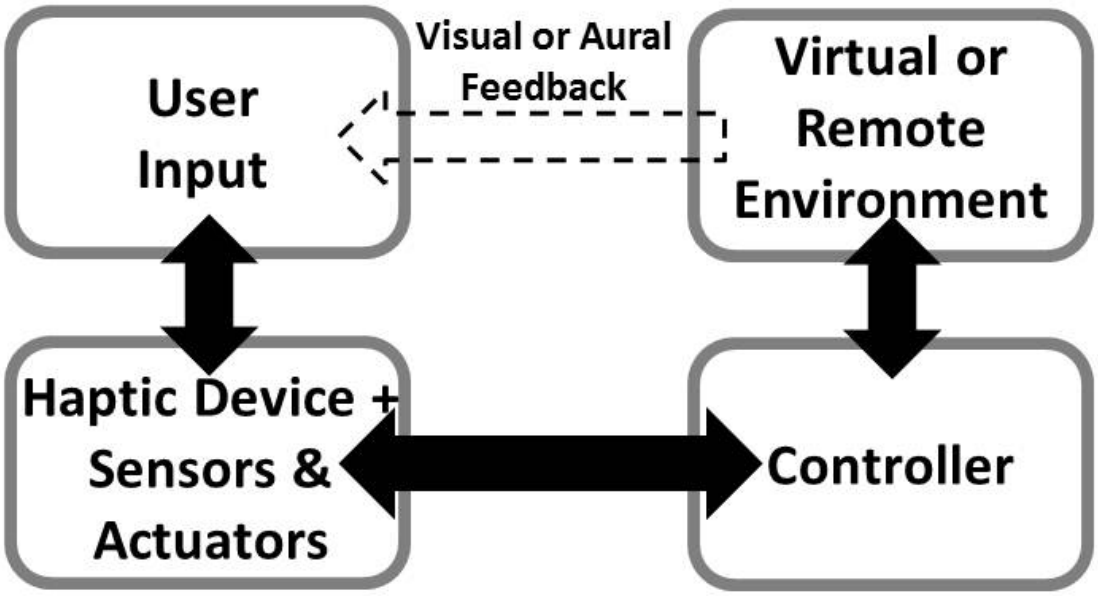

Figure 1.1: A schematic of the three components of a haptic interface: The haptic device itself, with accompanying hardware; the controller; and the virtual or remote environment, which typically provides visual or aural feedback to the user.

sion used in [76], which categorizes them as either force feedback devices or tactile devices. Force feedback devices provide kinesthetic stimuli. They display forces to users, enabling them to feel resistive forces, friction, and other surface properties of the environment with which they are interacting. Three examples of commercially available force feedback devices are shown in Figure 1.3. Ideally, the force that the user perceives from the device would correspond to the force that the user would feel if the device was not present and if instead, the user's hand was directly interacting with the remote or simulated environment. That is, an ideal haptic device is perfectly transparent. To achieve this, a force feedback device should have low inertia and friction and a balanced range, resolution, and bandwidth for sensing and force reflection [76]. Force feedback devices are often characterized

by their degrees of freedom (DOF), which refers to the number of variables required to completely define a device's pose [66]. A higher DOF device often has a larger workspace, the physical space in which the robot can move, but is often more expensive, as it requires more sensors and actuators than a lower DOF device.

Tactile devices, on the other hand, provide cutaneous stimuli. They convey tactile information, information related to pressure, vibration, and/or temperature, to the user. One of the primary advantages of tactile feedback, unlike force feedback, is that it can provide haptic feedback to users (typically through vibrations) without requiring a mediated device, such as a stylus. The use of tactile feedback may be particularly beneficial in touchscreen platforms, where users are directly interacting with a surface. In this case, tactile feedback can also be referred to as surface haptics, since the feedback is felt directly on the surface itself. Tactile devices can use a variety of actuators and sensors to provide haptic feedback (often at the fingertip) to the user [66]. In subsequent chapters, this dissertation provides examples of both tactile and force feedback devices, together with new applications and assessments in education.

Haptic feedback has been incorporated in several applications (see [76] for a good overview and Figure 1.2). Perhaps the simplest example of haptic feedback is the vibration of a cell phone, notifying the user of an incoming call. Even in this simple scenario, the benefits of haptic feedback are evident. First, haptic feedback provides direct interaction to the user, without disturbing others in close proximity (unlike if a cell phone would ring). Further, it enhances pure visual or pure auditory feedback, serving as another means of conveying information to the user. Haptic feedback also has applications in medicine, where it has been used in enhancing surgical training (Figure 1.2(a)) and rehabilitation,

(a)

(b)

(c)

Figure 1.2: Haptic feedback has been incorporated into several applications including (a) Surgical training systems such as the LapMentor^{TM} by SimBionix^{TM}, (b) Teleoperated systems such as the Raven, which has been used in underwater and surgical applications [73], and (c) Video games, such as this racing simulation from Disney Research [1].

particularly stroke-based rehabilitation [76]. It has also been used in telerobotic systems, including those for underwater exploration, assembly, manufacturing, military applications, and surgery (Figure 1.2(b)) [76]. Haptic feedback also has applications in entertainment and gaming, where it can immerse users in the gaming experience more realistically than through visual or audio feedback alone (see Figure 1.2(c)). Touchscreens and mobile devices, which were once passive touch input devices, are now becoming more interactive and can even be used to facilitate social and interpersonal communication through haptic feedback [76]. Similarly, recent advancements in accessibility to interfaces (such as mobile devices) for the blind or visually impaired has been propelled by the inclusion of haptic feedback [66]. Finally, there has also been a growing interest in developing haptic interfaces to enhance education and learning [76]. The potential benefits of haptic feedback in all of these areas are tremendous, as it enables users to interact with and manipulate virtual objects which they would otherwise passively observe, it provides an additional sensory channel through which users can "send and receive" information, and it can enhance user performance on specific tasks, some of which may have been impossible to complete without haptic feedback [22, 49, 66].

Despite these numerous applications and prospective benefits, however, current haptic technology is still in its infancy and has yet to be widely adopted [75]. This may be due to several challenges including their high cost, limitations in actuation technology, the lack of cross-application capabilities, and the level of realistic interaction haptic devices are currently able to provide [66, 75]. These challenges, however, make it an exciting time for the field of haptics, which has recently seen a proliferation in both commercial and research efforts in order to overcome these barriers [22]. There have been a number of commercially

Figure 1.3: Three examples of commercially available force feedback haptic devices: (a) The Novint Falcon (Novint Technologies, Inc.), (b) The Phantom Omni (Sensable Technologies, Inc.), and (c) The Maglev 200^{TM} Magnetic Levitation Haptic Interface (Butterfly Haptics, LLC).

available haptic devices that have come to market in recent years, including those produced by Novint Technologies, Inc, Sensable Technologies, Inc., Butterfly Haptics, LLC and Immersion Corp. (see Figures 1.3 and 3.1 for examples), among others [66]. Further, research efforts, ranging from investigating the science of touch to haptic device design and applications, have increased dramatically within the last decade [49,66]. It is predicted that as the cost of improved sensor and actuator technology falls and the demand for active human intervention within virtual and remote systems increases, there will be much greater accessibility to, and widespread adoption of, haptic devices in the next 10 to 20 years [66].

1.1.1 The Role of Haptics in Education

To date, haptics has largely remained an untapped sensory modality in teaching and learning, despite the perceptual power and the wealth of information that touch provides, and despite the fact that some of our earliest learning experiences occurred through touch [61].

This is due in part to some of the challenges mentioned above, particularly the high costs associated with haptic devices. However, the widespread adoption of haptic devices into educational settings is compounded by the fact that, aside from engaging students in the learning process, it is still unclear if and how haptic devices may enhance student learning. In a review of haptic applications in education, Minogue and colleagues observed that there is a large gap that exists between two equally important fields of research in haptics: the research on haptic perception and cognition and the research on haptics as an intervention for change. They conclude that the true potential of haptics in education will not be realized until these two fields are bridged, at which point, "armed with the theories and understandings of haptics built by psychologists and cognitivie scientists, we could rigorously investigate the effects of using the latest technologies in the field to create haptically rich learning environments," [61].

Addressing some of the above challenges to bridge haptics, engineering, and education and to faciliate the development and assessment of haptic devices in Science, Technology, Engineering, and Math (STEM) education is the focus of this dissertation. Developing low-cost haptic devices within an educational setting encompasses several challenges. First, designing a suitable device requires an understanding of the theories underlying haptic perception and cognition. Second, there are additional design constraints in the case of implementation within an educational setting in that the device need not only be low-cost, but also easily accessible, such that any educator or student could use it. Finally, from an educational perspective, the device must be easy to implement within a classroom and robust enough to be used by a number of students. Addressing the lack of cross-application capabilities requires flexible, adaptable, and portable device platforms. For teaching, this

requires a device that can be used to teach multiple lessons or even be used in multiple courses. A challenge in creating such devices is that the device alone is insufficient if it lacks associated curriculum. This requires the development of learning modules accompanying a given haptic device. Determining if haptic devices enhance student learning requires systematic assessments of the haptic intervention, as well as sound statistical analyses of the collected data. Challenges described above in haptic device design, implementation in the classroom, and assessment of learning benefits are addressed in this dissertation for two haptic devices, one that is force-feedback and used in an undergraduate mechanical engineering course and one that is tactile and used in math education of visually impaired students. Incorporating knowledge of haptics and engineering, this work aims to enhance understanding of the potential benefits haptic devices have in education. It is intended that results from this work will spur the adoption of such devices into classroom settings and impact current teaching and learning methods for a wide range of educators and students.

1.2 Related Work

Both force feedback and tactile devices have begun to be explored in educational contexts. The incorporation of haptic devices into educational settings is thought to be beneficial for several reasons. First, they enable active, hands-on learning, which has been shown to engage students and enhance their learning experience [18, 69]. Second, haptic devices can appeal to multiple sensory channels, and thus multiple styles of learners. In fact, kinesthetic learners, individuals who learn through touch, make up approximately 15% of the population, and would struggle to grasp concepts fully through visual or auditory feedback alone [47]. Further, haptics actively involves students in choosing to investigate proper-

ties of an object or system, which can be a powerful motivator and increase their attention to learning [61, 78]. Finally, interactive technologies, such as haptic devices, are likely to be a crucial component of educational curriculum for the current generation of students, who have grown up surrounded by technologies of all kinds and have expectations of higher learning technologies, and will likely be critical for future generations of students as well [21, 47].

A thorough review of the implementation of haptic feedback in the context of several educational settings can be found in [61]. Perhaps the largest area where haptics has been adopted into education is in medical training and aviation [61, 77]. In fact, many commerical and military pilots are now trained on flight simulators. Several simulators for medical applications, particularly those for endoscopic and laparoscopic surgeries, have also been developed within the last decade [85]. Currently, however, there does not exist a consensus on the benefits of haptic feedback in minimally invasive surgery, and only a little research has been done in the area of robot-assisted endoscopic surgical training, though results appear to be promising [85]. In this review, we limit the scope to include haptic devices in (1) K-12 education, where a relatively large number of innovations have occurred, (2) Engineering education, where fewer efforts exist, and (3) Math education of the blind, where a good deal of research has been done, but the potential benefits of surface haptics are just beginning to be recognized. The literature presented in this section is not meant to be exhaustive, but rather to provide examples of recent efforts of incorporating haptic devices in education and to review the state-of-the-art in these areas.

1.2.1 Haptics in K-12 Education

The majority of efforts to date have involved incorporating haptic devices at the K-12 level. Within this scope, there have been several studies that have used haptic feedback in teaching the sciences [79]. In biology, for example, commercially available haptic devices were used to teach middle and high school students about viruses [52]. Results showed significant increases in the level of engagement of the activity and in the number of virus characteristics that students were able to recall among the population who had the lesson incorporating a haptic device [52]. Another study used haptic feedback combined with a 3D virtual model of an animal cell to teach middle school students about the structure of cells. While haptic feedback enhanced students' ability to interpret the cell environment, no significant differences in cognitive benefit between students who received haptics and visual information versus those who received only visual information were found [62].

In the physical sciences, there have also been numerous efforts in using haptic devices to assist students in developing an understanding of abstract concepts. Williams and colleagues have developed a series of haptically augmented programs using a commercially available force-feedback joystick, the Microsoft Sidewinder, for teaching elementary students concepts associated with simple machines [94]. They developed five simulations to demonstrate concepts associated with levers, pulleys, inclined planes, screws, and wheels and axles. They conducted pilot studies asking users to rate the ease of use of the software and to rate its effectivness in helping students learn or review simple machines. Their results were positive, with majority of the users rating the technology as effective or somewhat effective and easy to use, but no quantitative data on its learning benefits were pre-

sented.

Using a similar approach, another study investigated the effectiveness of haptic simulations compared with non-haptic simulations for the purpose of teaching gears [48]. A commercially available force feedback joystick provided users with the feeling of the force they should apply to rotate gears and with information about the speed and rotation of the gears. Their results suggest that the haptic simulations were more effective than the non-haptic simulation in providing perceptual experiences and helping elementary students create representations of gear movements. In another study, the Phantom Desktop was combined with simulations to teach middle school students concepts associated with centripetal forces and gravity, though the results from this work were very preliminary and only qualitatively assess the ease of use and engagement of the device [99]. Yet another system, the HaptEK16, uses a Phantom Omni combined with a 3D simulation to investigate pressure and more complex hydraulic concepts in high school physics [47]. Results from this study suggest enhanced student learning via haptic feedback, though no statistical tests were performed.

1.2.2 Haptics in Engineering Education

Specifically in engineering education, there have only been a few studies which have incorporated haptics into the curriculum. Williams and colleagues extended their software activities from simple machines to augment teaching and learning in statics, dynamics, and physics at the undergraduate level [95]. Though no quantitative analyses of the learning benefits of these modules were presented, surveys assessing the effectiveness and engagement of the activities were positive. Another study used a tactile trackball combined with

a computer simulation to teach concepts of force fields to students [72]. Twelve graduate students with no background in physics participated in the study and were asked to draw representations of what they were feeling. Analyses of student drawings suggest that they could successfully construct a graphical representation of a force field, even without formal exposure to these concepts. The last example of haptic device implementation in engineering education was the implementation of the haptic paddle, a one DOF force feedback device used in teaching System Dynamics [44, 65]. This device, which is used in teaching system dynamics and controls concepts, will be described in more detail in Chapter 2.

The above studies exemplify innovative means of incorporating haptic feedback into K-12 and university settings. It is evident, however, that this area of study is still in its infancy. With the exception of [65], all of the other studies have used commercially available haptic devices combined with custom software. While taking advantage of commercially available hardware is likely a good idea in terms of ease of access and implementation within a classroom, many of the devices used, such as the Phantom Omni, are relatively expensive (approximately $2400). This is particularly problematic if numerous devices need to be purchased, and it hinders the ability for such methods to be widely adopted by other educators. Further, the majority of the assessments conducted on the effectiveness of the haptic devices in these educational settings have largely assessed valuable qualitative metrics such as ease of use, student engagement, and the effectiveness of the technology in specific scenarios, but have lacked empirical evidence of increasing student learning [61]. This lack of evidence in learning gains appears to be a critical "missing link" in understanding the benefits of haptic devices in enhancing student understanding and in permitting them from being widely adopted within educational settings.

1.2.3 Haptics in Math Education of the Visually Impaired

Unlike in K-12 and engineering education, research efforts in implementing haptic devices in education of the visually impaired are more common. This is likely due to the fact that the value of haptics for visually impaired students is more apparent, given that these students highly rely on other senses, such as hearing and touch, to compensate for their loss of vision. While auditory feedback is effective in conveying textual information, accessing visual and graphical material is more challenging because a direct translation to voice is nonexistent [89]. Thus, to date, many efforts in incorporating haptic feedback in education have been in subject areas such as mathematics, which have a large visual component (see [56] for an overview). This area is the focus of this literature review and dissertation work.

The most common technology currently used to display graphical content to visually impaired users is embossing [86]. Braille tactile graphics embossers represent both text and graphics through either raised dots or elevated regions on a page. Software, such as the Math Description Engine, which uses an input in equation form and converts it to a format that can be printed with Tiger embossing software, and MathTrax, which adds sonification and audio description files for graphs, are also available [2,3]. While embossers are commonplace, they produce only static images, requiring a new page to be printed for every new figure. Further, both the machines and the output documents are quite expensive [86]. Nonetheless, current methods of teaching the visually impaired rely on embossed documents or other creative materials, which will be discussed in the related work section of Chapter 3. While the need for more sophisticated tools is significant, there are several

challenges associated with developing a refreshable, robust tactile display. First, several actuators are often required to provide tactile feedback on a display, and they must be compactly housed within the platform, which ideally would be portable. Second, the device must be easy for educators and students to use in a classroom and should be robust to heavy student use. Due to these two challenges (both actuation and setup), developing such a device is expensive [89].

Prior work on displaying information through the sense of touch has focused on various kinds of pin array-based displays, which can be configured into fingerpad-sized arrays to display braille and other sensations to the fingertip, or larger arrays for the user's fingers to explore (see [66, 89] for reviews). The standard Braille cell consists of 6 to 8 pins, each actuated by a peizoelectric, and the average price of a single cell with accompanying electronics is approximately $90 [89]. If this were to be expanded into a display slightly larger than the size of a piece of paper, the cost goes up dramatically. In fact, commercial devices using multiple cells cost a few tens of thousands of dollars [89]. An example of a commercially available static refreshable display is METEC's DMD-12060 screen, which is a 159 $\times$ 59 pin array actuated via miniature solenoids and sells for $70,000 [87]. A refreshable 7200 pin-array device (see Figure 1.4(a)) capable of detecting multiple points of contact was also developed in the HyperBraille Project [4], though the cost and commercialization of this device is unclear. An alternate approach to actuating each pin individually is to actuate pins in a manner similar to that of writing or printing devices, where a mechanism similar to a plotting head moves along the display and pushes pins up accordingly. An example of a device such as this which uses electromagnetic actuators is presented in [63], though this device is not commercially available. Another pin array device that was specif-

ically adapted to education of the blind showed promising results in being able to convey maps and enable users to construct 3D poses out of 2D graphics [91]. However, as noted in [89], most existing pin-based display devices are research prototypes that are currently expensive to produce commercially, and the goal of an efficient, low-cost tactile display for the visually impaired has yet to be achieved. Portability and robustness to the wear and tear that students will impose on the device, both of which are significant challenges for many existing pin array designs, are also important in classroom applications.

There have also been several research efforts in the development of dynamic devices, displays that refresh underneath stationary fingertips. Perhaps the best known device in this category is the Optacon (OPtical to TActile COnverter) [59] and its successor Optacon II, which consists of a 20×5 pin array matrix and relies on piezoelectric actuators [89]. This device, however, is used to convey textual information that has not been transcribed into Braille. It is still unclear how effective these types of devices could be at displaying graphical information. Another proposed approach uses a tactile mouse (VT Player, VirTouch, Israel), shown in Figure 1.4(b), which is a computer mouse that has one or more tactile pin arrays embedded on the top of it [71]. An overview of several other efforts investigating novel actuation methods for dynamic displays including shape memory alloys, electromagnets, micromachined polymer actuators, miniature motors, and ultrasound transducers is presented in [89]. These devices are still under development and have not yet been employed in educational settings.

A number of innovative recent studies aimed at conveying graphical math concepts to visually impaired students through force feedback alone and in combination with auditory feedback have also been explored. One approach is to incorporate auditory feedback with

(a)

(b)

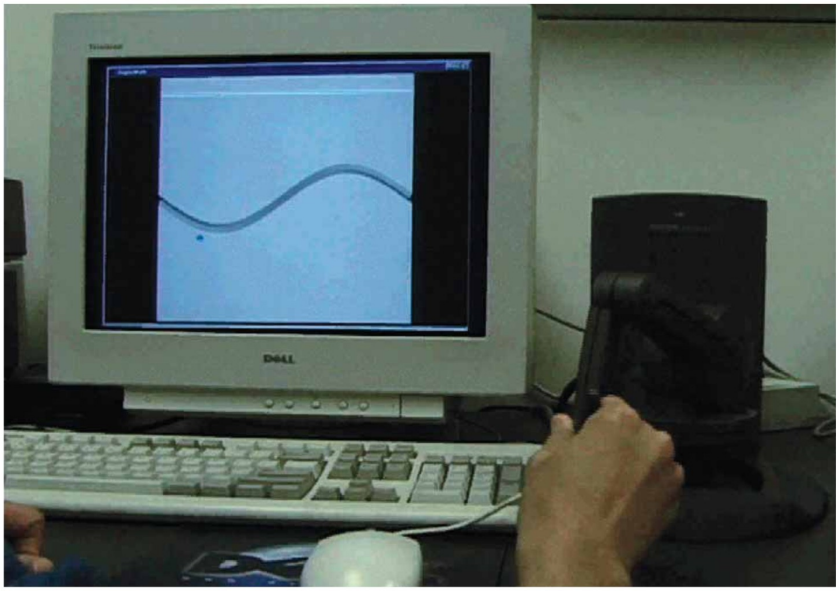

(c)

Figure 1.4: Three examples of haptic devices that have been developed for graphical display for the blind: (a) A refreshable pin-array device [4], (b) A tactile mouse called the VT Player (VirTouch) [5, 71], and (c) Force feedback devices, such as the Phantom, combined with software running on a PC [86] .

force feedback devices such as the SensAble Phantom or Logitech WingMan Force Feedback Mouse, as shown in Figure 1.4(c), to explore and create graphs [20, 24, 30, 70, 86, 100, 101]. Another approach combined a tactile pin-array device, a 3-D digitizer, and a tablet PC to allow students to draw and erase lines by moving a stylus along the tactile surface, which they could then explore with their fingertips [91]. Yet another approach that has been suggested as a means to convey graphical information to a user incorporates vibration feedback into a stylus that can write on a tablet screen [80]. Specifically developed to enable interaction with 3D virtual objects, the European Union GRAB project team has built a dual arm haptic interface accompanied with a haptic audio virtual environment (HAVE) [97]. Each arm of the interface has 3 DOF and can simulate many properties of virtual objects, including texture, hardness, and stickiness. Evaluations of this system through a simple interactive game showed that users could easily identify objects in the game and found the game to be an immersive experience [97].

While these prior studies illustrate some of the benefits that various haptic technologies can have in displaying graphical concepts, they have yet to be widely adapted into a classroom setting. This may be due to several factors (including some mentioned above), such as cost, portability, lack of educational curricula, perceptual challenges associated with stylus-mediated devices, or many other reasons. Toward addressing some of these challenges, this dissertation explores two facets of tactile touchscreens. First, we explore the use of commercially available vibratory touchscreens as educational assist devices for the visually impaired (Chapter 3). Then, we explore the feasibility of a custom built variable friction touchscreen for providing enhanced tactile feedback and for creating complex geometries on a flat surface (Chapter 4).

1.3 Dissertation Overview and Contributions

This introductory chapter presented an overview of haptic interfaces and motivation for their use in educational settings. Two haptic interfaces, tactile touchscreens and a force feedback joystick called the haptic paddle, were placed within the context of existing research on haptic interfaces in education, specifically in engineering education and math education of the blind. The subsequent chapters and the major contributions of this dissertation are summarized as follows:

- **Chapter 2 - Enhancements to, and Formal Assessments of, The Haptic Paddle:** The haptic paddle, a one DOF, custom-built force feedback joystick, was developed in the late 1990s and has been adopted by several universities as a teaching tool in System Dynamics [65]. Design, hardware, and software improvements are made to enhance the ease of use and robustness of the system and to reduce the cost to less than $100 for all components. These improvements, along with a comprehensive website containing all of the information needed for others to build the haptic paddle [6], may enhance classroom implementation in other educational settings and may spur its adoption among university and K-12 educators, and among individual students. Complementing prior qualitative assessments of this device, a 3-year systematic assessment of its learning benefits is conducted and results are presented. This assessment is the first of its kind exploring not only what concepts students are learning through the haptic paddle laboratories, but also investigating *when* students are learning the material, shedding light on the learning benefits of this device.

- **Chapter 3 - Vibratory Touchscreens as Educational Assist Devices for the Visually Impaired:**

  A new paradigm for teaching graphical math concepts to blind students using commercial tactile touchscreens and freely available software is proposed, and our vision of its classroom implementation is discussed. Custom developed software is presented that provides haptic and auditory feedback to users as they scroll their finger across an image on the screen. User studies investigating some of the first graphical concepts students learn in math are presented, with both sighted and blind individuals. Toward enhancing adoption of such a device, similar software was developed in the form of an application running on an Android tablet. The software developed in this work, however, is generalizable to tablets running on a variety of operating systems. This method has the potential to improve the way blind students are currently taught graphical math concepts tremendously, providing a refreshable, portable, robust display enabling students to take on a much more independent role in the learning process. Further, it would enable educators to teach a larger number of students, and even perhaps, enable one teacher to teach both visual and blind students simultaneously in one classroom.

- **Chapter 4 - Modeling and Experimental Validation of Variable Friction Touchscreens:**

  Toward enhancing the tactile feedback provided to users from a touchscreen, there has been recent research in the development of variable friction touchscreens [26,60], which rely on ultrasonic vibrations of plates via piezoelectric actuators to create

changes in friction on the plate's surface. Using classical thin plate theory, a computational model of glass plates actuated via any number of piezoelectric actuators at any plate location is presented. A physical prototype of a small touchscreen system is constructed. Optimization of the number and location of piezos is determined, and predicted and experimental results are compared. This work provides a theoretical basis for how to design variable friction touchscreens, which, to date, has largely been "ad hoc" and non-generalizeable. The methods presented here are generalizeable to any variable friction touchscreen design and provide insight into how vibration modes could be combined to create complex frictional patterns on a plate surface. With the use of piezoelectric actuators already being explored in commercial touchscreens, it is expected that these methods may greatly enhance the types of tactile feedback available to users and the geometries that can be created from a touchscreen platform, which in the future, could be used in several applications, one being math education of the visually impaired.

The dissertation concludes and future work is discussed in Chapter 5.

Chapter 2

Enhancements to, and Formal Assessments of, The Haptic Paddle

Haptic interfaces have the potential to serve a dual-purpose in education: engage students through a rich sensory channel and increase their understanding of abstract concepts by providing a physical basis in which to experience them. Further, by their very nature, haptic interfaces are "hands-on" devices, providing educators with a medium through which they can incorporate more active learning exercises into their classroom. Particularly in engineering education, haptic interfaces have the additional advantage that they can be explored from a mechanical, electrical, and computer engineering perspective, since they are a dynamic system with accompanying hardware and software. While several research groups have shown that haptic devices are engaging educational tools, widespread adoption of haptic interfaces into the classroom has not yet been realized.

Challenges that must be overcome to bring haptic interfaces into the classroom include (1) reducing the cost, (2) increasing accessibility and ease of classroom implementation, (3) creating educational curriculum accompanying them, and (4) validating their effectiveness as an educational tool. It is also important that these devices can be used to teach multiple lessons, or perhaps even multiple subjects. Using a simple force feedback haptic device called the haptic paddle as our platform, we address several of these obstacles. We have lowered the cost and ease of use by incorporating inexpensive, commercially available hardware and newly developed software. Creation of educational material is enhanced by modifying existing curriculum associated with the haptic paddle. Finally, we have performed the first formal assessment of its kind quantifying the learning benefits of

the laboratories associated with the haptic paddle.

The research described in this chapter was published in *The Proceedings of the American Society for Engineering Education 2012* [43] and has been submitted for publication in the *Journal of Science Education and Technology* [42]. It has also been successfully applied by collaborators in another undergraduate and graduate course in Mechanical Engineering, and has been the focus of a MathWorks, Inc. webinar [41]. Several other university educators have also recently expressed interest in adopting this version of the haptic paddle into their engineering curriculum.

2.1 Motivation and Related Work

The haptic paddle and an associated laboratory curriculum were developed in the late 1990s at Stanford University to provide a hands-on platform for students to physically interact with and "feel" simulated dynamic systems via force feedback [65]. Since then, haptic paddles have been adopted at multiple universities (see [7] for an overview) including Johns Hopkins [65], Rice [23], Michigan [38], Vanderbilt [6, 43], ETH Zurich [37], and Utah [7]. Generally agreed upon engineering education objectives [34] have spurred adoption of haptic paddles, including the desires to engage students with a variety of learning styles, enable students to connect theoretical principles to practical applications, and to provide students with cooperative learning experiences. The objectives of haptic paddles are in keeping with prior work incorporating hands-on demonstrations [12, 29, 31], computer simulations [35, 39, 93], design projects [25, 82], and laboratory experiences [33], which have been found beneficial in the context of many different undergraduate courses. For System Dynamics, a core mechanical engineering undergraduate course required at most

universities, haptic paddles provide a particularly good device upon which to build laboratory curricula [44, 65]. They are one of the simplest possible robots that a student can build, having only one motor and one degree of freedom (DOF). Yet the modeling, mechatronics, and control work required to accomplish the haptic paddle laboratories is directly generalizable to more complex systems with more degrees of freedom. The haptic paddle has the additional benefit that it is a haptic device, through which students can touch and feel dynamic system simulations.

Each university that has adopted haptic paddles has contributed to the evolution of the haptic paddle in mechanical design, educational curricula, and software in various ways (see Figure 2.1 for pictures of the various haptic paddle designs, and the central web repository EduHaptics [7] for more information). However, none of these modifications have fundamentally altered what the haptic paddle is; it remains a one DOF haptic device that students can construct and/or program and use. Most hardware changes have been aimed at increasing robustness, reducing costs (though even the initial work at Stanford emphasized cost-conscious mechanical design), and using readily available materials and components. The initial curriculum proposed at Stanford consisted of sequential laboratory exercises focused on constructing, calibrating, modeling, and controlling the paddle, before using it to interact with simulated dynamic systems [65]. While some curricular adaptations have been made at various universities to suit the learning objectives of their respective courses, the originally proposed curriculum has been used with only minor modifications at Stanford, Johns Hopkins, and Vanderbilt, and is the subject of the formal assessment described in this chapter. Prior assessments of the haptic paddle as a learning tool have all been qualitative and anecdotal in nature, illustrating that students respond enthusiastically to the

haptic paddle and that many students appeared to laboratory instructors to be developing a true understanding of core course concepts for the first time as they interacted with the haptic paddles [65].

There have also been a number of instances over the years where high school students and teachers have requested information and assistance from faculty and graduate students in building their own haptic paddles, having found information about them on the Internet. To address this, one of the main objectives in the initial work at Stanford was to enable broad dissemination at multiple educational levels. They sought to facilitate this adoption by making the haptic paddle mechanical components as low cost as possible. However, a major hurdle in the process of making haptic paddles accessible to the at-home and high-school settings has been the fact that the initial system at Stanford used an expensive D/A card, a desktop computer to host it, and a benchtop power supply. Thus, despite low-cost mechanical components, someone developing a haptic paddle setup from scratch needed to invest quite a bit of money in computer/electronics resources. They would also need to be sufficiently computer-savvy to be comfortable opening their computer case to install the card and then learning how to write a program to interface with it.

To address these challenges, in this chapter, we contribute enhancements to the haptic paddle infrastructure, as well as the first formal assessment of the learning that is facilitated by haptic paddle laboratories during a semester of System Dynamics. More specifically, we present (1) a new friction drive design, which is more robust than the original capstan drive (enhancing learning by mitigating student frustration with re-stringing the paddles whenever they make them go unstable), (2) a new electronics implementation featuring a low-cost Arduino microcontroller and amplifier ($\approx$\$55), which connects to a computer us-

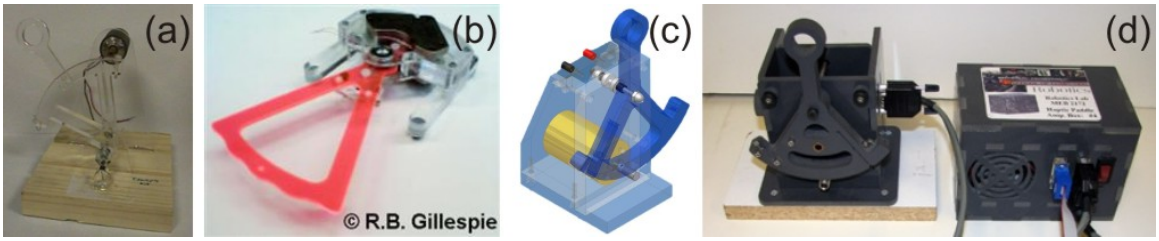

Figure 2.1: (a) The Stanford and Johns Hopkins Haptic Paddle. (b) The University of Michigan Haptic Paddle. (c) The Rice University Haptic Paddle. (d) The University of Utah Haptic Paddle.

ing a universal serial bus (USB) interface, making it possible to operate the paddle from a laptop, and (3) a new Matlab/Simulink (The MathWorks Inc.) software framework, which is consistent with and reinforces Matlab use throughout the course. Further, we complement prior qualitative assessments that evaluted student perception of the value of the haptic paddle laboratories with a formal assessment. The objective is to determine if and when students learn key course concepts: in lecture, in the lab activities themselves, or after reflecting on the lab activities while writing lab reports.

2.2 Haptic Paddle Hardware and Software Enhancements

The haptic paddle is similar in functionality to commercially available haptic devices (such as the PHANToM Omni by SensAble Technologies) in that it emulates interaction forces that occur when a user contacts an object, but it is simpler in design and construction since it is has just one DOF. As the user moves the paddle handle, the drive wheel attached to the motor rotates. The position of the drive wheel is sensed using a magnetic angle sensor

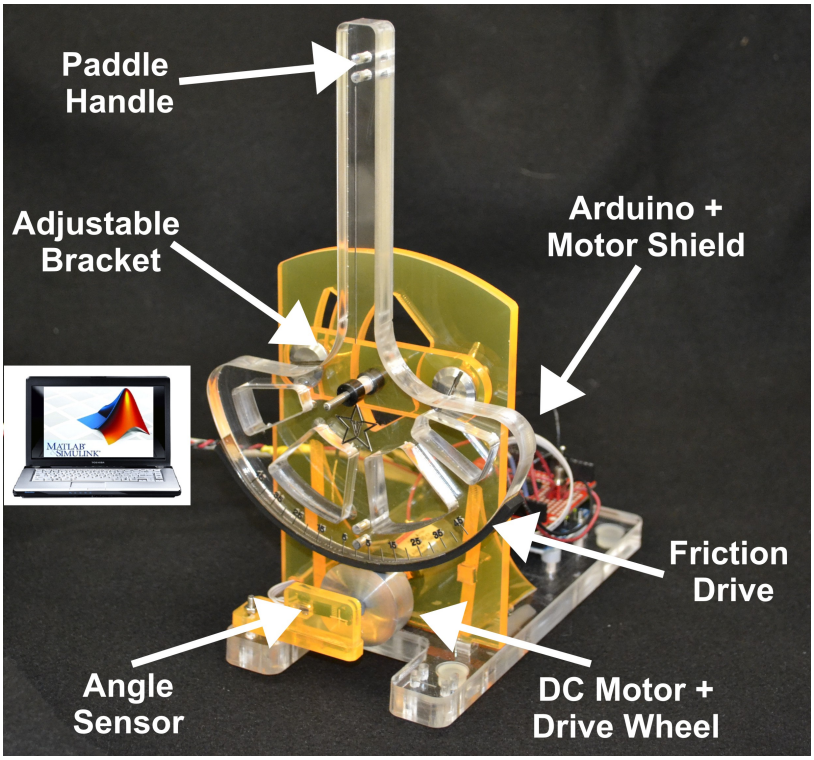

Figure 2.2: A schematic of the components of our Haptic Paddle, which relies on a friction drive design, runs in Matlab/Simulink, and uses a low-cost Arduino microcontroller for communication.

and the Arduino (see Section 3.2.2). The Arduino is used for bidirectional communication between the motor and Simulink. In Simulink, the position and velocity of the paddle handle are calculated and desired forces are computed. Then, the motor generates these desired forces, which are felt by the user holding the paddle handle.

2.2.1 Mechanical Design Enhancements

The basic haptic paddle design (Figure 2.1) consists of an acrylic handle coupled to a single motor through a capstan drive. As with prior haptic paddles, ours (Figure 2.2) is designed to be low-cost and easy to manufacture, consisting of laser-cut acrylic. All prior haptic

paddle designs have used capstan drives, with the exception of the Michigan haptic paddle (iTouch Motor), which uses a direct drive device without a transmission [38]. While there is nothing intrinsically disadvantageous with capstan drives (indeed, they are preferred in many commercial haptic devices for their low friction and smoothness), several years of experience in the laboratory have illustrated that they can be a source of significant frustration for students and teaching assistants (TAs) as implemented on haptic paddles. For example, when students cause paddle instability (which they often do when learning about control, and occasionally at other times in the lab) the string will pop off of the motor drive wheel. It then requires several hands working in a small space to re-wrap and tension the string, while tightening screws and nuts to fix both ends of the string to the capstan. This process takes anywhere from 2-10 minutes, depending on student experience and frustration level. If done incorrectly, the string may be too loose and slip around the motor spool.

To address this, we have replaced the capstan drive with a friction drive. The friction drive consists of a strip of neoprene rubber adhered to the bottom of the paddle handle that rolls in contact with an aluminum drive wheel fastened to the motor shaft, as shown in Figure 2.3. This new design is much easier to assemble. If the paddle goes unstable, the neoprene strip simply rolls out of contact with the drive wheel. To reset the paddle, all one needs to do is move the handle back into its normal vertical position. To ensure that the amount of contact force between the drive wheel and the rubber strip can be optimally adjusted (note that this only needs to be done once), we included an adjustable bracket that enables the entire paddle handle to move up and down, as shown in Figure 2.2.

While this friction drive trades off some haptic fidelity in exchange for robustness, we

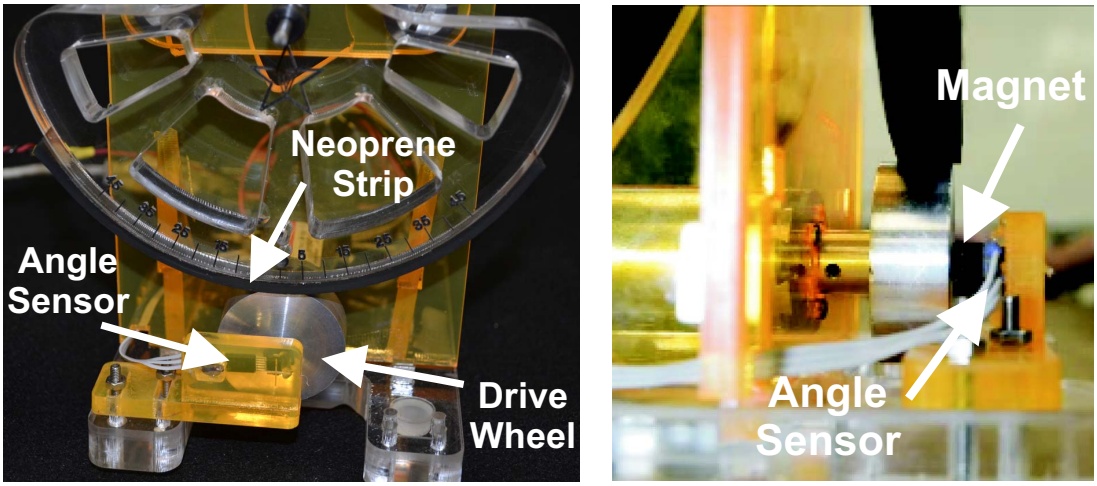

Figure 2.3: The new friction drive design of the haptic paddle consisting of a rubber strip at the bottom of the paddle handle which directly contacts the drive wheel on the motor. An inexpensive magnetoresistive angle sensor ($6, KMA199E, NXP Semiconductors), which measures the angle of the nearby rotating magnet on the drive wheel, provides the motor position.

have observed no practical reduction in learning benefit with this new design. Indeed, it is qualitatively difficult to perceive a noticeable difference between the friction drive and capstan drive. To quantitatively compare the friction and cable drive designs, we measured the friction and inertia of our new paddle compared to the Stanford haptic paddle using an experimental setup similar to that described in [11], which estimated these parameters for the capstan drive haptic paddle. To do this, we attached a load cell (Entran ELFM-T2E-25L) with a small acrylic square at the handle of both paddles. A user lightly grasped the acrylic square and moved the paddle randomly using a variety of velocities. Force and position values were recorded throughout paddle motion. We modeled the haptic paddle as a mass with Coulomb-plus-viscous friction and used a pseudoinverse technique to solve for

the mass (m), viscous friction coefficient (b), and Coulomb friction (f_c), as in [11]. Twenty trials were performed for each paddle design, and the results were averaged.

The resulting parameter estimates for the capstan drive paddle were $m = 0.0596$ kg, $b = 0.0926$ Ns/m, and $f_c = 0.1083$ N, and for the friction drive paddle were $m = 0.0466$ kg, $b = 0.1218$ Ns/m, and $f_c = 0.1146$ N. We observe that the equivalent mass, viscous friction, and Coulomb friction in both paddles are similar. While the viscous friction coefficient is higher in the friction drive paddle compared with the capstan drive paddle, both are low. Further, in [11], the viscous friction coefficient in the cable drive paddle was found to be between $b = 0.15 - 0.23$ Ns/m, showing that this parameter can vary depending upon the construction of the paddle and the components used. We also note that our equivalent mass was lower in the friction drive paddle compared with the capstan drive paddle. Our calculated effective masses at the paddle handle, including the 0.0075 kg load cell and acrylic square, were $m = 0.053$ kg for the friction drive paddle and $m = 0.052$ kg for the capstan drive paddle. These calculated values were comparable to the estimated values of mass from our model, but there were some small discrepancies between the two values for each paddle. These discrepancies were likely due to slight variations in how hard the user's finger pressed onto the force sensor when holding the paddle in each trial. We mitigated this variation as much as possible by reminding the user not to squeeze the force sensor before each trial; however, the compliance of the fingertip pad likely contributed to small variations in the grasp force. Compared to commercial haptic devices such as the Phantom Omni, which has an apparent mass at the tip of 0.045 kg and backdrive friction of 0.26 N [8], both haptic paddle designs perform well.

A minor additional mechanical change to the haptic paddle design was the incorporation

of the larger aluminum drive wheel, shown in Figure 2.3, onto the motor shaft. This adds some inertia and changes the gear ratio slightly of our new paddle compared to the original haptic paddle. However, it enables the motor spin down test (a Lab 1 exercise, see [65]) to be performed with no disassembly of the paddle, as was required in prior capstan drive versions. Now, all that must be done to perform the motor spin down test is to rotate the handle until the neoprene strip is out of contact with the aluminum drive wheel.

2.2.2 Low-Cost Electronics and Computer Interfacing

Toward lowering the overall cost and thus the bar for entry to new users of the haptic paddle, and in keeping with the general goals of the original Stanford project which sought a widely disseminable device, we have developed a new low-cost and easy-to-use electronics solution based on the Arduino microcontroller. While the original haptic paddle could be built for $30 in mechanical components, it was assumed that a D/A (Digital to Analog) solution was already available to the person implementing the paddle [65]. Initial instantiations of the design at Stanford and Johns Hopkins used Measurement Computing PCI cards which, at the time, retailed for between $1000 and $2000 and required a desktop computer. The recent introduction of the Arduino microcontroller has provided a low-cost microcontroller capable of D/A and (with the associated motor amplifier) motor control, that has catalyzed a large hobbyist community and has been introduced into the classroom at many universities over the past few years. For us, an ancillary benefit of Arduino use is that it reinforces the experience that students obtain in our undergraduate Mechatronics class, in which Arduino programming and interfacing are central topics. The Arduino is a USB-connected device (meaning the haptic paddle can now be run from a laptop) and

is inexpensive, with the Arduino UNO retailing for $30 and the Motor Driver Shield (amplifier) retailing for $25 from SparkFun Electronics, as of the time of this writing. The microcontrollers are easy to program, with extensive online documentation and examples. Using the Arduino language, which is simply a set of C/C++ functions, and the Arduino programming environment [9], we developed code to read the haptic paddle's angle sensor and control the motor using pulse width modulation (PWM).

We also upgraded the hall effect sensors used in the original design to a new $6 magnetic angle sensor (KMA199E, NXP Semiconductors) as shown in Figure 2.3. These analog sensors are much more reliable and robust to misalignment and exact distance to the magnet, and provide a larger voltage output range compared with the hall effect sensors used in the initial Stanford design. They are also linear with respect to angle, obviating the need for a 3^{rd} order model fit for calibration. We note that this calibration process, while perhaps useful educationally, was a significant source of frustration for students and TAs because the need for recalibration was frequent, as the sensors did not work well for imperfectly assembled paddles (i.e. those with distance variation between the magnet and sensor over the paddle sweep). To retain the educational aspects of calibration, we now include a calibration verification experiment in the lab, where students verify the linear relationship between handle angle and sensor output.

These electronics improvements have reduced the cost of the complete haptic paddle system to just under $90, ($55 D/A and motor control electronics + $6 angle sensor + $5 surplus motor + $20 Acrylic raw material). This lower cost may make it easier for universities, K-12 students and teachers, and hobbyists to adopt and use haptic paddles. This cost assumes that the user has a laptop or desktop computer and a power supply.

Many users will already have access to a power supply, but if not, low-cost options such as a 12V Regulated Power Adapter, rated for 5A, can be easily found on several online retailers (e.g. Replacement AC Adapter, 12V, 5A Power Supply from Stiger) for less than $9. To connect this to the haptic paddle, an appropriate connector (e.g. CP-024B-ND, DigiKey Corporation, $3) will be needed, or one could simply cut off the plug and use the individual wires.

2.2.3 Matlab/Simulink Control Software

We have also modified the software interface that controls the haptic paddles, moving from C++ to Matlab/Simulink (The MathWorks, Inc.). Simulink's Real Time Windows Target and the 3D animation packages enable us to control the haptic paddle in real time and to create realistic visualizations and convenient user-interfaces for students. All of the code to do this is freely available at [6].

The move to Matlab/Simulink was made for two reasons. First, we use Matlab in the lecture portion of the class for model evaluation and dynamic simulation, and it is preferable to keep a consistent software language throughout the class. Note that many Mechanical Engineering students have only superficial knowledge of programming and little comfort with it, despite having a required programming course as freshmen or sophomores. Thus, often, one must re-teach many basic programming concepts in System Dynamics, and switching languages can cause confusion.

Second, the original paddles were programmed using C++, and students were provided only with executables, which limited their ability to develop a deep understanding of what is going on inside the haptic paddle system "black box". Simulink's graphical interface en-

ables students to build block diagrams, connecting what they have learned in class directly to hardware, and makes it easier for students to understand how the computer program works. Since students are now able to program the paddle themselves, they also have much more accountability during lab activities. Rather than blaming the TAs, the computer in the lab, the course instructor, or the university for any bugs they encounter, they are automatically inclined to begin debugging themselves, rather than relying on the TA to "fix" the system for them. We have qualitatively observed students to be more engaged and more enthusiastic in the lab with the interactive software environment provided by Simulink, than when simply double clicking in an executable.

2.2.4 Updates to the Original Stanford Laboratory Curriculum

The mechanical, electronic, and software changes described above have reduced the complexity and cost of the entire system while also providing students with a flexible software interface through which they can quickly develop real-time models and interface them with their haptic paddle. While these changes have required some curricular changes (notably the simpler design does not require most of one lab for paddle construction, and the improved sensor design has saved about half of another lab by eliminating sensor calibration), the learning objectives of the lab exercises remain comparable to the original Stanford and Johns Hopkins labs. These time savings have enabled us to devote more lab time to teaching the students Simulink and how to interface simulation and hardware.

Similar to the original Stanford curriculum, each of the five sequential lab assignments focuses on a different aspect of the haptic paddle, which relates to concepts covered in lecture. The following are descriptions of the current lab assignments (also posted at [6]),

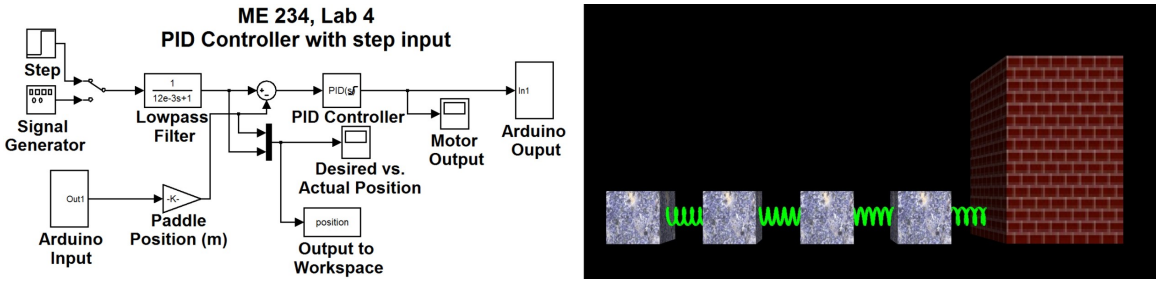

Figure 2.4: (Left) The Simulink model students build to investigate feedback control in Lab 4. (Right) The 3D visualization of a mass-spring-damper system students interact with using the haptic paddle in Lab 5.

including minor modifications enabled by the hardware/electronics/software changes described above.

In the first lab, students are introduced to Simulink by creating simple models of virtual springs and dampers and then use the paddle to feel these virtual objects while changing their properties. Then, they conduct a motor spin down test as an example of a first order system and compare their experimental results with predicted results they obtain from their Simulink simulation of their motor. Students then include Coulomb friction in their simulation and compare the differences between it and their simulation with only viscous damping. Finally, they use their simulation results to estimate damping in their motor and compare it with the best fit damping constant they obtain from their analytical solution. In the second lab, students experimentally measure the torque constant and Coulomb friction in the motor and analyze the paddle handle by measuring its moment of inertia through a bifilar pendulum experiment.

In the third lab, students first perform a calibration exercise with the magnetic sensor. Then, they use Simulink to make their haptic paddle behave as a second order underdamped

system in order to determine the equivalent mass, stiffness, and damping of the system. Finally, students build a pure simulation of a second order system and compare their predicted and experimental results. In the fourth lab, students investigate PID (proportional-integral-derivative) control by developing a Simulink model to command step and sinusoidal inputs (as shown in Figure 2.4 (Left)), altering PID gains, and observing the paddle's response. Then, students add weights to the top of their paddle handle to make it an unstable system (inverted pendulum) and use feedback control to stabilize the paddle. In the fifth lab, students interact with a multiple DOF mass-spring-damper system and explore its modes of vibration using the paddle and a real-time 3D visualization of the system, shown in Figure 2.4 (Right).

2.3 A Formal Assessment of Student Learning: Methods

This section addresses the formal assessment, based on analyses of three years of data, of the learning that takes place in haptic paddle laboratories in the context of a System Dynamics course. This assessment seeks to determine if students are learning key educational objectives for each lab and to determine when that learning took place (in lecture, during the lab itself, during report writing, etc.). In conducting this assessment, we had the distinct advantage of having a large class (approximately 70 students, varying slightly from year to year) that was subdivided into four lab sections, which enabled us to randomize quiz presentation to determine when learning occurred. Each lab section met for three hours on a different day of the week, five times throughout the semester. During the three hour lab periods, students completed one of the five lab exercises described in Section 2.2.4. Within each lab section, teams of 2-3 students work together, as shown in Figure 2.5. These teams

Figure 2.5: Small teams of 2-3 students interacting with the haptic paddle during a lab activity.

are self-selected by the students, and they remain in roughly the same groups for the duration of the semester.

To assess student learning, we constructed a 25-question multiple choice quiz (5 questions/lab $\times$ 5 labs, see Appendix I) covering the core concepts of the lecture and the lab exercises [6]. Each question had 4 possible answers, with one being correct. The three remaining incorrect choices were chosen to include common wrong answers or misconceptions that students often have. In a few questions, we asked students to "Choose all of the answers that apply," instead of selecting just one. This 25-question assessment was administered at the beginning of the semester to all students in order to assess their initial understanding of all of the course material and to provide a baseline measurement for statistical analyses and again at the end of the semester as a final evaluation. This 25-question assessment was then broken down into 5 quizzes, each containing 5 questions.

Each of these 5-question quizzes corresponded to key concepts from one lab (1 quiz/lab, see Appendix I). We note that the 5 questions on each quiz were pulled directly from the original 25-question assessment, and the corresponding 5-question quiz was the assessment administered during the lab session.

To explore *when* student learning was occuring, we randomized the presentation of the 5-question lab quiz among the four sections at (1) the beginning of the lab session, (2) after a pre-lab lecture, (3) after completing the lab, or (4) after completing the lab report (typically 1-2 weeks after completing the lab), as shown in Table 2.1. The first time point enabled us to assess the value of the in-class lecture alone. The second time point enabled us to assess students' listening and recall skills after having heard a short introductory lecture on the lab objectives. The third time point enabled us to assess the benefit of the lab activities in enhancing student learning, and the fourth time point enabled us to assess the value of the lab report. Though the timing of the lab quiz differed between student sections, the same lab quiz was administered to each. Using this approach, each student section took one quiz for each lab, varying only by the time point at which they took it. The time at which the 5-question lab quizzes were administered to each section was systematically rotated (see Table 2.1) to remove any potential bias in data collection. Students were given a 10% extra credit bonus on each of their lab report grades for completing the respective lab quiz. These points were given based on completion of the quiz, not based on correctness of student answers. Students were aware of this grading policy, and thus, it is possible that they may not have always tried their hardest in answering the questions correctly. We note, however, that lab TA's stressed the importance of the quizzes to the students and provided ample time in lab for students to complete them. For assessment purposes, we recorded 1

Table 2.1: Quiz placement for each lab for each student section. S1-S4 represents each of the four student sections.

Placement	**Lab 1**	**Lab 2**	**Lab 3**	**Lab 4**	**Lab 5**
Beginning	S1	S4	S3	S2	S1
After Pre-Lecture	S2	S1	S4	S3	S2
After Lab	S3	S2	S1	S4	S3
After Lab Report	S4	S3	S2	S1	S4

point for every correct answer and 0 points for every incorrect answer. Means and standard deviations were computed for each of the students' quizzes.

Below, we present three years of data collected from the assessments, with $N_1 = 63$ students, $N_2 = 71$ students, and $N_3 = 74$ students, where N_x represents the total number of students in the class for each of the three years. As stated earlier, each student class was divided into four sections ranging in size from 15-20 students in each, for the lab activities. We note that appropriate IRB approval was obtained for this study. In year 1 (Y1), we used the original Stanford version of the haptic paddle (subsequently used at Johns Hopkins University) and its C-executables, in year 2 (Y2), we used the inverted paddle design with a cable drive (similar to the Rice University design) and Matlab and Simulink software, and in year 3 (Y3) we used the friction drive paddle and Matlab and Simulink. The lab content and objectives were similar in all three years, as were the assessments.

2.3.1 Research Questions

The research questions we sought to answer analyzing quiz data are as follows:

1. Overall, did the students learn the core course concepts at some point in time during the semester? Statistically, we were interested in determining if there was a significant increase in mean quiz score from the beginning to the end of the semester.

2. Did the lab activities increase student understanding of the course material? Statistically, we were interested in determining if there was a significant increase in mean quiz score from the beginning of the semester to after completing the lab.

3. When did the students learn the material? Statistically, we were interested in determining if there were any significant differences between mean quiz scores from the beginning of the semester to any of the time points at which the quizzes were administered.

In order to address the first question, paired t-tests were performed to compare the mean quiz score on the pre-test with the mean quiz score of the post-test. To assess the value of the labs, we performed paired t-tests to compare the mean quiz score on the pre-test with the mean quiz score of the appropriate student section after completing the lab activity. Finally, to assess *when* student learning was occurring, we performed paired t-tests comparing the mean quiz score of the pre-test to the mean quiz score of the appropriate student section at various time points for each lab. Note that all analyses consist of pairwise comparisons, in order to not compare across student sections and implicitly assume that each student section is equivalent at every time point throughout the lab. This was done to ensure valid

interpretations of our results. For further insight into each analyses on the magnitude of the difference in mean quiz scores, we also computed the effect size between the two means of interest using Cohen's *d* with a pooled standard deviation. A positive value of d suggests an increase in student performance on the quiz at the specified time compared to the pre-test, and a negative value of d indicates a decrease in student performance on the quiz at the specified time compared to the pre-test.

Note that in all discussions, figures, and tables presented, significance at the 95% confidence level ($\alpha = 0.05$) and 90% confidence level ($\alpha = 0.10$) were determined from the paired t-test analyses, and the interpretations made on effect size were based upon the Cohen's *d* computation. We note that these two statistical analyses are complementary to one another, with the t-tests providing insight on whether or not quiz means were significantly different from one another, and the effect sizes providing insight on the magnitude of this difference. In our discussions of effect size, we follow the standard interpretation that $d = 0.2$ is a small effect, $d = 0.5$ is a medium effect, and $d = 0.8$ is a large effect, where the value of *d* indicates the difference between two means as a fraction of the pooled standard deviation. All statistical analyses were performed in R 2.11.1, and the results are presented in Section 2.4.

2.3.2 Verification of Normality and Comparable Student Sections

Before performing the above statistical analyses, we sought to verify three things: (1) Normality of our data, (2) No significant difference between student sections' initial cumulative pre-test scores for each year, and (3) No significant difference between student sections' initial pre-test scores *for each lab*, for each year. We assessed the normality of each student

section's data for each year by creating quantile-quantile plots that included both pre-test scores and lab quiz scores for each student section. All 12 (4 student sections $\times$ 3 years) plots suggest a linear trend, but for simplicity, only one representative plot is shown in Figure 2.6. From this, we can infer that our data is approximately normally distributed and that parametric statistical tests, such as the t-test, are applicable in our subsequent analyses. Second, we ensured that student sections within each year were comparable in their initial cumulative understanding of the course material by comparing the mean cumulative pre-test score (all 25 questions) of each student section with the other 3 student sections using a two-sample t-test with unequal variances. Finally, we ensured that student sections within each year were comparable in their initial understanding of the course material *for each lab* by separating the 25-question pre-test up into 5 parts, corresponding with the 5 lab quizzes, and comparing the mean quiz scores on each part between each student section using a two-sample t-test with unequal variances. The null hypothesis for all tests was that no difference in mean pre-test score existed between any two sections.

From the Y1 data, we observed a significant difference between student section 1 and student section 2 (p-value = 0.04) in their *cumulative* pre-test score, but found no significant differences at the 95% confidence level ($\alpha = 0.05$) between student sections on individual parts of the pre-test. For this reason, we only omit the cumulative pre-test scores of student sections 1 and 2 in appropriate subsequent analyses. From the Y2 data, we observed no significant differences at the 95% confidence level ($\alpha = 0.05$) between any student sections'*cumulative* pre-test score, but found a significant difference between section 1 and section 4 on the Lab 5 portion of the pre-test (p-value = 0.04), with section 1 having a significantly higher average on this portion of the material. Because of this, student sec-

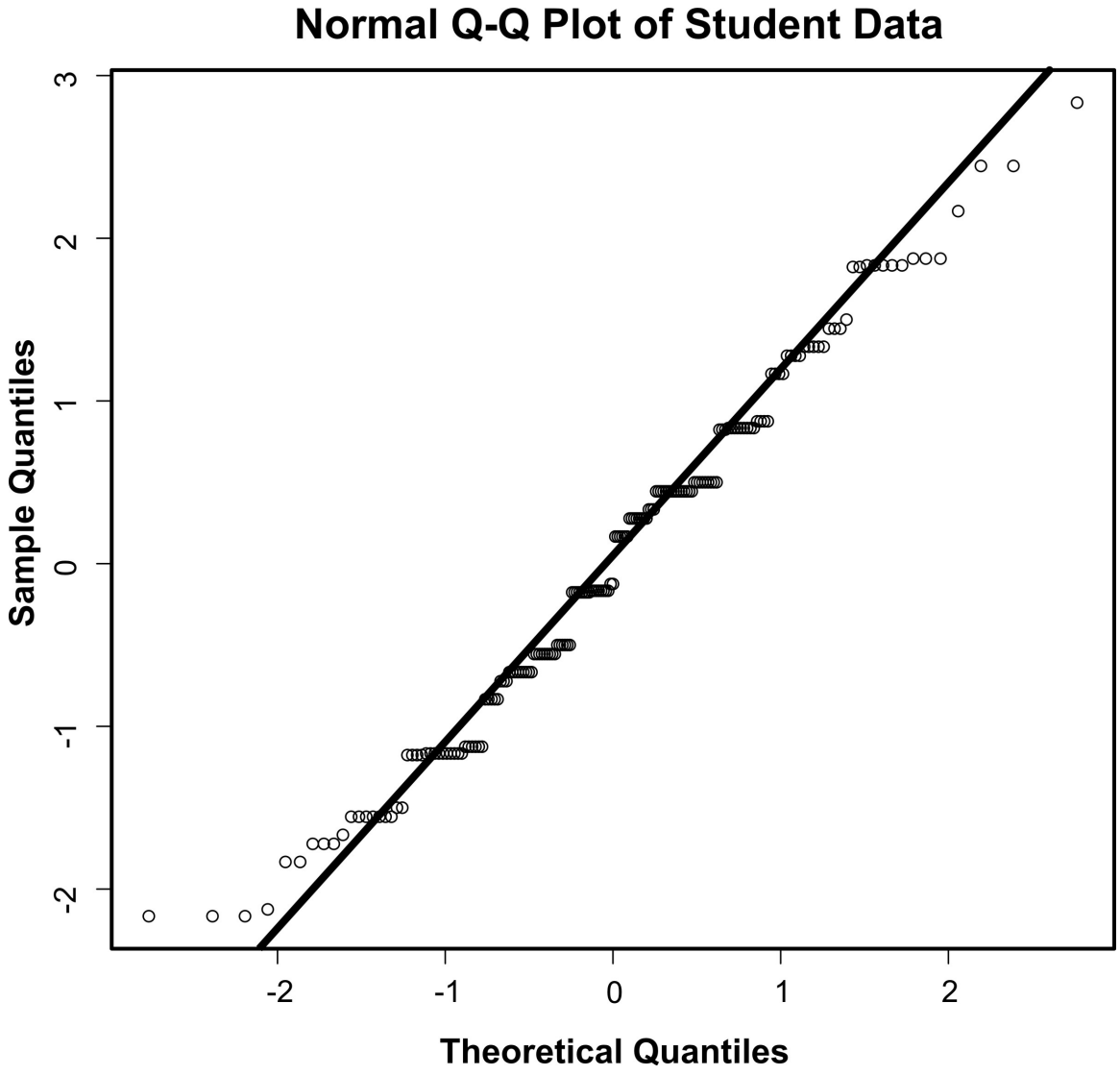

Figure 2.6: A Q-Q plot from one student section assessing the normality of our data. The linearity of this plot suggests that the data follows an approximate normal distribution. Q-Q plots were created for each student section for each year (4 student sections $\times$ 3 years), for a total of 12 plots. The plot shown is representative of all 12 plots, and thus we can infer that each student section followed an approximately normal distribution.

tion 1's data was omitted in the Lab 5 analyses for Y2. Only section 1's data was omitted because there were no significant differences between any combination of sections 2, 3,

and 4's scores on the Lab 5 portion of the pre-test. From the Y3 data, we observed no significant differences at the 95% confidence level ($\alpha = 0.05$) between any student sections' *cumulative* pre-test score, but found a significant difference between section 1 and section 4 on the Lab 2 portion of the pre-test (p-value = 0.02), with section 1 having a significantly higher average on this portion of the material. For this reason, we omit student section 1's data in the Lab 2 analyses for Y3. Again, only section 1's data was omitted because there were no significant differences between any combination of sections 2, 3, and 4's scores on the Lab 2 portion of the pre-test.

2.4 Formal Assessment: Results and Discussion

2.4.1 Educational Benefit from Course

We first sought to answer whether or not the students learned and retained the course concepts after completing the entire course. This enabled us to generally assess if the combination of learning opportunities we are providing (lectures, homework assignments, labs, lab reports) is beneficial for students. To address this question, we performed a paired t-test comparing all students' cumulative mean score on the pre-test with their cumulative mean score on the post-test. Because we found a significant difference in cumulative scores from this comparison, we then separated the pre-test and the post-test into 5 parts (corresponding with the lab quizzes), and performed paired t-tests comparing all students' mean quiz score on one part of the pre-test with their mean quiz score on that same part of the post-test. This latter analysis allowed us to observe the cumulative learning of portions of the course material, in order to pinpoint which areas appear more difficult for students to grasp and

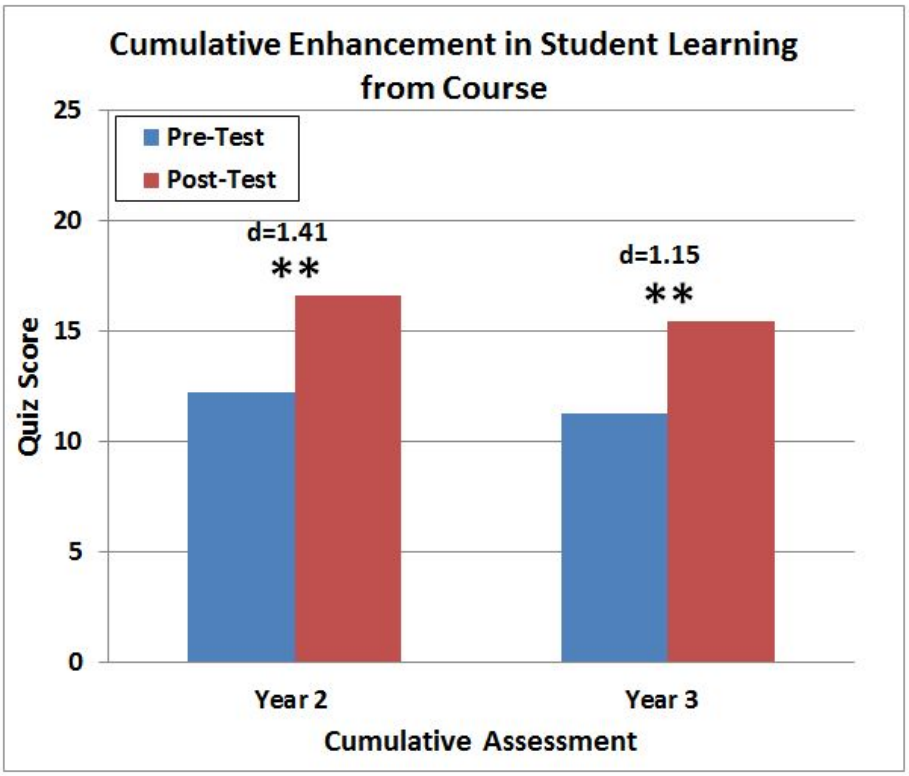

Figure 2.7: The cumulative mean (out of 25) of all students' pre-test score compared with their post-test score for years 2 and 3. Significant differences in quiz scores from the paired t-test are denoted with a ** at $\alpha = 0.05$ and a * at $\alpha = 0.1$, and the corresponding p-values are shown in Table A.1 in Appendix A. The effect size, d, between the two means is shown above the bars.

may benefit from more emphasis in the future. In both analyses, we also computed the effect size, d, of the difference in means. The results of this study are presented in Figures 2.7 and 2.8 and can be found in tabular form in Appendix A, Table A.1. Note that post-test data was only available for Y2 and Y3, and thus no data is presented from Y1.

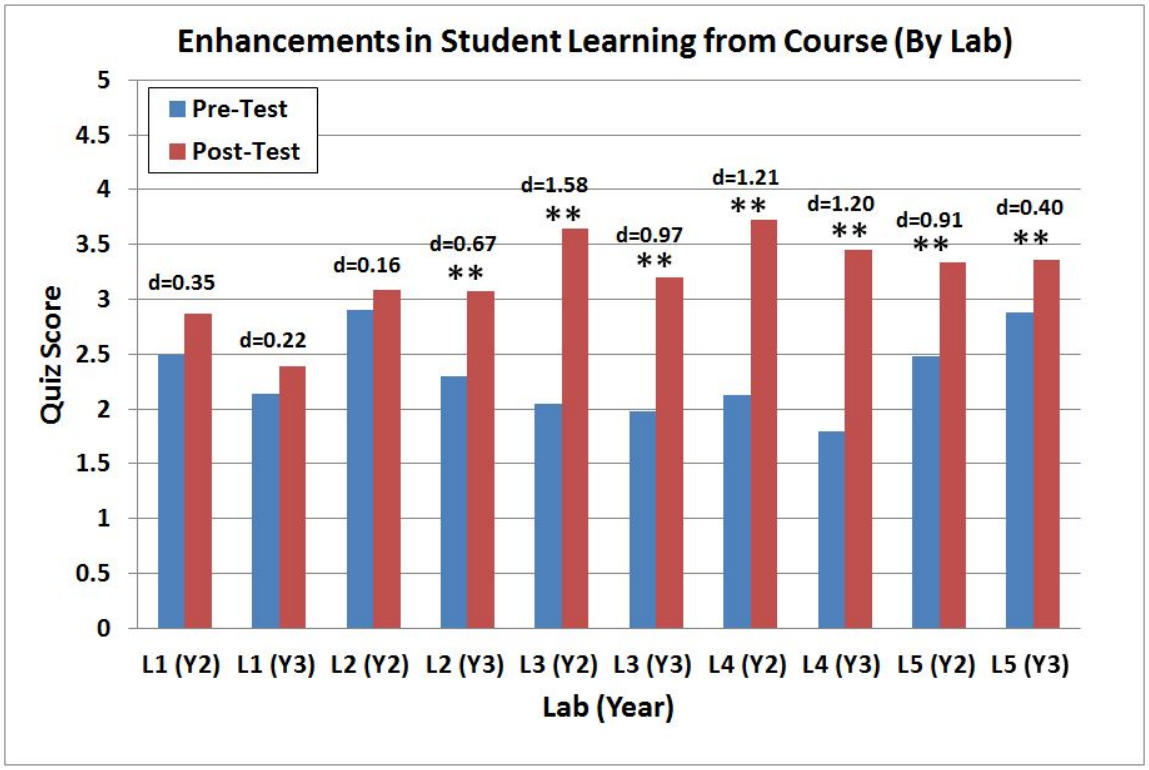

Figure 2.8: The means (out of 5) of all students' pre-test score compared with their post-test score for years 2 and 3. Significant differences in quiz scores from the paired t-test are denoted with a ** at $\alpha = 0.05$ and a * at $\alpha = 0.1$, and the corresponding p-values are shown in Table A.1 in Appendix A. The effect size, d, between the two means is shown above the bars.

Discussion of Educational Benefit from Course

The results presented from the first study suggest that students learned and retained majority of the core course concepts throughout the semester. From Figure 2.7, we observe that students achieved a significantly higher cumulative score on the post-test compared to the pre-test in both years. Large effect sizes ($d > 0.8$) were also observed. This suggests that the learning opportunities provided to the students throughout the semester were successful

in enhancing students' overall understanding of the course material. After looking at the pre-test and post-test scores separated by lab (Figure 2.8), we observe that students did significantly better on the quizzes focusing on concepts from Labs 2, 3, 4, and 5 in at least one of the two years presented. Moderate to large effect sizes ($d > 0.5$) were also observed in these same labs. This suggests that students learned and retained these concepts throughout the duration of the course. Though quiz score increases are observed for Lab 1 in both years and Lab 2 in Y2, there were no significant differences between the pre-test and post-test scores in these cases, and the observed effect sizes were small ($d < 0.5$). For further insight into these latter results, we look to the next assessment focusing on the educational benefit from the lab itself.

2.4.2 Educational Benefit from Lab

The second question we addressed was if students increased their conceptual understanding of the course concepts immediately after having participated in the lab activity. To assess this, we performed a paired t-test comparing the mean quiz score obtained after completing the lab with the mean quiz score obtained on the corresponding section of the pre-test for each lab. We also computed the effect size, d, for the difference in means from pre-test to after lab. For both analyses, we compared student section 3's scores from pre-test to after lab for Lab 1, student section 2's scores from pre-test to after lab for Lab 2, and so on, as shown in Table 2.1. The results are shown in Figure 2.9 and can be found in tabular form in Appendix A, Table A.2.

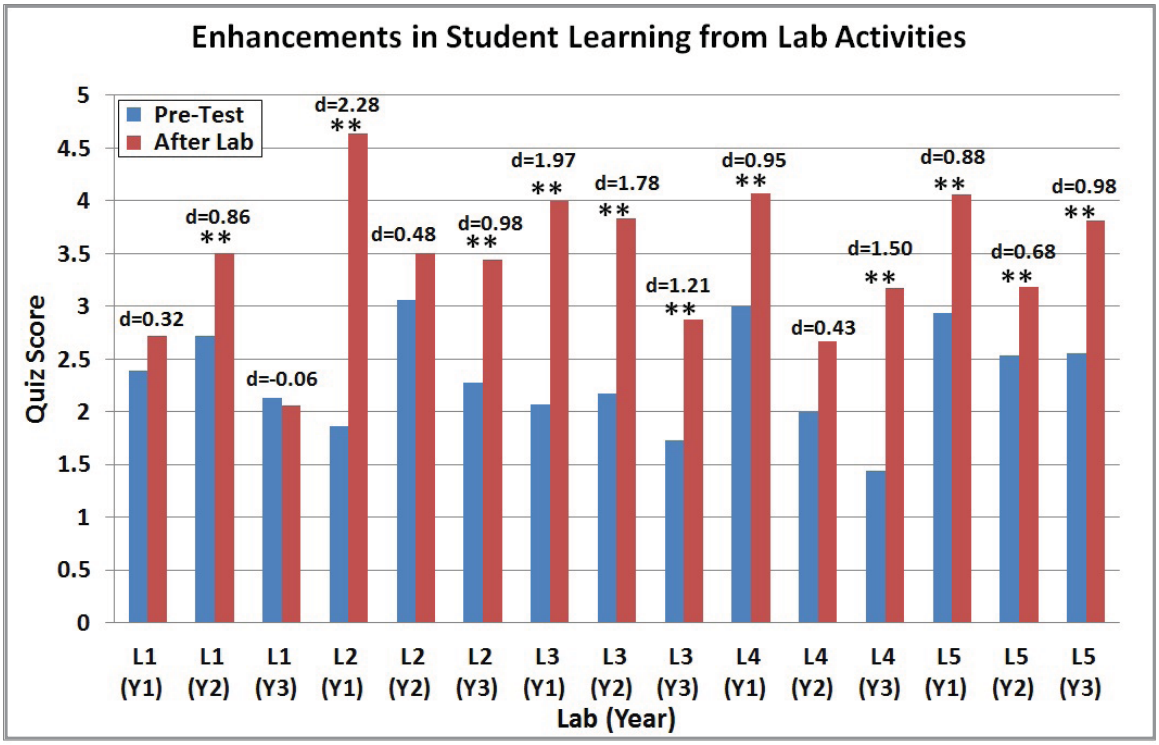

Figure 2.9: The means of the appropriate student section's quiz score (out of 5) on the pre-test compared with the quiz score taken after completing the lab for year 1 (Y1), year 2 (Y2), and year 3 (Y3). Significant differences in quiz scores from the paired t-test are denoted with a ** at $\alpha = 0.05$ and a * at $\alpha = 0.1$, and the corresponding p-values are shown in Table A.2 in Appendix A. The effect size, d, between the two means is shown above the bars.

Discussion of Educational Benefit from Lab

The results from this second study are positive, as students achieved significantly higher quiz scores after having participated in the lab activity, for all of the labs, in at least one of the three years of data collected (see Figure 2.9). Large effect sizes ($d > 0.8$) were also observed in each of the labs in at least one of the three years of data collected. Looking at

each year individually, we observe that students achieved significantly higher quiz scores in 4 of the 5 labs for Y1 and Y3 and in 3 of the 5 labs for Y2. A similar trend was observed in looking at effect sizes, with moderate to large effects ($d > 0.5$) being observed in 4 of the 5 labs for Y1 and Y3 and in 3 of the 5 labs for Y2. For further insight into these results, we look at the individual labs separately.

We begin with the Lab 1 material, which appears to be the most challenging for students to understand, as it was the only lab that did not have a significant increase in quiz score immediately after completing the lab exercise in Y1 or Y3. A significant increase was observed in Y2, however no significant increase was observed when comparing the pre-test scores to the post-test scores for Lab 1 in Y2 (see Figure 2.8). These results suggest that Lab 1 would benefit from further improvements to enhance student understanding and retention of the material.

In Lab 2, we observe that there was a large significant increase from pre-test to after lab for Y1 and Y3, but there was not a significant increase in quiz score from pre-test to after lab for Y2 (see Figure 2.9). Some changes were made between the three years in the Lab 2 curriculum which may have contributed to this discrepancy, though the changes were primarily hardware and software rather than lab content. We note, however, that an unpaired, two-sided t-test at the 95% confidence level comparing the mean pre-test scores for Lab 2 between all three years revealed that the Y2 Lab 2 pre-test score was significantly higher than the Y1 Lab 2 pre-test score (p-value = 0.02) and significantly higher than the Y3 Lab 2 pre-test score (p-value = 0.05). This suggests that the students from Y2 had a better understanding of the Lab 2 material at the beginning of the course compared to the students in Y1 and Y3. A similar trend was observed in the assessment of the educational

benefit over the entire course for Lab 2 (see Figure 2.8), as the pre-test score for Y2 was significantly higher than the pre-test score for Y3 (p-value = 0.01, from an unpaired, two-sided t-test at the 95% confidence level). Thus, part of the reason we may not observe a significant increase in Y2 Lab 2, may be due to the fact that students already knew a large portion of the material initially. Nonetheless, the results suggest that Lab 2 could also be a focus for future improvements.

The results for Labs 3, 4, and 5 show significant learning enhancements. Lab 3 particularly appears to be beneficial for students, as we observe significant increases in quiz scores and large effect sizes ($d > 0.8$) from pre-test to after lab (see Figure 2.9) in all 3 years and from pre-test to post-test (see Figure 2.8). This suggests that the Lab 3 exercises are successful in increasing student understanding and retention of the material associated with Lab 3. Almost equally as promising is Lab 4, where we observe a significant increase in quiz score and a large effect size from pre-test to post-test in Y2 and Y3 (see Figure 2.8) and from pre-test to after lab in Y1 and Y3. The one exception is the Lab 4 data from Y2, which does not show a significant increase in quiz score from pre-test to after lab, and has a small to moderate effect size ($d > 0.2$). This result may be due in part to the fact that the sample size for this particular lab was relatively small due to several students switching lab sessions or not completing the quiz. The significant increase in Lab 4 in Y2 from pre-test to post-test, however, suggests that majority of the students learned the Lab 4 material, perhaps benefiting especially from the lab report and lecture discussions following the lab. The results from Lab 5 are also very encouraging, as there was a significant increase in quiz score and moderate to large effect sizes ($d > 0.5$) from pre-test to after lab in all three years and from pre-test to post-test, suggesting that the exercises in this lab were beneficial in en-

hancing student understanding and retention of the material. Even with the few exceptions mentioned above, the results presented both after lab (see Figure 2.9) and at the end of the semester (see Figures 2.7 and 2.8) suggest that the haptic paddle labs significantly enhance student understanding and retention of the core concepts in the course.

2.4.3 Educational Benefit of Other Learning Opportunities

The last question we sought to answer in this study addressed if and *when* students were learning the material. In other words, we wished to pinpoint at what stage(s) learning was occurring. In order to assess this, we analyzed the components of the learning process in a separate, but cumulative fashion.

To assess the value of the in-class lecture, we conducted a paired t-test with unequal variances to compare the mean quiz score from the appropriate part of the pre-test to the mean quiz score from the student section who took the quiz at the very beginning of the lab. We also calculated the effect size, d, between the difference in means from pre-test to the very beginning of lab. From Table 2.1, the pertinent data used in this analysis was student section 1's scores for Lab 1, student section 4's score for Lab 2, and so on. The results, which will be discussed in detail in Section 2.4.3, are shown in Figure 2.10 and can be found in tabular form in Appendix A, Table A.3. They suggest that the lecture was beneficial for the concepts covered in Labs 3 and 4.

We then assessed the value of the in-class lecture and the pre-lab lecture combined by comparing the mean quiz score on the appropriate part of the pre-test with the mean quiz score from the student section who took the quiz after the pre-lab lecture, but before the lab activity. We did this using a paired t-test with unequal variances and by computing the

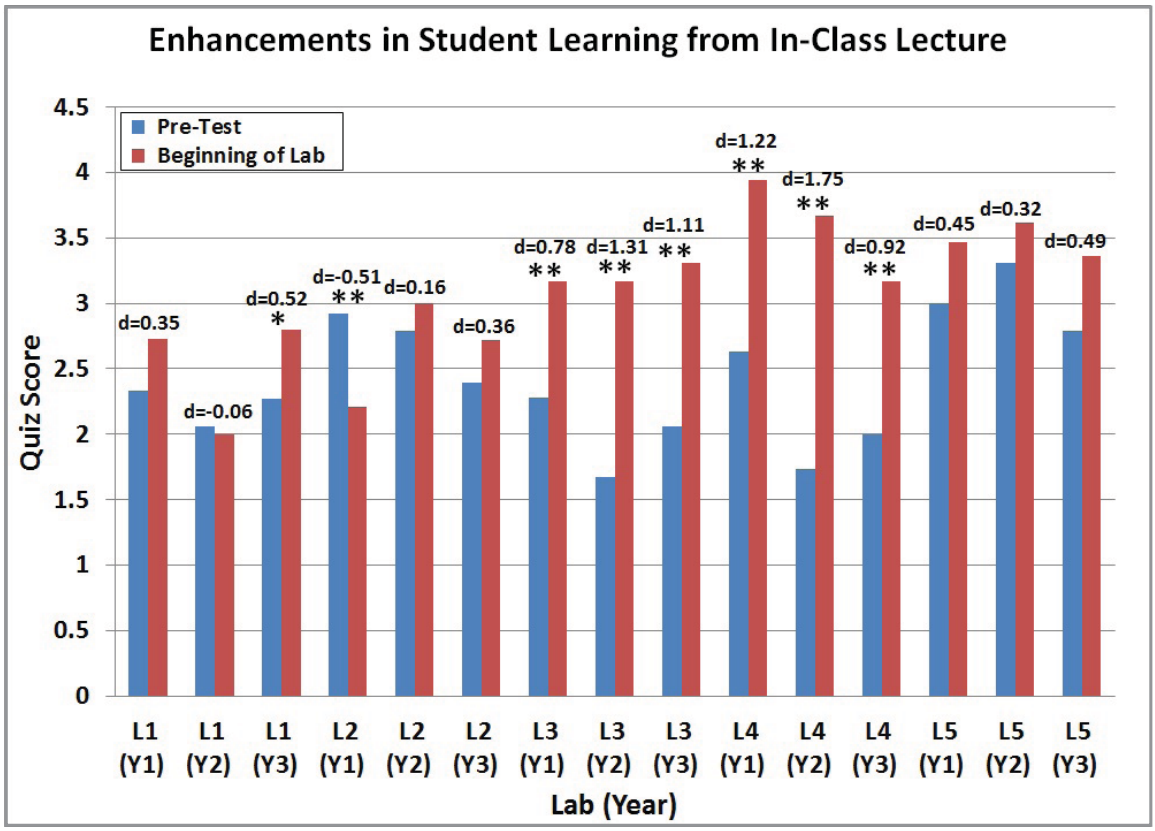

Figure 2.10: The means of the appropriate student section's quiz score on the pre-test compared with the quiz score taken at the beginning of lab for year 1 (Y1), year 2 (Y2), and year 3 (Y3). Significant differences in quiz scores from the paired t-test are denoted with a ** at $\alpha = 0.05$ and a * at $\alpha = 0.1$, and the corresponding p-values are shown in Table A.3 in Appendix A. The effect size, d, between the two means is shown above the bars.

effect size between the two appropriate means. From Table 2.1, the pertinent data used in this analysis was student section 2's scores for Lab 1, student section 1's score for Lab 2, and so on. The results are shown in Figure 2.11 and can be found in tabular form in Appendix A, Table A.4. They will be discussed in more detail in Section 2.4.3, but they suggest that the pre-lab lecture is a beneficial component of the lab, enhancing students'

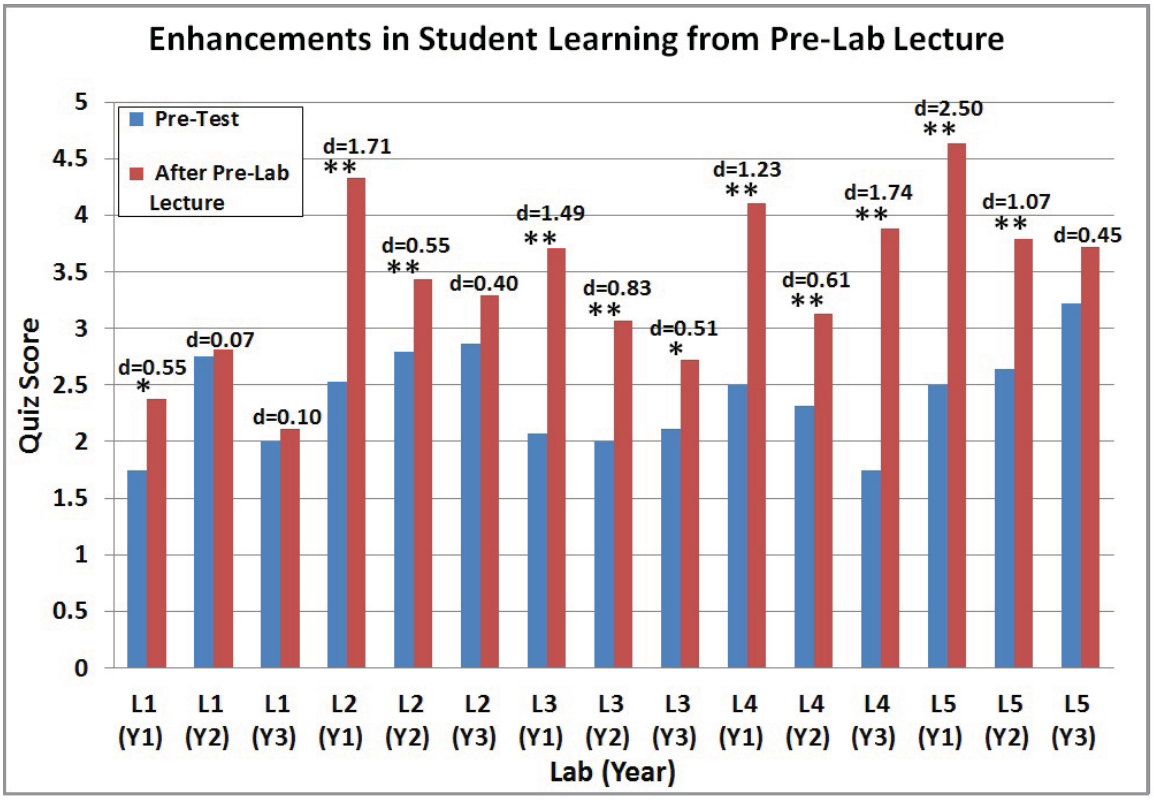

Figure 2.11: The means of the appropriate student section's quiz score on the pre-test compared with the quiz score taken after the pre-lab lecture for year 1 (Y1), year 2 (Y2), year 3 (Y3). Significant differences in quiz scores from the paired t-test are denoted with a ** at $\alpha = 0.05$ and a * at $\alpha = 0.1$, and the corresponding p-values are shown in Table A.4 in Appendix A. The effect size, d, between the two means is shown above the bars.

immediate recall of the material in all of the labs.

Because the value of the lectures and the lab combined are presented above in Figure 2.9, we omit them here. Finally, to assess the value of all learning components (lectures, lab, and lab report), we conducted a paired t-test with unequal variances to compare the mean quiz score from the pre-test to after the lab report. We again computed the effect size, d, of the difference between the two means. From Table 2.1, the pertinent data used in

this analysis was student section 4's scores for Lab 1, student section 3's scores for Lab 2, and so on. The results, also discussed in more detail in Section 2.4.3, are shown in Figure 2.12 and can be found in tabular form in Appendix A, Table A.5. They suggest that the lab report is also a necessary component of the lab activity, as it enabled students to apply and retain the material they learned in four out of the five labs.

Discussion of Educational Benefit from Other Learning Opportunities

In this last study, we sought to gain a better understanding of when student learning was occurring, by looking at the individual learning opportunities. From Figure 2.10, which shows the value of the in-class lecture alone, we observe that students scored significantly higher on quizzes for Labs 3 and 4 even before participating in the lab itself. Strong effect sizes ($d > 0.8$) were also observed in these two labs. This suggests that the in-class lecture is particularly beneficial for the concepts associated with Labs 3 and 4. We also observed a significant increase ($\alpha = 0.1$) in the Lab 1 material for Y3, however this was not observed in the other two years of data collection, and this resulted in only a moderate effect size in this case. We also note that the Y1 students had a significant decrease in quiz score (and a moderate effect size ($d > 0.5$)) from pre-test to the beginning of lab for Lab 2. This suggests that students may have become confused by the in-class lecture on this material. In Y2 and Y3, however, we observe increases in quiz scores for this material, though they are not significant and the effects are small. Taken together, these results suggest that the lecture itself, while beneficial, was simply not enough in enhancing student understanding of majority of the material and reiterate the need for additional learning opportunities outside of the lecture.

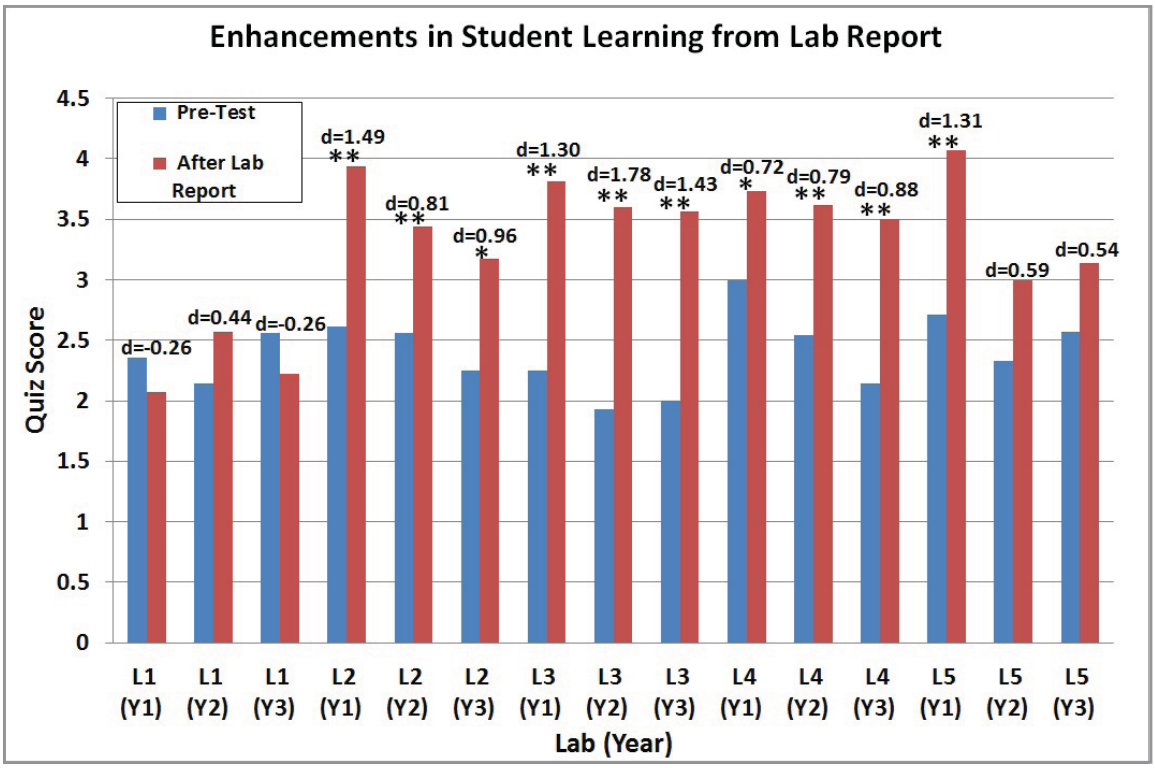

Figure 2.12: The means of the appropriate student section's quiz score on the pre-test compared with the quiz score taken after completing the lab report for year 1 (Y1), year 2 (Y2), year 3 (Y3). Significant differences in quiz scores from the paired t-test are denoted with a ** at $\alpha = 0.05$ and a * at $\alpha = 0.1$, and the corresponding p-values are shown in Table A.5 in Appendix A. The effect size, d, between the two means is shown above the bars.

Before students perform a lab exercise, they are given a short pre-lab lecture, specifically addressing the learning objectives of the lab. These objectives correspond directly with the concepts covered in the quiz, such that if students paid close attention during this introductory lecture, they should know every answer on the quiz. Thus, this quiz primarily

tested students' listening and recall skills. In order to assess the value of the in-class lecture and the pre-lab lecture, we compared pre-test scores with quiz scores taken after the pre-lab lecture but before completing the lab. From Figure 2.11, we observe that students appeared to listen and benefit from these pre-lab lectures, as reflected in the significantly higher quiz scores after hearing the pre-lab lecture in all of the labs, in at least one of the three years of data collected. Moderate to large effect sizes ($d > 0.5$) were also observed in this same labs. We suspect that the discrepancies between years is due in part to different TAs providing the lectures. Though we cannot directly decouple the in-class lecture from the pre-lab lecture in this analysis, we speculate that the pre-lab lecture had a significant benefit on its own when comparing the results from the in-class lecture individually (Figure 2.10) and the results including both the in-class and pre-lab lectures (Figure 2.11). From these two figures, we see that students performed significantly better on more of the quizzes after the pre-lab lecture than after the in-class lecture. Overall, these results suggest that students' immediate recall of the material appears to be good and that a pre-lab introduction is a useful component of the lab itself.

After finishing a lab exercise, we ask students to complete a lab report where they answer questions about the lab exercises and analyze and interpret the data they collected in lab. The purpose of these lab reports is to teach students how to be reflective learners, give them another opportunity to connect theoretical concepts to their lab activities, and to enhance their ability to write technical reports. To assess the value of the lectures, lab, and lab report together, we compared pre-test scores with quiz scores taken after completing the lab report and computed corresponding effect sizes. From Figure 2.12, we again see that students scored significantly higher on quizzes for all of the labs in at least one of the three

years of data collected, except for Lab 1. Large effect sizes ($d > 0.8$) are also observed in at least one of the three years of data collected in all labs except Lab 1. These results suggest that the lab report is beneficial in helping students translate and retain the concepts they learned in the lab and reiterate the need to improve Lab 1.

2.4.4 Summary of Results

Overall, we found that the in-class lecture alone, though beneficial, is not sufficient for enhancing student understanding of the material, as reflected by t-tests revealing that students only scored significantly higher on quizzes relating to 2 of the 5 labs, (Labs 3 and 4), and one year in Lab 1. Large effect sizes for the in-class lecture comparison were also only observed for Labs 3 and 4. Further, we found that the haptic paddle labs (including the pre-lab introduction, the lab activity, and the lab report) were very successful in increasing student understanding of the core concepts, as students scored significantly higher on quizzes in 4 of the 5 labs after completing all parts of the lab experience in one of the three years of data collected and in 3 of the 5 labs in the other two years. A similar trend was observed when looking at effect sizes of the differences in quiz scores after completing the lab activity. Specifically looking at the pre-test scores compared to the after lab scores, we observed that students scored significantly higher on all 5 of the lab quizzes in one of the three years of data collected. This finding is also supported by observing large effect sizes on all 5 of the lab quizzes in one of the three years of data collected. Finally, our results suggest that student retention of the material is also good, with significantly higher scores attained in 4 of the 5 labs in one of the two years of data collected, and cumulatively, on the post-test compared with the pre-test in both years. These conclusions are supported by

similar findings when observing effect sizes for each case.

2.5 Conclusion

In this chapter, we have introduced a new, robust, inexpensive design of the haptic paddle, a force feedback device which has been adopted by several universities in teaching System Dynamics. Our haptic paddle relies on a friction drive, which we have experimentally shown is comparable in performance to the original, widely accepted, capstan drive, but is much more robust to classroom use. Further, by using the low-cost Arduino microcontroller for communication, our complete haptic paddle kit can be constructed for less than $100 including all electronics except a computer, and can be operated from a laptop, making it more portable than prior haptic paddle systems. We also transitioned the software from its original C-executable files over to Matlab and Simulink, software that enables students to take on a much more independent role in programming their haptic paddle and provides a convenient, engaging user interface.

We have also formally assessed the benefits of the haptic paddle laboratories, probing both what material students are learning and when they are learning it. Our formal assessments, using 3 years of student data, suggest that the haptic paddle laboratories are successful in enhancing student understanding of core concepts in this course. The results of our study show that the lab activities complement and enhance the in-class lecture and significantly increase student performance on conceptual quizzes. These results, combined with prior qualitative assessments of the haptic paddles [65], suggest that this set of laboratories engages students, provides an inexpensive, versatile platform for educators to use, and results in significantly higher scores on multiple-choice conceptual quizzes in System

Dynamics.

In order to encourage the adoption of the haptic paddle by other educators and interested university or K-12 students, we have developed a comprehensive website containing all of the information one needs to build the haptic paddle and conduct the lab exercises [6]. This website contains all of the part files required to manufacture the paddle, a complete bill of materials and assembly guide for constructing the paddle, all of the lab handouts and lab report questions, all of the Arduino and Simulink files needed to complete the lab exercises, and all of our assessments. In addition, with support from The MathWorks, Inc., we have made an introductory video to the haptic paddle labs, which provides a discussion of the hardware and software of the paddle, examples of using Real Time Workshop in Simulink in combination with external hardware, an overview of the lab exercises, and our "lessons learned" on using the haptic paddle laboratories. We are also working with collaborators at California State University Long Beach to implement the haptic paddle in a freshman introduction to engineering course and in a graduate level course on teleoperation. The material developed for these courses will be made freely available on our website in the near future.

Our analyses also enable us to pinpoint areas for future improvement in the haptic paddle lab exercises. In subsequent years, our primary focus will be on revising Lab 1, which was the lab that consistently appeared to be the most difficult for students in the analyses discussed in this paper. One possible thought in addressing this issue is to split Lab 1 up into two labs. The first "lab" session would simply be an introduction to the lab and the equipment, and the second lab session would be the actual first lab, with modifications from previous years. The motivation behind this is to allow students more time to get

acquainted with the hardware and software of the haptic paddle before performing any in-depth analysis. Another area of future work is to take advantage of the flexibility and functionality of Simulink to provide simulations of additional dynamic systems beyond the mass-spring-damper system already used in the labs. We also plan to explore how the haptic paddle can be used in teaching other subjects at both the university and K-12 level, and will work with educators to develop lab modules around these ideas. One idea is to incorporate the haptic paddle in a physics lesson and compare its effectiveness using the standardized Force Concept Inventory as our assessment. Finally, we will continue using assessments like the one presented here to evaluate and improve the haptic paddle laboratories, as well as future laboratories where it may be used. We believe that this type of assessment and reflective analysis has the potential to significantly improve the educational experience and performance of both teachers and students.

Chapter 3

Vibratory Touchscreens as Educational Assist Devices for the Visually Impaired

As discussed in Chapter 1, haptic feedback can be provided through either force or tactile feedback. Choosing which type of feedback is most appropriate depends upon the educational goals. To date, most of the devices that have been implemented within an educational setting have provided force feedback to the user. This may be partially due to the fact that most of the currently available commercial haptic devices provide force feedback. Further, in many cases where students are learning about physical phenomena, there may also be particular benefit to feeling actual forces, as opposed to feeling textures or vibrations. This was the case in Chapter 2, where we demonstrated the effectiveness of a force feedback device in a mechanical engineering undergraduate course.

One of the primary advantages of tactile feedback, unlike force feedback, is that it provides users with feedback directly at their fingertips (not mediated by an additional device, such as a stylus). For this reason, it can also be referred to as surface haptics, since the feedback is felt directly on the surface itself. The use of surface haptics may be particularly beneficial in touchscreen platforms, where users are directly interacting with a surface.

The incorporation of tactile feedback into touchscreens has only recently come to fruition. Despite this, however, mobile phones and touchscreens have already begun to incorporate tactile (typically vibratory) feedback in order to enhance the user's experience and tap into an additional sensory modality for conveying information. Though there are several innovative methods being developed to endow touchscreens with enhanced tactile feedback

(discussed further in Chapter 4), most of these techniques are still restricted to research labs. In current commercial tactile touchscreens, vibratory feedback, where a small embedded motor vibrates the entire screen, is the most common approach. Though this may appear to be a very simple means of providing tactile feedback, it can still convey a great deal of information to the user. Further, commercially available tactile touchscreens have the additional benefit that they have already been rigorously tested and validated. This will likely lead to more rapid dissemination in classroom settings, since it is typically easier to adopt and implement readily available hardware rather than custom solutions that have not yet been tested for robustness.

Toward realizing the potential benefits of touchscreens in education, this chapter explores the use of tactile (vibratory) feedback in two commercially available touchscreens, with the goal of developing a refreshable, portable, robust interface as an educational assist device for the visually impaired. Here, we propose a new education paradigm for teaching visually impaired students that can be implemented on inexpensive and robust commercially available hardware using freely available software components. We then present user studies showing that subjects can differentiate between lines of different slopes, but have difficulty differentiating fully filled in shapes from one another. These experiments demonstrate that users can perceive and understand basic math concepts displayed on a touchscreen using tactile and auditory feedback and provides suggestions for areas of improvement in future work. In this chapter, we also perform initial pilot studies with blind students and show that their results appear qualitatively comparable to user studies in sighted cohorts. Finally, we describe our initial experiences adapting touchscreens to the public school setting, where we received overwhelmingly positive feedback about the

system from users initially predisposed to doubt that it would be effective.

The work presented in this chapter was published in *The Proceedings of the IEEE WorldHaptics Conference 2011* [84] and has been submitted for publication in the *Journal of Special Education and Technology* [40]. Several commericial partners, such as Apps4Android, have shown interested in the software developed in this work. Having the application be made freely available on the open source markets such as the Android Market will help broadly disseminate this software for others to test and use. This work has also laid the foundation for several future studies, both from a perceptual and educational standpoint.

3.1 Motivation and Related Work

Approximately 285 million people are visually impaired worldwide, 39 million of whom are blind [92]. Current methods of teaching graphical concepts such as math to visually impaired students are labor intensive. A separate instructor typically accompanies each student to class and manually constructs shapes or graphs by placing objects on tactile graph paper or using cork boards and pushpins [32, 101], or via similar use of magnetic boards or swell paper (which creates tactile bumps in response to ink). As mentioned in Chapter 1, embossing graphical material ahead of time is another commonly used method, but this limits interactive learning and precludes answers to questions that stray from the specific lesson plan. A major drawback of manually constructed tactile graphics (in addition to the time and effort required from the instructor) is the time lag experienced by students while the instructor constructs replicas of the visual material drawn on the board by the primary classroom teacher, which often creates a temporal mismatch between what

is “seen” through touch, and what is being verbally discussed. Another drawback is the fact that the student being taught does not feel a sense of independence; the presence of an individual instructor underscores the disability and the sense of being different from one’s peers.

As discussed in Chapter 1, prior work on displaying information through the sense of touch has focused on various kinds of pin array-based displays and on using force feedback devices combined with auditory feedback. There has also been several efforts in using pure auditory feedback (e.g. [100, 101]) to convey graphical concepts. For example, the Accessible Graphing Calculator (ViewPlus Technologies, Corvallis, OR, USA) generates a sonified wave form to represent a line on a graph. Pure auditory feedback has also been used specifically for making touchscreen content more accessible to people with visual impairments. These efforts include programs like Voiceover (Apple Inc., Cupertino, CA, USA), eyes-free texting and typing methods including BrailleTouch (e.g. [36]), as well as touchscreen overlays [53, 54]. These new auditory touchscreen interfaces foreshadow a future in which computers will be much more accessible to blind users. It has also been noted that adding haptic feedback might increase the usefulness of these auditory touchscreen interfaces [54], and a review of haptic technologies for touchscreens was presented in Chapter 4.

While these prior studies illustrate some of the benefits that various haptic technologies can have in displaying graphical concepts, pin array-based displays and force feedback devices have yet to become widely used in classroom education. This may be due to lack of portability, high cost, lack of educational curricula, or many other factors. Further, in the case of force feedback devices, interactions with graphical material are mediated by

a stylus. It is possible that there may be user perception advantages to direct interaction with onscreen material through the fingertips rather than stylus-mediated interaction, since this more closely parallels the way blind students currently explore physically constructed tactile images.

Thus, in this chapter, we explore the possibility of combining many of the ideas individually proposed in the references above (vibratory feedback, touchscreen interfaces, combinations of auditory and haptic feedback, and haptics to teach math, among others), toward use of the new class of portable, inexpensive, vibration-capable touchscreens that have recently come to market in mathematics education. These devices are specifically designed for portability and robustness, are already on the commercial market, and share a small number of common operating systems (e.g. the Android operating system), meaning that software can be widely and rapidly disseminated through online app stores. These characteristics provide a unique opportunity for quick adoption of vibratory touchscreens into mathematics education for the blind, provided that surface vibrations are capable of displaying graphical information with sufficient fidelity to assist in conveying graphical mathematics concepts to users.

3.2 System Description

3.2.1 Overview of Touchscreen Classroom Concept

We envision a classroom in which each blind student has a touchscreen that is wirelessly networked to the teacher's touchscreen (or possibly tablet or smart board, if the teacher is not also blind). The classroom is set up in the manner of a traditional classroom in that

there is one teacher and multiple students. As the teacher draws a graph or figure on his or her input device (touchscreen, tablet, smart board, etc.), this same image will immediately appear on the student's touchscreen. The student can then explore the screen and receive haptic and/or auditory feedback (which they could listen to using headphones to block out crosstalk with auditory signals from other students' devices – in this case the teacher would use a microphone that wirelessly transmits speech to all sets of headphones). The students' touchscreens would be able to transmit to the teacher's or other students in the manner of current networked laptop classrooms where students and the teacher can share material with one another.

We believe that this approach will enable visually impaired students to take on a much greater role in the learning process and will enable them to become much more involved and interactive in class, while also enabling one teacher to teach a larger number of students. It is also likely to give the students a sense of independence, since a dedicated teacher need not be provided for each visually impaired student. The feasibility of setting up networked classrooms such as this is indicated by the fact that some schools are already adopting laptops or touchscreens such as the iPad (Apple Inc., Cupertino, CA, USA) in the classroom [51, 64].

3.2.2 Hardware: Touchscreens

Though we intend for the touchscreen classroom concept to eventually be platform independent, enabling students to use any touchscreen with vibration capability they happen to own, we have initially explored software implementation and user studies on the Immersion TouchSense Demonstrator Series 1000 (Immersion, Inc. San Jose, CA, USA), which was

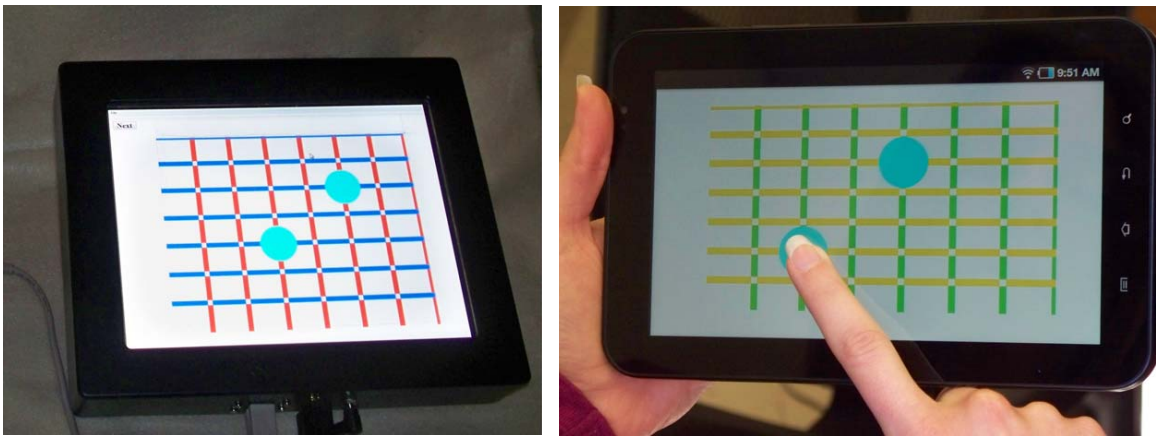

Figure 3.1: The two commercially available vibratory touchscreens used in this work. (Left) Immersion TouchSense Demonstrator which has a 10.4" screen and (Right) Samsung Galaxy Tab 7.0" (Model #:GT-P1010).

one of the first commercial touchscreens with vibration capability to be released. Then, to explore cross-platform portability and create a more portable demonstration, we also implemented our software (described in Section 3.2.4) on the recently released Samsung Galaxy Tab 7.0" (GT-P1010, Samsung, Ridgefield Park, NJ, USA), using Immersion's MOTIV^{TM} Software Development Kit (SDK).

The TouchSense Demonstrator (Fig. 3.1(Left)) consists of a 10.4-inch LCD capacitive touchscreen with 4 Johnson Electric A1110 actuators and a TouchSense controller integrated into a package 270 mm $\times$ 222 mm $\times$ 47 mm, similar in size to a laptop computer. The touchscreen itself is 210 mm $\times$ 158 mm with a resolution of 1024 $\times$ 768 pixels, resulting in approximately 123 ppi (pixels per inch). The actuators have a nominal weight of 22 g each and are rated for 4 **g** at 20 Hz for 100 hours. The surface capacitive touchscreen requires a 5.4 ms minimum finger contact and is rated for a lifetime of more than 1 million touches. The device operates in conjunction with a PC using 2 USB cables and 1 VGA

HDB-15 video cable. Immersion provides the TouchSense Application Programming Interface (API) which has 50 built-in haptic effects grouped into eight base effects classified as "pop click", "crisp click", "pulse click", "high frequency click", "double click", "constant vibration", "pulse vibration", and "single/double vibration". Within each of these categories, the effects vary in magnitude and duration. The subset of these many haptic effects used in our user studies are experimentally characterized in Section 3.2.3.

The Galaxy Tab (Fig. 3.1(Right)) is a Wi-Fi capable Android tablet running with Samsung's TouchWiz interface. The dimensions of this tablet are 190 mm $\times$ 120 mm $\times$ 12 mm, and it weighs 13.58 oz. The actual display size is 154 mm $\times$ 90 mm with a resolution of 1024 $\times$ 600 pixels, resulting in approximately 169 ppi. Recently, several additional sizes of this tablet have been released. It has an embedded vibration motor controlled using Immersion's MOTIV^{TM} SDK and TouchSense technology, which provides over 100 built-in haptic effects and the capability to generate custom designed effects.

3.2.3 Haptic Feedback Characterization

In our user studies, we used three different vibration sensations on the Immersion TouchSense Demonstrator: a "crisp click" with a relative magnitude of 10 out of 10 and a duration of 50 ms, a "pop click" with a relative magnitude of 4.5 out of 10 and a 10 ms duration, and a "constant vibration" with a relative magnitude of 6 out of 10 and a duration of 45 ms. To quantitatively characterize these vibrations, we directly measured the vibration of the screen using a Conoprobe Mark 3, (Optimet Optical Metrology Ltd., Jerusalem, Israel), a conoscopic holography-based system which uses a laser to obtain highly accurate distance measurements. Because the screen vibrates laterally, we used vinyl cling and tape to attach

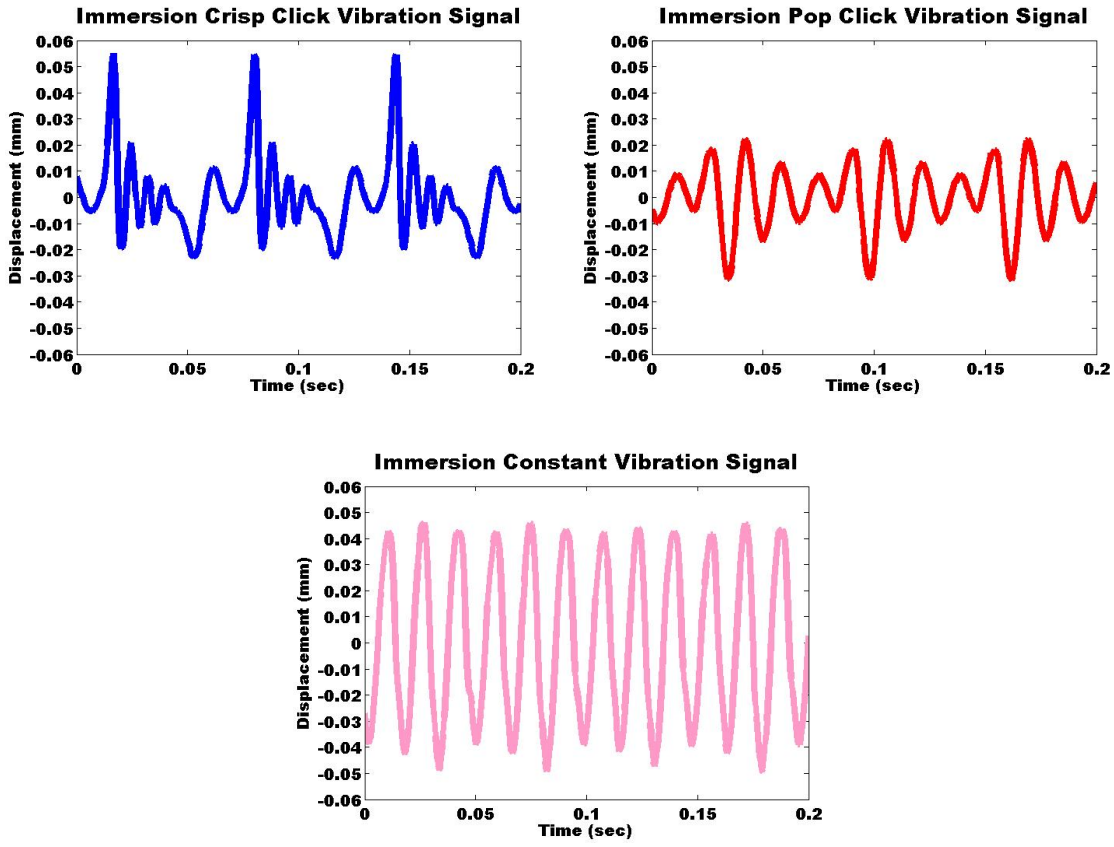

Figure 3.2: Conoprobe measurements of TouchSense Demonstrator vibrations: crisp click, pop click, and constant vibration, used in later user studies.

a lightweight, hollow plastic rectangle on the surface of the screen. We then aligned the Conoprobe with the laser pointing parallel to the touchscreen at the rectangle. To ensure that we were capturing vibrations that included the effects of finger-screen interaction, we touched the screen lightly with a fingertip and commanded the various vibration sensations described above. Plots of the resulting vibrations are shown in Figure 3.2.

These signals are similar in frequency and differ from one another in amplitude and pattern of vibration. They were selected from among the many sensations available as a set that produced distinctly different sensations, but no rigorous testing was conducted to determine which of the many sensations (and levels of sensation) available on the TouchSense

Demonstrator were optimal. It is also worth noting that sighted individuals seem drawn to vibrations of maximum amplitude (at least in initial testing), while blind subjects tend to prefer more mild vibrations, suggesting that the strong vibrations saturate their sense of touch and produce a similar sort of mild discomfort as might be felt by a sighted individual who suddenly walks from a dim room outdoors into full sunshine.

3.2.4 Haptic and Aural Exploration Software

Our software uses Immersion's TouchSense API and consists of a multi-threaded C++ application built on the open-source user interface (UI) framework Qt (Nokia, Oslo, Norway). The program contains two modes. The first, (*Explore Mode*), enables users to explore touchscreen content while receiving haptic and/or auditory feedback. The second, (*Sketch Mode*), enables the user to create a new drawing for later exploration. In these modes, users can interact or draw with lines of different "colors" which are represented by different haptic sensations and/or auditory tones, in much the same way that a teacher might draw on a chalkboard using different colors of chalk, or on a whiteboard with different marker colors. This software was adapted to the Galaxy Tab as an Android 2.2.1 application.

3.3 Experimental Methods

The Immersion touchscreen was used in two user studies to explore the feasibility of touchscreen display of basic graphical math concepts. The first study (Section 3.4) was designed to evaluate whether users could find desired Cartesian (x,y) locations and could identify points on a grid. The second study (Section 3.5) evaluated whether users could differentiate between shapes and lines of varying slopes. These exercises were chosen because they

Figure 3.3: A user interacting with the touchscreen during the user studies. The user was able to touch the screen, but not view it, and the user's ears were shielded to prevent auditory feedback from touchscreen actuators during haptic experiments.

represent some of the first graphical concepts taught to children, and they are generally presented visually. Points and lines are typically introduced at the beginning of algebra (6th or 7th grade) and are considered fundamental concepts [83]. Our experiments were designed to evaluate both haptic and auditory feedback and combinations of the two.

The user studies were first performed on sighted individuals (N = 10, mean age 27, two left-handed, two female). The studies were completed in two sessions conducted within 1 to 5 days (mean = 1.8 days) of one another, with an average session time of less than one hour. Half of the users were randomly assigned to perform the haptic grid session first, and the other half performed the auditory grid session first. In each session, users navigated

to desired (x,y) locations (Section 3.4.2), and then identified and located both haptic and auditory points that were displayed (Section 3.4.3). In the session with the haptic grid, subjects then performed the shape/line discrimination experiment (Section 3.5) with haptic feedback. Similarly, in the session with the auditory grid, subjects performed shape/line discrimination with auditory feedback. When all haptic feedback was provided, users listened to background music of their choice and wore sound isolating earmuffs to mask the sounds of the touchscreen actuators. During portions that involved combined haptic and auditory feedback, users wore the earmuffs and listened to white noise. The earmuffs were not required during the purely auditory feedback portions of the experiments.

During all experiments, the touchscreen itself was shielded from the user's view by a box with an opening at the front, allowing them to touch the touchscreen without viewing it (Figure 3.3). Users were allowed to explore the screen using only one finger, since the touchscreen used did not support multiple points of contact simultaneously. If a user forgot this and touched the screen with more than one finger, the experimenter would remind the user to only use one finger for exploration.

3.4 Point/Coordinate Experiment

In this experiment, we sought to answer 3 questions: (1) Can users navigate to a given (x,y) location on a grid, (2) Can users find displayed points on a grid, and (3) Can users determine the (x,y) location of these points on a grid.

3.4.1 Experimental Setup and Grid Display

To investigate these questions, we created figures in Matlab (MathWorks Inc., Natick, MA, USA) of 7×7 grids, both with and without points on them, as shown in Figure 3.4. The total grid area was 157.5 mm wide (x) × 126 mm tall (y), meaning that each physical grid unit was 19.5 mm (x) × 15 mm (y). Grids that contained points contained two points located randomly at grid intersections. Points were displayed as 22.5 mm diameter circles.

In order to help the user discriminate between the grid lines, all of the horizontal grid lines were displayed using one haptic or auditory effect, and all of the vertical grid lines were displayed using a different haptic or auditory effect. The horizontal grid lines were displayed using a crisp click in the haptic session, and a repeating beep of 400 Hz with a duration of 100 ms in the auditory session. The vertical grid lines were displayed using a pop click in the haptic session, and a repeating beep of 500 Hz with a duration of 50 ms in the auditory session. The frequency and amplitude of vibration for both of these signals is shown in Figure 3.2. We note that the haptic and audio effects repeated as long as the user's finger was on the line, enabling them to trace or stop along a line and continue to receive feedback. Both vertical and horizontal grid lines had a thickness of 3.5 mm.

To remove ambiguity exactly at grid intersections, no effect was displayed, as shown by the small white boxes at the intersections in Figure 3.4. To ensure that users had a fixed reference for where the grid was located on the screen at all times, we attached thin strips of transparent vinyl cling around the perimeter of the grid (each 3.5 mm thick), and placed a circle (12.5 mm in diameter) of the vinyl cling at the origin, as illustrated by the black lines and circles in Figures 3.4 and 3.5.

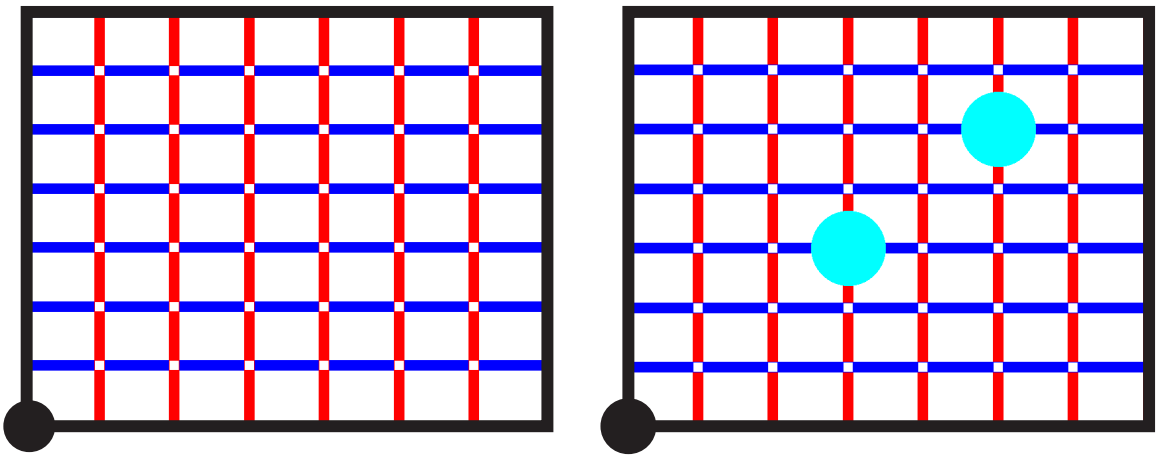

Figure 3.4: Examples of the information displayed to the user in the Point/Coordinate Experiment. The black lines and circle represent the vinyl cling attached to the screen to create raised physical borders and an origin for the grid. (Left) A blank grid. (Right) A grid with two points displayed.

3.4.2 Finding a Desired Grid Intersection

To determine whether users could find a desired coordinate location on the grid, we conducted the following experiment. We introduced users to the grid with an initial training period where no data was recorded. During this period, they were first allowed to explore only vertical grid lines and then only horizontal grid lines. In both cases, they were verbally told what was being displayed, and they were allowed to explore it for as long as they liked. Next, both vertical and horizontal grid lines were displayed together as the complete grid, and users were instructed to familiarize themselves with the grid and determine the number of units in the x and y directions. During this part of the training, the experimenter provided verbal feedback to the user on whether or not the grid size was determined correctly. If the user did not correctly identify the grid size, the experimenter provided verbal assistance as

necessary until the user determined the grid to be 7×7. These training procedures were designed to introduce subjects to the device and were conducted in the same way for each subject.

Next, the user was given a specific (x,y) location verbally and was instructed to find it on the grid, as shown in Figure 3.4 (Left). Between one and three practice trials were performed until the user was comfortable with the task. During practice, users received verbal feedback on whether or not they reached the correct location and were told what location they had actually reached if they had reached an incorrect location. The location reached was identified as the closet grid intersection to the user's position when the user verbally indicated that he/she believed the desired location had been reached. After the practice trials were completed, three trials were performed in which the experimenter provided no feedback or assistance and recorded whether the correct or incorrect final location was achieved.

Results of this coordinate finding experiment are shown in Table 3.1. The mean and standard deviation of the correct number of locations (out of 3) found by sighted users on both the haptic and auditory grids are presented. From these results, we can see that users were able to reach the correct location over 66% of the time using haptic and auditory feedback. To determine if there was a significant difference between the haptic grid and auditory grid for sighted users, we performed a Wilcoxon Signed Rank Test with continuity correction ($\alpha = 0.05$) and obtained a p-value of 0.68. This suggests that there was no statistically significant difference between sighted user performance with haptic versus auditory grids in our experiment.

Table 3.1: The mean and standard deviation (σ) of the correct number of locations (out of 3) reached by sighted users for the grid intersection location portion of the Point/Coordinate Experiment.

	Haptic Grid	**Auditory Grid**
Mean	2.30	2.10
σ	0.82	0.88

3.4.3 Identifying a Displayed Point

After the user had finished finding specified grid intersections (with no points displayed), points were added to the grid as shown in Fig. 3.4 (Right), and users were asked to identify and determine the locations of these points. Point locations were chosen randomly within (but not on the borders of) the grid. Points were displayed with constant vibration or a repeating beep of 600 Hz with a duration of 275 ms. The frequency and amplitude of the constant vibration is shown in Fig. 3.2.

At the beginning of this experiment, a short training session was conducted to familiarize the user with the method of displaying points. Two points were displayed without the grid, before presenting the two points together with the grid. In both cases, the user was able to explore the screen for as long as they liked. Then, the user was asked to find the points and determine their locations on the grid. One or two practice trials were completed to ensure the user understood the task. During the practice trials, users received verbal feedback and assistance as needed. After this training procedure, the experiment

Table 3.2: The mean and standard deviation (σ) of the number of displayed point locations correctly identified (out of 6) on the grid by users. The H stands for haptic, with A for auditory; the first letter in a pair denotes the grid, and the second the points.

	H,H	**H,A**	**A,A**	**A,H**
Mean	5.4	5.30	5.00	5.30
σ	1.07	1.06	1.63	1.06

commenced, and three trials were performed, during which the experimenter provided no verbal feedback. In the experiment, subjects identified and determined the location of 6 total points, presented two at a time. This process was done for both haptic and auditory points in both the haptic grid session and the auditory grid session.

All users were able to find all of the points successfully, regardless of the feedback mode of the points or the grid. Thus, a total of 240/240 points (10 subjects $\times$ 6 points $\times$ 4 cases) were found. Results for the correct number of (x,y) locations determined by the users are shown in Table 3.2. We observe that 80% of the users determined the correct location for at least 5 of the 6 points. Typical errors involved miscounting either horizontal or vertical grid lines by one unit. We note, however, that the highest scoring user was not the same user in each feedback case. To determine whether any conclusions can be drawn from this data about which combination of haptic and audio feedback is optimal, we performed a Wilcoxon Signed Rank Test with continuity correction for all possible feedback cases, but found no statistically significant differences at the $\alpha = 0.05$ level.

3.4.4 Point/Coordinate Experiment Discussion

Users were able to locate the correct grid intersection with no displayed points over 66% of the time, which was consistent for both haptic and auditory feedback. When points were displayed on the grid, users found 100% of the points, and 80% of the users correctly determined at least 5 out of 6 coordinate locations of those points in all feedback cases. Taken together, these results indicate that much of the desired information was successfully conveyed to the subjects. While the true test of whether these numbers are sufficient will be the development and use of various mathematics lesson plans, with an evaluation of learning outcomes, they are encouraging. Further, though the grid used in the above experiments was 7×7, it is likely that this grid could be scaled up to a larger size, containing smaller grid units or containing major and minor grid units. Determining an optimal grid layout requires further psychophysical tests investigating parameters such as grid line spacing and line width.

The lack of statistically significant differences between auditory and haptic feedback suggests that for simple mathematical shapes, both information channels may be valuable. These results agree with the mixed user preference results for haptic vs. auditory feedback found in [74]. It has also previously been noted by Yu et al. that multimodal (haptic and auditory) representation can enhance a user's ability to interpret graphs using a force feedback device in some cases [100]. In our study, personal preference indicated by users for haptic vs. auditory feedback was highly variable, as was the strength of the preference. User preference in a post-study questionnaire was highest for combined feedback where a haptic grid and auditory points (or vice versa) were used, rather than the use of solely

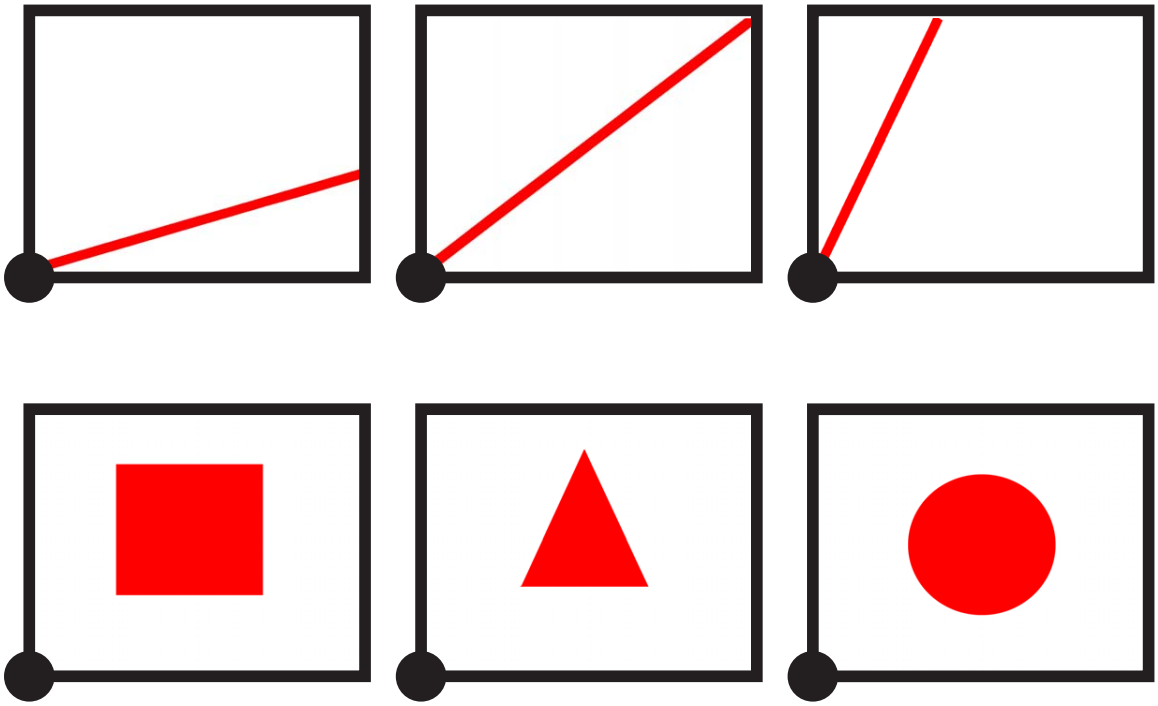

Figure 3.5: The figures displayed on the touchscreen in the Shape/Line Discrimination Experiment.

haptic or solely auditory feedback.

3.5 Shape/Line Experiment

In this portion of our experiments, we explored the following questions: (1) Can users differentiate between shapes and lines, (2) Can users determine the general slope of a line, and (3) Can users perceive different shapes. To investigate these questions, we created lines (5 mm thick) with slopes of 22.5°, 45°, or 67.5° as well as a solid square, triangle, and circle (see Fig. 3.5). All of the shapes were approximately the same size and were located at the center of the screen. No grid was displayed with any of these figures, but the vinyl cling axes and origin remained on the screen, affixed as previously described.

These objects were presented to each user in random order. The user then explored the screen and verbally classified them, with lines classified as less than, greater than, or equal to 45°. Objects were presented using haptic feedback during the haptic grid session described in Section 3.4, and auditory feedback during the auditory grid session described in the same section. The type of haptic or auditory feedback (magnitudes, durations, tones, etc.) were the same as those used for the vertical grid lines in the Point/Coordinate Experiment. Users first completed 1-2 practice trials, in which they were given verbal feedback on whether their answer was correct or incorrect and were told the correct answer if they responded incorrectly. The experiment then commenced, and each user completed 12 trials (two of each image), during which no verbal feedback was provided by the experimenter. Users were not told how many objects would be presented or that each image option would be presented twice.

Experimental results are shown in Table 3.3. With both haptic and auditory feedback, we observe that users were able to differentiate lines from shapes and lines from other lines more accurately than shapes from other shapes. A Wilcoxon Signed Rank Test with continuity correction suggests a significant difference between the correct number of lines and shapes identified in both cases (haptic p-value=0.01 with 95% confidence interval: (1.5, 3.0), auditory p-value=0.02 with 95% confidence interval: (1.5, 3.5)). There were not, however, significant differences between haptic lines and auditory lines or haptic shapes and auditory shapes at the $\alpha = 0.05$ level.

Table 3.3: The mean and standard deviation (σ) of the correct number of lines and shapes (both out of 6) correctly identified by sighted users for both haptic (H) and auditory (A) feedback in the Shape/Line Experiment.

	H Lines	**H Shapes**	**A Lines**	**A Shapes**
Mean	5.80	4.00	6.00	4.20
σ	0.42	1.15	0.00	1.55

3.5.1 Shape/Line Experiment Discussion

These experiments indicate that users are able to distinguish lines from shapes with high accuracy, and similarly differentiate between the three slope conditions of the lines. It was more challenging for users to discriminate filled-in shapes from one another. We suspect that shape identification was more challenging partly due to some users employing ineffective exploratory procedures (no specific exploratory procedure was suggested or prescribed in our experiments). Successful users often employed a search for corners, but not all users realized that corners were a good way to differentiate between different shapes. Also, user survey feedback indicated that it might be useful to enable the user to "mark" features or locations to which they wished to return later (e.g. the locations of corners of a shape). Making the touch screen interactive in this way is straightforward and is a promising direction for future development.

3.6 Pilot Studies with Blind Students

To determine whether blind students (Fig. 3.6) would enjoy interacting with the touch-screen and achieve performance levels comparable to the sighted users in our experiments in Sections 3.4 and 3.5, we conducted the following study. Three visually impaired students (mean age 17, one left-handed, two female) were recruited from the Metropolitan Nashville Public School System under a Vanderbilt University Institutional Review Board approved protocol, with approval from the relevant school system administrators, teachers, and parents. These students completed the same studies, using the same experimental setup, training, and protocols, described in Sections 3.4 and 3.5. The time between user studies spanned from 2 to 15 days, depending on students' school schedules and availability.

Table 3.4 shows results of the grid intersection location experiment (Section 3.4.2). The students were able to reach the correct location over 66% of the time using haptic and auditory feedback, which is comparable to the results obtained by sighted users. We also note that each time users missed the correct location, they were only off by one unit in either the x or y direction. Further, we observe that 2 of the 3 users successfully located all of the correct grid locations, with one user finding all 3 locations using both the haptic and the auditory grid. In post-experiment questionnaires, all blind users rated the ease of navigating on the haptic and audio grids as a 3 or higher (on a scale from 1 to 5 with 1 being very difficult and 5 being very easy).

In identifying displayed points (Section 3.4.3), as with sighted subjects, all blind students were able to successfully find 100% of the points displayed, regardless of the feedback mode. Results are shown in Table 3.5. The most promising result from this experi-

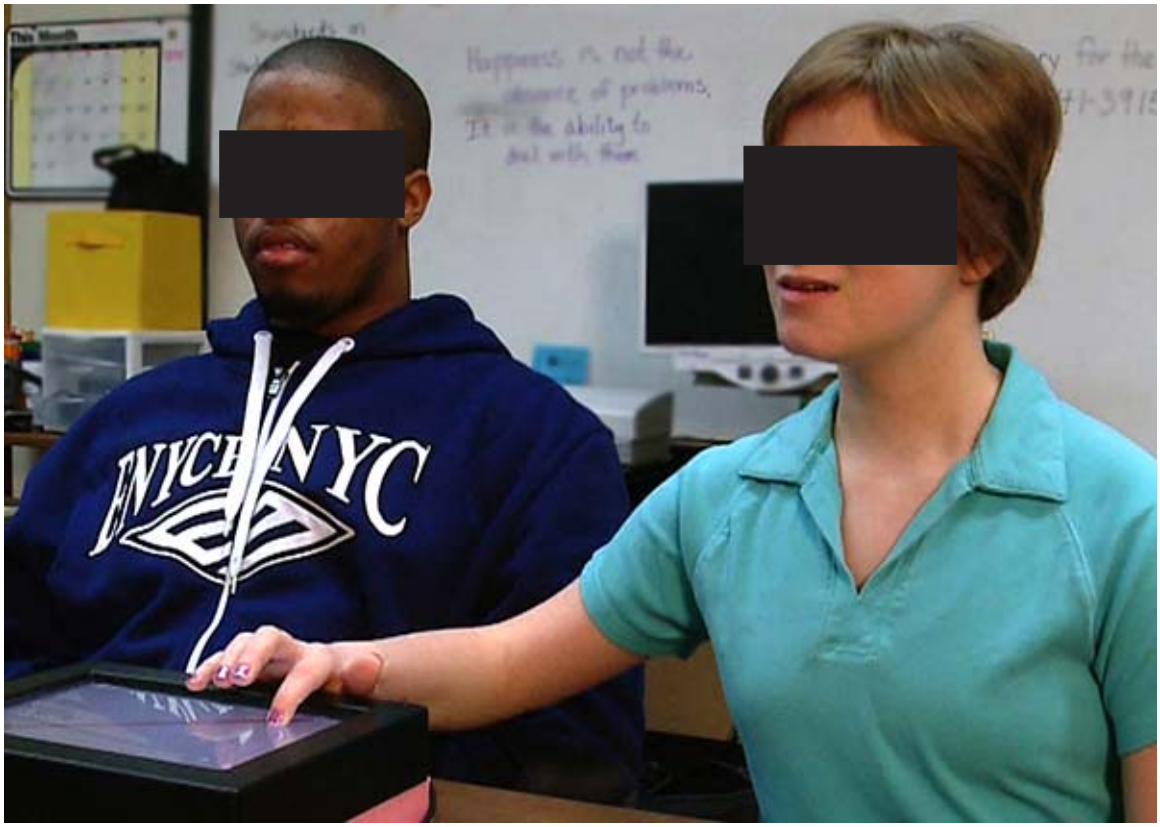

Figure 3.6: Two blind students using the Immersion touchscreen during a visit (but not an actual user study) at the school.

ment is that every user correctly located all of the points in at least one of the four cases presented, suggesting that users can find and locate points on the grid using the feedback provided. In post-experiment questionnaires, blind users, like sighted users, rated the ease of finding points on the grid highest for combined feedback (with an average rating of 4 on a scale from 1 (very difficult) to 5 (very easy)), rather than for pure haptic or pure auditory feedback. We also note that in the combined case of an auditory grid with haptic points, 2 of the 3 users found all 6 point locations. These results, accompanied by interviews with blind users, lead us to believe that a combination of haptic and audio cues will likely be more valuable than either stimulus in isolation. Providing users with the ability to per-

Table 3.4: The correct number of locations reached by blind users (out of 3) in the grid intersection location portion of the Point/Coordinate Experiment (Section 3.4.2).

	Haptic Grid	**Auditory Grid**
User 1	2.00	3.00
User 2	2.00	2.00
User 3	3.00	3.00
Mean	2.33	2.67

sonalize their touchscreen and choose their desired feedback is a feasible path forward in widespread deployment of a touchscreen platform.

Blind users also performed the Shape/Line Experiment (Section 3.5), with results shown in Table 3.6. As with sighted users, blind users were able to differentiate lines from shapes and lines from other lines more accurately than shapes from other shapes. Two of the three users were also able to correctly identify all of the lines in both the haptic and auditory cases, and the remaining user was able to correctly identify all of the lines in the auditory case. On average, the users rated the ease of discriminating lines and shapes as 3.33 (on a scale from 1 (very easy) to 5 (very difficult)) for both haptic and auditory feedback. As with sighted users, differentiating solid shapes from one another was more challenging, with some users doing well and some doing poorly. We hypothesize this variability in performance may be at least partially due to a variability in exploratory procedures used (as mentioned in Section 3.5.1). Despite challenges, however, blind users still expressed excitement at the possibility of using the touchscreen for learning shapes. Several suggestions

Table 3.5: The number of displayed point locations correctly identified (out of 6) on the grid by blind users in the Point/Coordinate Location Experiment (Section 3.4.3). The H stands for haptic, with A for auditory; the first letter in a pair denotes the grid, and the second the points.

	H,H	**H,A**	**A,A**	**A,H**
User 1	5.00	3.00	6.00	6.00
User 2	4.00	6.00	3.00	2.00
User 3	5.00	3.00	5.00	6.00
Mean	4.67	4.00	4.67	4.67

from blind users were obtained to make shape identification easier, including only showing the shape border or using different types of feedback for the shape border and the shape fill.

3.6.1 Participant Feedback

One of the more interesting qualitative observations from these studies was the rapid rise in enthusiasm for the touchscreen from both students and teachers during our experiments. While the teachers and students began the experiments neutral or even mildly doubting the effectiveness a touchscreen might have in our intended application, by the end of the study, all expressed a great deal of enthusiasm. One blind student commented, “At first, I didn’t think this would help me, but after I started using it I found that it can be very helpful.” Another reflected, “The biggest obstacle was getting the correct mental images. However,

Table 3.6: The correct number of lines and shapes (both out of 6) correctly identified by blind users for both haptic (H) and auditory (A) feedback for the Shape/Line Experiment (Section 3.5).

	H Lines	**H Shapes**	**A Lines**	**A Shapes**
User 1	6.00	3.00	6.00	2.00
User 2	6.00	4.00	6.00	4.00
User 3	2.00	0.00	6.00	0.00
Mean	4.67	2.33	6.00	2.00

once you get the knack, it gets fairly easy." The students also indicated that they would have great motivation to use such a device if it were available, because it would enable them to interact with the rest of the class in a similar manner to sighted students and not require a dedicated instructor for each student. In the words of one blind student, "It would really help to have something like this because it makes us equal to everyone else."

Similar excitement was evident in the teachers who work with the visually impaired students who participated in our study. One teacher observed, "One of these haptic tablets would allow them [the students] to keep up much better [in class]. If I didn't have to attend class with them, it would also make them feel more independent." The teacher also pointed out that since the touchscreen is capable of simultaneous visual, auditory, and tactile feedback, it could be used by students with varying degrees of visual impairment, since there is a large population with partial blindness. The teacher summarized her reflection on the experiments as follows: "When [the researcher] first approached me with the idea, I thought

it would be interesting and might be some small help. The more experience I have with it, the more valuable I think it could be. It makes the work more accessible."

3.7 Conclusions and Future Work

In this chapter, we have taken initial steps in exploring the feasibility of a new touchscreen-based teaching paradigm for math education for visually impaired students, enabled by the recent mass market introduction of low-cost, robust, and portable, vibration-capable touchscreens. The potential benefits of this new paradigm include a reduction in teacher workload, an increase in the timeliness with which graphical information can be presented to a visually impaired student in the classroom, and the ability to include visually impaired students into traditional classrooms with their sighted peers in a streamlined and interactive way that does not draw attention to the disability.

We performed user studies with sighted and blind individuals, toward verifying that vibration feedback and combined vibration/auditory feedback can convey "building block" graphical mathematical concepts from which more complex lessons can be constructed. We first evaluated the ability of users to understand and make use of grids, and find points using them. While users did not achieve perfect performance (sometimes miscounting grid lines), the facts that all users found all points displayed and that they correctly identified their locations a high percentage of the time are encouraging. Further, there are several enhancements that can be made to make grid navigation and point location easier, including aural feedback informing the user which grid line he/she is on or having every *Nth* grid line provide a different type of feedback, where N is the major incremental unit on the graph. Similarly encouraging was the fact that users were always able to distinguish lines from

shapes, and that they were able to select between three slope options correctly a high percentage of the time. The fact that users could not easily distinguish between filled-in shapes indicates that if the screen is to be used for teaching basic shapes, further study is needed investigating whether outlined shapes, new interaction modes (e.g. enabling users to mark positions to return to later), prescribed exploratory procedures, or alternate haptic/audio effects will be able to increase performance.

However, we note that user performance using a touchscreen display need not be perfect to achieve educational benefit, just as a chart or graph displayed on a noisy or dim projector or monitor may still have educational value – particularly when combined with verbal descriptions. We also note that our studies were not designed to investigate learning curve effects (nearly all experiments were done at time of first user experience with the touchscreen), but there is reason to believe that experience will result in improved performance, as indicated via qualitative feedback from blind students. Another positive factor is that the manner of feedback need not be the same for each user. If a particular user prefers (and performs better with) all haptic feedback, they can set the device to provide it, and similarly with the user who prefers all auditory feedback. Our initial studies and qualitative feedback from users indicate that mixtures of haptic and auditory feedback are best from a performance point of view, which is in agreement with previous studies [100], and with the intuition that taking advantage of a rich a set of input sensations into the human user will enable more information to be conveyed. Lastly, we note that in our initial feasibility studies, we have experimented only with a few, qualitatively selected, vibration signals where the screen surface vibrates along its own plane.

Many other vibration modes and directions are possible, including variable friction

from high frequency vibrations [26] (as discussed in Chapter 4), electrostatic displays [17], and displays actuated via piezoelectrics [55, 57], to name a few. Much psychophysical research remains to be done in this new field of surface haptics, and any new advancements will be beneficial within the education paradigm we have proposed in this chapter. Thus, we believe it is noteworthy that one of the first vibratory touchscreens available (the Immersion TouchSense Demonstrator), with qualitatively selected haptic sensations and beginner users, was capable of conveying many of the initial "building block" mathematical objects presented in our user studies.

There are several pathways forward in this work. In parallel with doing further psychophysical studies, and investigating the use of novel surface haptics technologies in this application as they arise (see Chapter 4), we intend to work with teachers to develop specific math lessons that make use of the touchscreen. These will enable us to evaluate outcomes, comparing the learning benefits of the device and associated lessons against control groups of students taught the same concepts using traditional methods. Intrinsic to this will be exploring different classroom dynamics and information flow paths with a system of networked tablets, drawing upon the literature already available for networked laptop and tablet-based classroom paradigms. Also important will be the construction of a large library of devices and software, which will involve the ongoing evaluation of new surface-haptics-capable screens for this application as they are brought to market, and the establishment of an open-source lesson and code base for developers and teachers. The availability of app stores for mass market release of various educational software modules is expected to facilitate the dissemination of the concept and educational modules developed.

In summary, we believe that touchscreens hold great potential for enhancing educa-

tion in various ways. Sighted students may benefit from interactive modules involving visual touchscreens, visually impaired students will likely benefit from screens that provide touch and/or auditory feedback, and students who are both blind and deaf may benefit from purely haptic touchscreens. Achieving these potential benefits on a large scale will require advancements in display technology, a better psychophysical understanding of user-touchscreen interaction, and purpose-designed educational materials that take advantage of the capabilities provided by touchscreens. Given their many potential uses in education, as well as the rapidly expanding variety and capability of modern touchscreen technology, touchscreens appear poised to become powerful educational tools in the near future.

Chapter 4

Modeling and Experimental Validation of Variable Friction Touchscreens

With touchscreens only recently becoming widely used, there is still much to be understood in terms of designing their interfaces and incorporating appropriate feedback into them. Because touchscreens themselves are a new technology, the exploration of providing haptic feedback from touchscreens is still in its infancy. There are only a few haptic touchscreens currently available (though they are rapidly becoming more common), despite the large number of commercially available touchscreens. In Chapter 3, we explored the potential of two commercially available tactile touchscreens in teaching math to blind students.

This chapter focuses on a novel technology for providing enhanced tactile feedback from a touchscreen platform, which has the potential to enrich the information that can be conveyed to the user. There are several challenges associated with developing tactile touchscreens, including the additional expense of incorporating actuators into a touchscreen to create tactile feedback and the design challenges associated with adding these actuators and electronics into the already very limited space available. Further, while current tactile effects can convey a great deal of information, they tend to lack a sense of realism [58]. Another way to describe this is that touch interactions with most current devices are "flat," meaning that all interface objects still feel like the same plastic or glass of the touch surface itself [58]. Thus, the exploration of novel actuation techniques and new methods for providing haptic feedback from a surface are worthy endeavors that will likely serve as a springboard for wider adoption of haptic feedback into touchscreens.

Toward exploring the possibilities of enhancing touch interaction with surfaces, this

chapter focuses on a new class of touchscreens called variable friction displays, that rely on surface haptics [26, 60]. These surfaces, often thin glass plates, use ultrasonic vibrations to modulate friction on the surface of the plate. This friction modulation enables users to perceive various textures and levels of low or high friction, with the potential to provide users with a sense of realism that current tactile touchscreens lack [58]. In this chapter, we discuss the current state of variable friction touchscreens and explore the theoretical principles by which they operate. We model ultrasonic plate vibrations based on plate and piezoelectric interactions. This model enables prediction of plate displacements (which correspond to friction level) at every point on the plate as a function of the number of piezoelectric actuators and their placement on the plate. Additionally, the model faciliates design optimization of variable friction displays. With a physical prototype, we experimentally validate our model predictions. We then present design guidelines and recommendations for the future development of variable friction displays. These studies form a theoretical foundation for realizing the potential of variable friction displays and surface haptics in providing a more realistic user-touchscreen interaction. The work presented in this chapter will be submitted for publication in the *IEEE Transactions on Haptics*.

4.1 Introduction

Touchscreens are becoming increasingly commonplace, changing the way users interact with information displayed on a screen. What once required the push of a physical button or the click of a mouse, now requires a simple finger tap. While touchscreens have enhanced users' ability to quickly and conveniently access information, they have replaced physical interactions with simple touch-based gestures. Toward reviving the tactile sensation of

these physical interactions and providing a more engaging user experience, there has been recent interest in incorporating haptic feedback into touchscreens (see e.g. [14, 16, 19, 26, 46, 68]). This haptic feedback (typically vibratory) is designed to enable users to "feel" virtual objects displayed on screen, to improve their performance on tasks such as data entry [50] and target acquisition [13, 58], and to enable them to complete tasks more efficiently [57, 67]. An overview of the advantages of haptic and tactile feedback can be found in [27].

There are several challenges associated with incorporating haptic feedback into touchscreens. First, as touchscreens become thinner and more portable, there is less room available for the actuators needed to generate this tactile feedback. Second, even in this small form factor, the tactile feedback provided must have high enough fidelity that it convincingly creates sensations the user finds helpful. Finally, haptic touchscreens must be able to quickly adapt and respond to the user's input, which is constantly changing. Despite these challenges, there have been several actuation methods developed to create tactile feedback in touchscreens. These include the use of vibration motors, piezoceramics [57], dielectric elastomers [15], and electrostatics [17]. The latter is an innovative approach that requires no mechanical components, but instead, uses periodic electrostatic forces to create sensations of vibrations or friction [17].

Variable friction devices [26, 60, 81, 98] are an alternative class of haptic surfaces that create the illusions of textures or surface features on the fingertip by controlling the lateral forces applied to it. In [98], friction between a thimble (which the user rests their finger in) and the display itself was varied using electrostatic forces. A similar setup was used in [81], but friction modulation was achieved via surface acoustic waves. The first variable friction device capable of controlling surface roughness on a bare finger was developed by

Watanabe and Fukui [90] using an ultrasonic vibrating steel plate.

More recently, pioneering work on surface haptics (i.e. variable friction displays created by surface vibration) [26,58,60] has been done by Colgate and Peshkin and their associates. Their approach uses piezoelectrics to vibrate a glass plate at ultrasonic frequencies, which are audibly imperceptible to users. Thin glass plates are used because they are transparent, enabling them to be integrated with existing LCD displays. Piezoelectric actuators are appealing because they have a small form factor, enabling an increase in screen surface area without a large increase in overall size. When the plate is actuated in the 20-40kHz range, resonant modes of the plate are excited, which create modal shapes on the plate surface. These modal shapes are defined by nodal lines, locations on the plate at which the displacement is zero. On these nodal lines, users perceive the surface to have a higher coefficient of friction. Off of these nodal lines, however, a thin film of air, called a squeeze film, is created between the plate and the finger, reducing the friction of the surface perceived by the user. By turning plate vibrations on and off, areas of high and low friction, resembling textures, edges, or other surface features, can be perceived by the user. Recently, Marchuk et al. constructed the LATPaD (Large Area Tactile Pattern Display), a $3" \times 3" \times 0.125"$ glass plate actuated by a single 0.5mm piezoelectric disk [60]. Surface friction maps were created for four resonant plate modes, and a combination of these maps was used to take advantage of the low friction areas in all of the modes. User studies with the LATPaD show that the programmable friction interface enhances user performance on targeting tasks and provides users with increased engagement [58].

4.1.1 Contributions

To date, the design of these variable friction touchscreens has largely been ad hoc, focusing on functionality and feasibility of the device as opposed to a generalizable design approach. Toward better understanding the modal responses of these surfaces and providing a tool to guide the design of these touchscreens, we present a comprehensive model, simulation, and experimental validation of variable friction touchscreens. We model the coupled system of the plate and the piezoelectric, accounting for the electromechanical coupling effects between the two. Our simulation enables modal shape prediction of variable friction touchscreens of any size, with any number and location of piezoelectric actuators. We validate our simulation experimentally, demonstrating its effectiveness in multiple scenarios. The simulation enables quick prediction of nodal line placement on the surface and can be used in guiding the design of variable friction touchscreens.

In the sections that follow, we first present a derivation of the coupled system model (Section 4.2) used in our simulation. We then present our simulation environment, a discussion of boundary conditions, and two physical prototypes of a variable friction surface we constructed, which are similar to the LATPaD [60] but contain newly designed boundary constraints, in Section 4.3. Two experiments validating our simulation are presented and discussed in Section 4.4, and two experiments showing the flexibility of the simulation under changes in parameters are presented in Section 4.5. This is followed by a discussion of our findings and and of future steps in enabling optimized designs of variable friction surfaces (Sec. 4.6). The chapter concludes in Section 4.7.

4.2 Modeling of Coupled System

In this section, we present the coupled model of our plate and piezoelectric system, following the method proposed by Hagwood et al. [45]. The model is based on a generalized form of Hamilton's principle for coupled electromechanical systems. While one could model the plate alone, using Kirckhoff-Love theory for thin plates, this would not account for the coupling between the plate and the piezoelectric actuator(s) nor the additional mass and stiffness of the piezo actuator(s) (which could become significant when multiple actuators are used). For this reason, we chose to model the plate and the piezoelectric actuators as a coupled system. First, we discuss the assumptions of our model before presenting the governing equation of the coupled system. We then define each of the parameters within the coupled system equation for our system. Finally, we present the state space representation of our model which is used in developing the plate simulation.

4.2.1 Assumptions

The first assumption is that our plate is square and "thin," the latter of which is based upon the criteria proposed in [88]. Here, a plate is considered thin if $8 \leq a/h \leq 100$ where a is the plate length in either dimension and h is the plate thickness. In our case, this ratio is 24, putting it within the thin plate realm. We also assume our boundary conditions reflect a simply supported plate (see Section 4.3.2 for further discussion on boundary conditions). We also adopt the assumptions associated with the Kirchhoff-Love theory for thin plates [88], which include:

- The plate material is elastic, homogeneous, and isotropic.

- The plate is initially flat.
- The deflection of the mid plane is small compared with the thickness of the plate.
- The straight lines initially normal to the mid plane before bending remain straight and normal to the mid plane during deformation, and the length of such elements is not altered.
- The stress normal to the mid plane is small compared with the other stress components and may be neglected in the stress-strain relations.
- Since the displacements of a plate are small, it is assumed that the mid plane remains unstrained during bending.

There are additional assumptions included in the coupled model as stated in [45]. Briefly, these assumptions include that the entire system remains an elastic body, the dynamics of the piezo element are dervied using a Rayleigh-Ritz formulation and adhere to the assumptions associated with it, the electric field is constant throughout the thickness of the piezo element, the forces from the piezoelectric actuator act as discrete, external point forces, and the voltages of all of the piezoelectrics are either zero or some other value as a function of time. Assumptions of the piezoelectric actuator itself, in terms of poling directions and electric fields, are also stated in [45]. Additionally, we assume that our piezoelectric actuators are square, which is a valid assumption even though our experimental actuators are circular because the discrepancies in overall surface area are small.

4.2.2 Plate and Piezoelectric Actuator Model

The governing equation of our coupled system, as derived in [45], is

$$(M_s + M_p)\ddot{q}_{mn} + (K_s + K_p)q_{mn} = \Theta v, \tag{4.1}$$

where M_s is the structure (plate) mass matrix, M_p is the piezo mass matrix, K_s is the plate stiffness, K_p is the piezo stiffness, Θ is an electromechanical coupling matrix, v is a voltage input to the piezo, $q_{mn}(t)$ is the plate displacement in the *generalized* coordinates, and m and n are the x and y indices of the modal pair, respectively.

We now mathematically define the quantities in Equation 4.1 in the general case and then in the simply supported case, since that it is our assumed boundary condition. First, we define a few intermediate variables that appear often in the equations below. V is the volume, ρ is the density, h is the thickness, Y is Young's Modulus, and ν is Poisson's Ratio, and a subscript s or p on any of these terms indicates the plate or the piezo, respectively. Further, a and b are the plate length in x and y respectively, $\phi_{mn}(x,y)$ is the assumed mode shape function based on the boundary conditions, and p and r are the x modal indices represented as m, and q and s are the y modal indices, represented as n. In this work, we have chosen the boundary conditions to be simply supported on all sides of the plate (meaning that the position of the plate edges are fixed, but the slope of the plate at the edge is free). The simply supported mode shape function is defined as

$$\phi_{mn}(x,y) = sin(\frac{m\pi}{a}x)sin(\frac{n\pi}{b}y). \tag{4.2}$$

The structure mass matrix, M_s is defined as

$$M_s = \int_{V_s} \phi_{mn}(x,y)^T \rho_s(x) \phi_{mn}(x,y)\, \mathrm{d}V_s,$$
$$= \rho_s h_s \int_0^a \int_0^b \phi_n(x,y)\phi_m(x,y)\, \mathrm{d}x\mathrm{d}y, \tag{4.3}$$

For a simply supported plate, M_s becomes

$$M_s = \begin{cases} \frac{1}{4}ab\rho_s h_s & \text{if } p = r \text{ and } q = s; \\ 0 & \text{if } p \neq r \text{ and } q \neq s. \end{cases}$$

The structure stiffness matrix, K_s, is defined as

$$K_s = \int_{V_s} \phi_{mn}(x,y)^T {L_u}^T C_s L_u \phi_{mn}(x,y)\, \mathrm{d}V_s, \tag{4.4}$$

where L_u is the structural differential operator, expressed as

$$L_u = \begin{vmatrix} -z\frac{\partial^2}{\partial x^2} \\ -z\frac{\partial^2}{\partial y^2} \\ -2z\frac{\partial^2}{\partial x \partial y} \end{vmatrix}, \tag{4.5}$$

and C_s is the stiffness matrix, expressed as

$$C_s = \begin{vmatrix} \frac{Y_s}{1-\nu_s^2} & \frac{Y_s \nu_s}{1-\nu_s^2} & 0 \\ \frac{Y_s \nu_s}{1-\nu_s^2} & \frac{Y_s}{1-\nu_s^2} & 0 \\ 0 & 0 & \frac{Y_s}{1+\nu_s^2} \end{vmatrix}. \tag{4.6}$$

Substituting these quantities into Equation 4.4, we obtain

$$\begin{aligned} K_s = & \frac{Y_s I_s}{1-\nu_s^2} \int_0^a \int_0^b \frac{\partial^2 \phi_n}{\partial x^2} \frac{\partial^2 \phi_m}{\partial x^2} \\ & + \frac{\partial^2 \phi_n}{\partial y^2} \frac{\partial^2 \phi_m}{\partial y^2} + \nu_s \left(\frac{\partial^2 \phi_n}{\partial x^2} \frac{\partial^2 \phi_m}{\partial y^2} + \frac{\partial^2 \phi_n}{\partial y^2} \frac{\partial^2 \phi_m}{\partial x^2} \right) \\ & + 2(1-\nu_s) \frac{\partial^2 \phi_n}{\partial x \partial y} \frac{\partial^2 \phi_m}{\partial x \partial y} \, \mathrm{d}x\mathrm{d}y. \end{aligned} \tag{4.7}$$

where $I_s = \frac{h_s^3}{12}$, which is the moment of inertia of the plate.

For a simply supported plate, K_s becomes

$$K_s = \begin{cases} \frac{D_s b \pi^4}{4a^3} [p^2 + (\frac{a}{b})^2 q^2]^2 & \text{if } p = r \text{ and } q = s; \\ 0 & \text{if } p \neq r \text{ and } q \neq s. \end{cases}$$

We now define the piezo mass and stiffness matrices. To do this, we first define the following intermediate variables:

$$s_1^{\zeta\pm} = \left| \frac{\zeta}{2} \pm \frac{sin(2p\pi\zeta)}{4p\pi} \right|_{\zeta_1}^{\zeta_2} \tag{4.8}$$

$$s_1^{\eta\pm} = \left| \frac{\eta}{2} \pm \frac{sin(2q\pi\eta)}{4q\pi} \right|_{\eta_1}^{\eta_2} \tag{4.9}$$

$$s_2^{\zeta\pm} = \left| \frac{sin(p-r)\pi\zeta}{2(p-r)\pi} \pm \frac{sin(p+r)\pi\zeta}{2(p+r)\pi} \right|_{\zeta_1}^{\zeta_2} \tag{4.10}$$

$$s_2^{\eta\pm} = \left| \frac{sin(q-s)\pi\eta}{2(q-s)\pi} \pm \frac{sin(q+s)\pi\eta}{2(q+s)\pi} \right|_{\eta_1}^{\eta_2}, \tag{4.11}$$

where $\zeta = \frac{x}{a}$ and $\eta = \frac{y}{b}$, and x_1, x_2, y_1, y_2 are the x and y edges of the piezo element, respectively.

The piezo mass matrix, M_p is defined as

$$\begin{aligned} M_p &= \int_{V_p} \phi_{mn}(x,y)^T \rho_p(x) \phi_{mn}(x,y) \, \mathrm{d}V_p, \\ &= \rho_p h_p \int_{x_1}^{x_2} \int_{y_1}^{y_2} \phi_n(x,y) \phi_m(x,y) \, \mathrm{d}x\mathrm{d}y. \end{aligned} \tag{4.12}$$

For a simply supported plate, M_p becomes

$$M_p = ab\rho_p h_p \left\{ \begin{array}{ll} s_1^{\zeta-} & \text{for } p = r \\ s_2^{\zeta-} & \text{for } p \neq r \end{array} \right\} \left\{ \begin{array}{ll} s_1^{\eta-} & \text{for } q = s \\ s_2^{\eta-} & \text{for } q \neq s \end{array} \right\}. \tag{4.13}$$

The piezo stiffness matrix, K_p is defined as

$$K_p = \int_{V_p} \phi_{mn}(x,y)^T {L_u}^T R_s^T C_p R_s L_u \phi_{mn}(x,y)\, \mathrm{d}V_p, \tag{4.14}$$

where L_u is defined above, R_s is a rotation matrix commonly used in elasticity (see [28]) which becomes

$$R_s = \left| \begin{array}{ccc} 1 & 0 & 0 \\ 0 & 1 & 0 \\ 0 & 0 & -1 \end{array} \right|, \tag{4.15}$$

and C_p is the piezo stiffness matrix, defined as

$$C_p = \left| \begin{array}{ccc} \frac{Y_p}{1-\nu_p^2} & \frac{Y_p \nu_p}{1-\nu_p^2} & 0 \\ \frac{Y_p \nu_p}{1-\nu_p^2} & \frac{Y_p}{1-\nu_p^2} & 0 \\ 0 & 0 & \frac{Y_p}{1+\nu_p^2} \end{array} \right|. \tag{4.16}$$

Substituting these quantities into Equation 4.14, we obtain

$$\begin{aligned} K_p = & \frac{Y_p I_p}{1-\nu_p^2} \int_{x_1}^{x_2} \int_{y_1}^{y_2} \frac{\partial^2 \phi_n}{\partial x^2} \frac{\partial^2 \phi_m}{\partial x^2} \\ & + \frac{\partial^2 \phi_n}{\partial y^2} \frac{\partial^2 \phi_m}{\partial y^2} + \nu_p \left(\frac{\partial^2 \phi_n}{\partial x^2} \frac{\partial^2 \phi_m}{\partial y^2} + \frac{\partial^2 \phi_n}{\partial y^2} \frac{\partial^2 \phi_m}{\partial x^2} \right) \\ & + 2(1-\nu_p) \frac{\partial^2 \phi_n}{\partial x \partial y} \frac{\partial^2 \phi_m}{\partial x \partial y} \, \mathrm{d}x\mathrm{d}y. \end{aligned} \tag{4.17}$$

where $I_p = \frac{h_s^2 h_p}{4} + \frac{h_s h_p^2}{2} + \frac{h_p^3}{3}$, which is the moment of inertia of the piezo.

For a simply supported plate, K_p becomes

$$K_p = \frac{D_p ab\pi^4}{a^4}\Big[p^4 s_1^{\zeta-} s_1^{\eta-} + (\frac{a}{b})^4 q^4 s_1^{\zeta-} s_1^{\eta-} + 2\nu_p(\frac{a}{b})^2 (pq)^2 s_1^{\zeta-} s_1^{\eta-} + 2(1-\nu_p)(\frac{a}{b})^2 (pq)^2 s_1^{\zeta+} s_1^{\eta+}\Big]$$

for $p = r$ and $q = s$,

$$K_p = \frac{D_p ab\pi^4}{a^4}\Big[p^4 s_1^{\zeta-} s_2^{\eta-} + (\frac{a}{b})^4 (qs)^2 s_1^{\zeta-} s_2^{\eta-} + \nu_p(\frac{a}{b})^2\big[(ps)^2 s_1^{\zeta-} s_2^{\eta-} + (pq)^2 s_1^{\zeta-} s_2^{\eta-}\big] + 2(1-\nu_p)(\frac{a}{b})^2 (p^2 qs) s_1^{\zeta+} s_2^{\eta+}\Big]$$

for $p = r$ and $q \neq s$,

$$K_p = \frac{D_p ab\pi^4}{a^4}\Big[(pr)^2 s_2^{\zeta-} s_1^{\eta-} + (\frac{a}{b})^4 q^4 s_2^{\zeta-} s_1^{\eta-} + \nu_p(\frac{a}{b})^2\big[(ps)^2 s_2^{\zeta-} s_1^{\eta-} + (rq)^2 s_2^{\zeta-} s_1^{\eta-}\big] + 2(1-\nu_p)(\frac{a}{b})^2 (q^2 pr) s_2^{\zeta+} s_1^{\eta+}\Big]$$

for $p \neq r$ and $q = s$,

$$K_p = \frac{D_p ab\pi^4}{a^4}\Big[(pr)^2 s_2^{\zeta-} s_2^{\eta-} + (\frac{a}{b})^4 (qs)^2 s_2^{\zeta-} s_2^{\eta-} + \nu_p(\frac{a}{b})^2 s_2^{\zeta-} s_2^{\eta-}\big[(ps)^2 + (rq)^2\big] + 2(1-\nu_p)(\frac{a}{b})^2 (prqs) s_2^{\zeta+} s_2^{\eta+}\Big]$$

for $p \neq r$ and $q \neq s$.

Finally, the electromechanical coupling matrix, Θ, which provides a relationship between the voltage applied to the piezo actuator and the plate displacement, is defined as

$$\Theta = \int_{V_p} \phi_{mn}(x,y)^T {L_u}^T R_s^T e^T R_e L_\phi \phi_v(x,y)\, \mathrm{d}V_p, \tag{4.18}$$

where $\phi_{mn}(x,y)$, L_u, and R_s are defined above, e is a matrix relating stress to the applied electrical field and is defined as

$$e = \begin{vmatrix} 0 & 0 & 0 \\ 0 & 0 & 0 \\ d_{31}(C_{p_{11}} + C_{p_{12}}) & d_{31}(C_{p_{11}} + C_{p_{12}}) & 0 \end{vmatrix}, \tag{4.19}$$

where d_{31} is a piezoelectric charge constant defined in reference to the local poling direction of the piezoelectric. The $C_{p_{ij}}$ terms in Equation 4.19 refer to the capacitance constants of the piezoelectric. R_e is a matrix of direction cosines defined as

$$R_e = \begin{vmatrix} 1 & 0 & 0 \\ 0 & -1 & 0 \\ 0 & 0 & -1 \end{vmatrix}, \tag{4.20}$$

L_ϕ is the electrical differential operator defined as

$$L_\phi = \begin{vmatrix} 0 \\ 0 \\ -\frac{\partial}{\partial z} \end{vmatrix}, \tag{4.21}$$

and ϕ_v is the assumed potential distribution defined as

$$\phi_v(z) = \frac{z - \frac{h_s}{2}}{h_p}. \tag{4.22}$$

Substituting these quantities into Equation 4.18, we obtain

$$\Theta = ab \int_{\zeta_1}^{\zeta_2} \int_{\eta_1}^{\eta_2} \frac{d_{31} E_p S_p}{h_p(1-\nu_p)} \left[\frac{1}{a^2} \frac{\partial^2 \phi_{mn}}{\partial \zeta^2} + \frac{1}{b^2} \frac{\partial^2 \phi_{mn}}{\partial \eta^2} \right] \mathrm{d}\eta, \mathrm{d}\zeta, \tag{4.23}$$

where $S_p = \frac{h_p^2 + h_p h_s}{2}$.

For a simply supported plate, Equation 4.18 becomes

$$\Theta = \frac{d_{31}E_pS_pb}{ah_p(1-\nu_p)}\frac{1}{pq}\left(p^2+(\frac{a}{b})^2q^2\right)\Big[cos(p\pi\zeta)\Big]_{\zeta_1}^{\zeta_2}\Big[cos(q\pi\eta)\Big]_{\eta_1}^{\eta_2}.$$

4.2.3 State Space Model

Having fully defined all of the parameters in Equation 4.1, we now develop a state space model of the coupled system, which we will use in our simulation. First, we rewrite Equation 4.1, such that

$$M\ddot{q}_{mn} + Kq_{mn} = \Theta v, \tag{4.24}$$

where $M = M_s + M_p$ and $K = K_s + K_p$.

Using the classical state space representation,

$$\begin{aligned} \dot{x} &= Ax + Bu \\ y &= Cx + Du \end{aligned} \tag{4.25}$$

we will now define our state variables and state matrices. The states of our system are the generalized displacements and velocities of the plate, $[x]_{2j\times 1} = [q_1 ... q_j \;\; \dot{q}_1 ... \dot{q}_j]^T$ where j is the number of modes of interest. Our input is the voltage applied to the piezo element, such that $u_{k\times 1} = v_{k\times 1}$, where k is the number of inputs. Our output, $y_{o\times 1}$, is the displacement of the plate in (x,y) coordinates, where o is the number of outputs. Our state matrices are as follows:

$$A_{2j\times 2j} = \begin{bmatrix} 0_{j\times j} & I_{j\times j} \\ (-M^{-1}K)_{j\times j} & (-2\zeta\sqrt{\lambda})_{j\times j} \end{bmatrix}, \tag{4.26}$$

$$B_{2j\times u} = \begin{bmatrix} 0_{j\times u} \\ M^{-1}\Theta_{j\times u} \end{bmatrix}, \tag{4.27}$$

$$C_{o\times 2j} = \left[\phi_{mn,o\times j}, 0_{o\times j}\right], \tag{4.28}$$

$$D_{o\times u} = \left[0_{o\times u}\right], \tag{4.29}$$

where M is the mass matrix, K is the stiffness matrix, ϕ_{mn} is the mode shape function, and Θ is the electromechanical coupling matrix (all defined above), and 0 is a matrix of zeros, I is an Identity matrix, ζ is the damping coefficient, and λ is a diagonal matrix of the eigenvalues of K and M.

4.3 Methods

We now describe the implementation of the above model in simulation, describing the user inputs and the simulation outputs. We then discuss the boundary conditions assumed in the simulation and implemented in our variable friction surface prototype used in validation experiments.

4.3.1 Model Implementation

The state space model of the coupled system described in Section 4.2.3 was implemented in Matlab R2011a. The input parameters defined by the user are the number and location of piezoelectric actuators. The input voltage signal(s) applied to the piezoelectric(s), the number of modes included in the model, and the properties of the plate and the piezoelectric

can also be changed if needed. In our simulation, we chose to include all modes that were at least two times the highest frequency of interest (40kHz), but no higher to ensure quick computation. This resulted in using 49 modes total, the point at which no change in simulation predictions was observed and at which all modes less than 100kHz were included. Plate displacement was computed at 40×40 locations, evenly spaced on the plate, which provided enough output locations to capture accurate representations of modal shapes. The resonant modes of the system are identified from the frequency response of the coupled system, by observing the peaks in the bode plot within the 20-40kHz range. The modal response of the coupled system at these resonant frequencies is then computed by multiplying the system eigenvectors by the assumed modal shape function, at each output location. Surface plots of these resonant modes are generated for visualization of modal shape.

4.3.2 Boundary Conditions

Prior hypotheses on the behavior of variable friction touchscreens have suggested that they qualitatively respond similar to free plates or point-supported plates, however there have not been attempts in modeling them due to several factors including the complexity of these boundary conditions [60]. Toward developing the simplest model of variable friction touchscreens possible, we chose to model our system as simply supported, the least mathematically complex boundary condition, but one which qualitatively produces similar mode shapes to that of free or point-supported plates (with some slight descrepancies at the actual edges themselves, discussed in more detail in Section 4.6). Thus, in this work, we sought to assess the effectiveness of using a simply supported model in predicting mode shapes of

variable friction touchscreens, dependent upon number and location of piezo actuators, as well as in varying plate thicknesses.

4.3.3 Experimental Setup

To validate our simply-supported simulation, we constructed several physical prototypes of variable friction surfaces with different numbers and locations of piezoelectric actuators. Our prototypes are similar to the LATPaD described in [60], with a newly designed plate housing. Our surface is a 3" $\times$ 3" $\times$ 0.125" borosilicate glass plate (McMaster-Carr, Part #: 8476K131) with a piezoelectric actuator (SparkFun Electronics, Part #: 7BB-20-6L0) 20mm in diameter $\times$ 0.42mm thick epoxied to the bottom. In some cases, multiple piezoelectric actuators were attached, as shown in Figure 4.6. We used a function generator (Tektronix, AFG 3012B) and a stereo power amplifier (Adcom GFA-555) to provide the input signal to the piezoelectric actuator(s).

In [60], the glass plate was pressed into a thick foam-core, to provide a free-like boundary condition on the plate. In making multiple prototypes of these touchscreens, we found the foam-core to be difficult to make repeatably and consistently, leaving some plates confined tighter than others. Further, we found that the foam would "loosen" over time, resulting in plates slipping on some edges and sitting uneven in the core. For repeatable experimental validation and practical manufacturing of these touchscreens, a more robust housing is needed. For this reason, we designed two different mounting arrangements, shown in Figure 4.1. In Figure 4.1 (Left), the plate is constrained by 4 wooden braces placed on each end, each with 2 nails protruding out. The tips of the nails hold the glass plate in place by resting in small cone-shaped impressions drilled lightly into the edge of

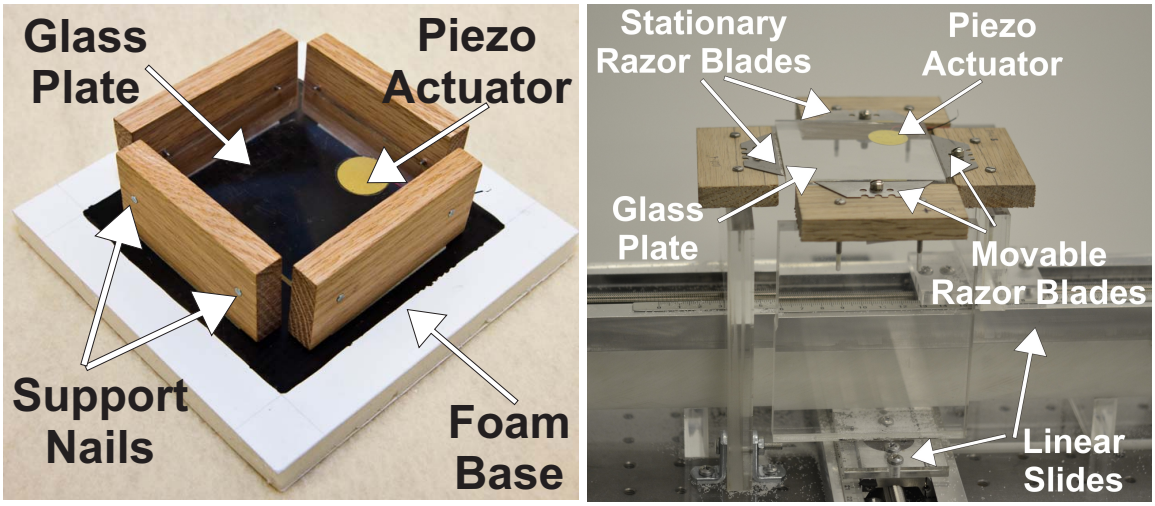

Figure 4.1: The two physical prototypes we constructed of variable friction touchscreen constraints. (Left) The plate is constrained via 2 small nails which protrude from each wooden side and contac the plate edge, sitting in pinpoint-size cone-shaped holes. (Right) An adjustable constraint for variable friction touchscreens that constrains the plate using 4 razor blades, 2 of which were stationary, and 2 of which could be moved in and out on linear slides. While both designs provided a repeatable way of constraining the plate, the adjustable razor blade setup enabled easy switching of plates in and out of the experimental tested. In both pictures, the piezoelectric actuator (the gold circle) is bonded directly to the glass plate.

the glass, resembling a very small point contact on the plate edge. The wooden braces are secured to a foam-base, providing a stable platform for the entire setup. While this design worked well in securing the plate, a new setup had to be manufactured for each plate. Though this may not be problematic for commercial manufacturing, we found it to be time consuming for testing purposes. For this reason, we developed a second design, that enabled easy switching between plates.

The second design, shown in Figure 4.1 (Right) sought to provide a more adjustable and interchangeable testing platform. We also sought to provide a more evenly distributed boundary condition on the plate edges to more closely match that of a very "light" simply supported condition and to provide a means of adjusting the force of contact between the plate and its constraints. This was done by using four thin razor blades that contacted the plate edges, one on each side. Two of the razor blades perpendicular to one another were attached to fixed supports mounted on an acrylic base, such that their position could not be adjusted. The other two blades were mounted onto supports attached to linear slides, such that their position, and thus the force between the plate and the razor blade, was adjustable.

To compare the modal response of the plate with one piezo actuator in the corner from its original foam core constraint presented in [60] to these two new design mountings, we tested a glass plate with one piezo actuator bonded in the corner in each configuration. In each case, we performed a manual frequency sweep of a sinusoidal voltage input between 20-40kHz, in 0.1kHz increments. When a modal shape was excited, exhibited by movement of the salt on the plate), the frequency sweep increment was reduced to 0.01kHz in order to more finely locate the mode. We then recorded the modal shapes observed and their corresponding frequenices. We observed no major changes in the shapes or the corresponding frequencies of the responses generated, as shown in Figure 4.2. This suggests that the nail or razor blade design does not qualitatively change the plate response, but provides a more robust and practical platform from which experiments can be conducted. We note, however, that it was possible to change the strength of the mode (observed by how vigorously the salt on the plate was moving) with the razor blade design. For example, if the razor blades were very tightly pushed up against the plate edges, the strength of the mode

was lessened and could even be dampened out. Thus, in our experimental validations, we ensured that the plate was constrained just enough such that it had stability within the setup, but that the modal responses of the plate were strong. Because of its ease in interchanging plates and its ability to accomodate various sizes of plates, we used the razor blade setup in our validation experiments discussed in Section 4.4.

4.4 Validation Experiments and Results

To validate our simulation, we performed two experiments using a plate with one piezo actuator attached in the corner (one diameter from each edge), similar to the configuration proposed in [60]. From a design perspective, a surface with only one piezo would be the simplest and most cost-effective setup to manufacture. The corner location was chosen because these variable friction surfaces are meant to be overlayed onto LCD screens, making it desirable to locate the piezos on the edges such that they do not obstruct the user's view of the onscreen content they are interacting with. The two validation experiments compared the predicted and experimental frequency response of the coupled system and the qualitative agreement between predicted and observed modal shapes.

4.4.1 Frequency Response Validation Experiment

The frequency response validation experiment was conducted to assess how well our simulation predicts the number of resonant modes that exist between 20-40kHz. To do this, we first generated a Bode plot of our coupled system from our simulation, identifying its resonant modes by the number of peaks in the Bode plot, as shown in Figure 4.3. We then experimentally measured the frequency response of our physical system by attaching

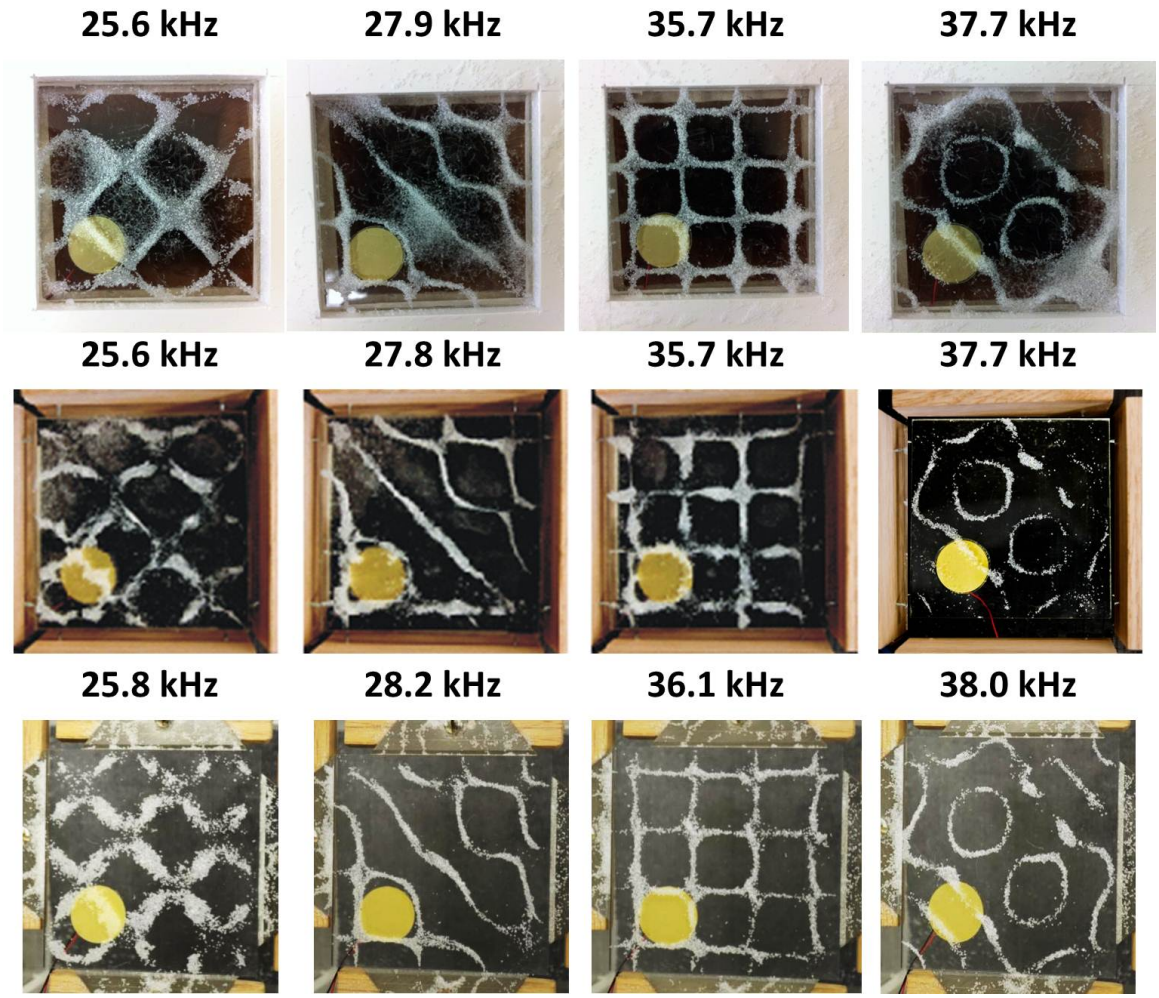

Figure 4.2: The modal shapes observed between 20-40kHz in the foam core constraint (top), the new nail contact setup (middle), and the new adjustable razor blade design (bottom). We note that we see good agreement in the observed modal shapes and their corresponding frequencies regardless of the three constraint designs, suggesting that the nail design or the razor blade constraints do not sacrifice performance but are more practical in terms of robustness, manufacturability, and repeatability.

a small, lightweight accelerometer (PCB Piezotronics, Model #: 352C22) to the plate using wax and exciting the plate with a random noise voltage signal. We recorded the input

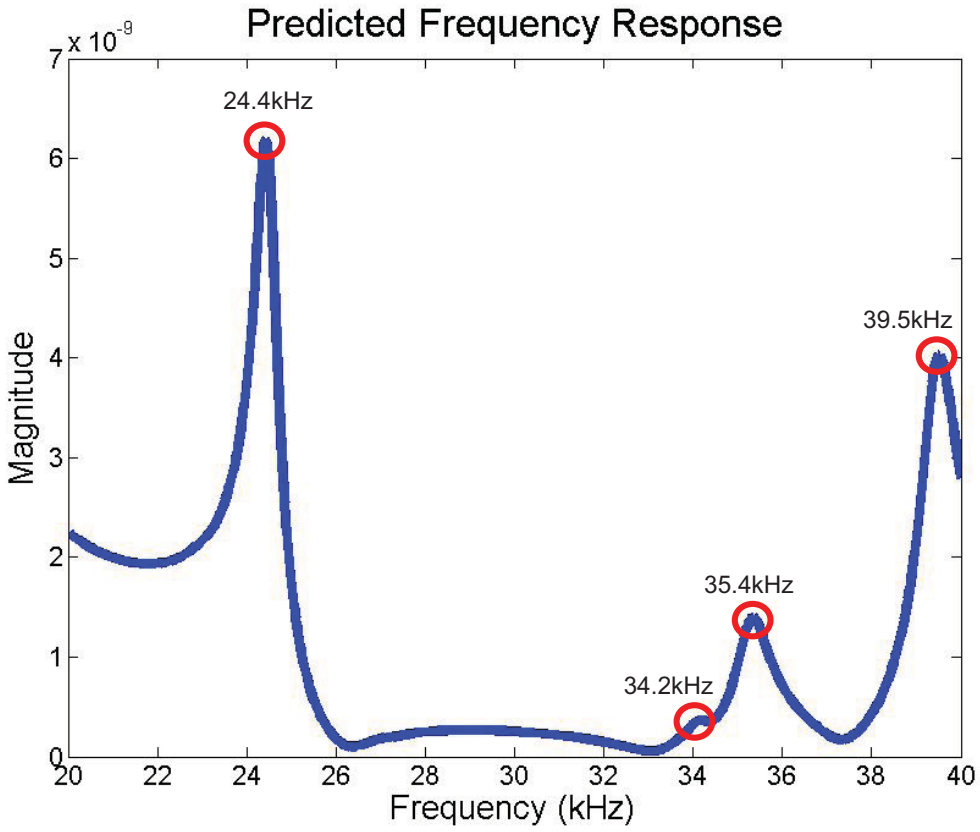

Figure 4.3: The predicted frequency response of the coupled system with one piezo actuator in the corner of the plate from the simulation. Four resonant peaks (modes) are observed occuring at 24.4kHz, 34.2kHz, 35.4kHz, and 39.5kHz.

voltage signal applied to the piezo and the output acceleration from the accelerometer. The frequency response of the system was then computed offline in Matlab 2011a using the *spectrum* command. The resulting frequency response is shown in Figure 4.4.

In comparing our predicted versus experimental frequency response, we observe that our simulation predicts 4 resonant modes, corresponding to the 4 peaks in the Bode plot of the simulated coupled system (Figure 4.3). This is in agreement with the 4 resonant modes observed experimentally, indicated by the peaks observed in the frequency response of the

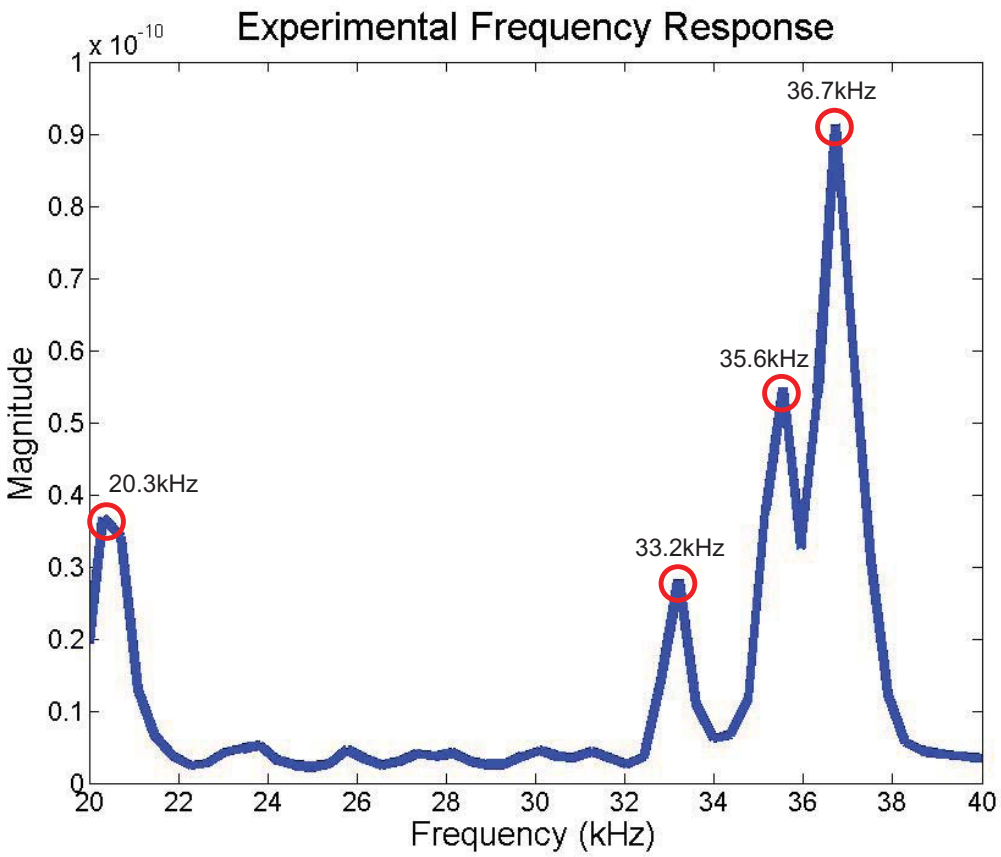

Figure 4.4: The experimentally measured frequency response of the coupled system with one piezo actuator in the corner of the plate. Four resonant peaks (modes) are observed occuring at 20.3kHz, 33.2kHz, 35.6kHz, and 36.7kHz.

physical system (Figure 4.4). We note that the strength of these resonant modes, indicated by the magnitude of the peaks in the bode plot, differs slightly between the experimental and the simulated case. Qualitatively, the last 3 modes observed experimentally appeared to be stronger, as the salt moved more violently on the plate in these modes. This is consistent with the magnitudes measured in the experimental bode plot. Discrepancies in our simulated and experimental system parameters, such as plate properties or piezo locations, may contribute to the discrepancy in the predicted magnitudes of the modes. The slight

differences observed between the predicted and measured frequency values are likely due to the additional mass of the accelerometer on the plate in the experimental case. We note, however, that the number of predicted and measured frequencies corresponding to the resonant modes are the same in the two cases, and that they are in relatively good agreement with one another. This suggests that the model is sufficient for predicting the number of resonant modes within the 20-40kHz range.

4.4.2 Modal Shape Agreement Experiment

The second experiment explored the qualitative agreement between the modal shapes predicted in simulation with those observed experimentally for the plate with one piezo in the corner. To experimentally observe the resonant modes, we placed salt on the glass plate and performed a manual frequency sweep of sinusoidal inputs over the range of 20-40kHz, in 0.1kHz increments. When movement of the salt was observed (which suggested a mode being close to excitation), the frequency sweep increment was reduced to 0.01kHz in order to more finely locate the mode. A mode was considered a resonant mode when the salt would bounce up and down on the plate and propogate to nodal lines, creating geometric patterns on the plate. The shape and frequency of each mode were recorded. Note that in this experiment, the accelerometer was removed from the plate surface. To generate predicted modal shapes in our simulation, we computed the modal shapes which most closely corresponded to the resonant frequencies identified in the simulated Bode plot of the coupled system. We note that for each resonant frequency, there were 2 potential mode shapes to choose from (differing only by a rotation of 90°, because the plate is assumed to be square. For example, the mode pair 1,3 occurs at almost the same frequency as the mode

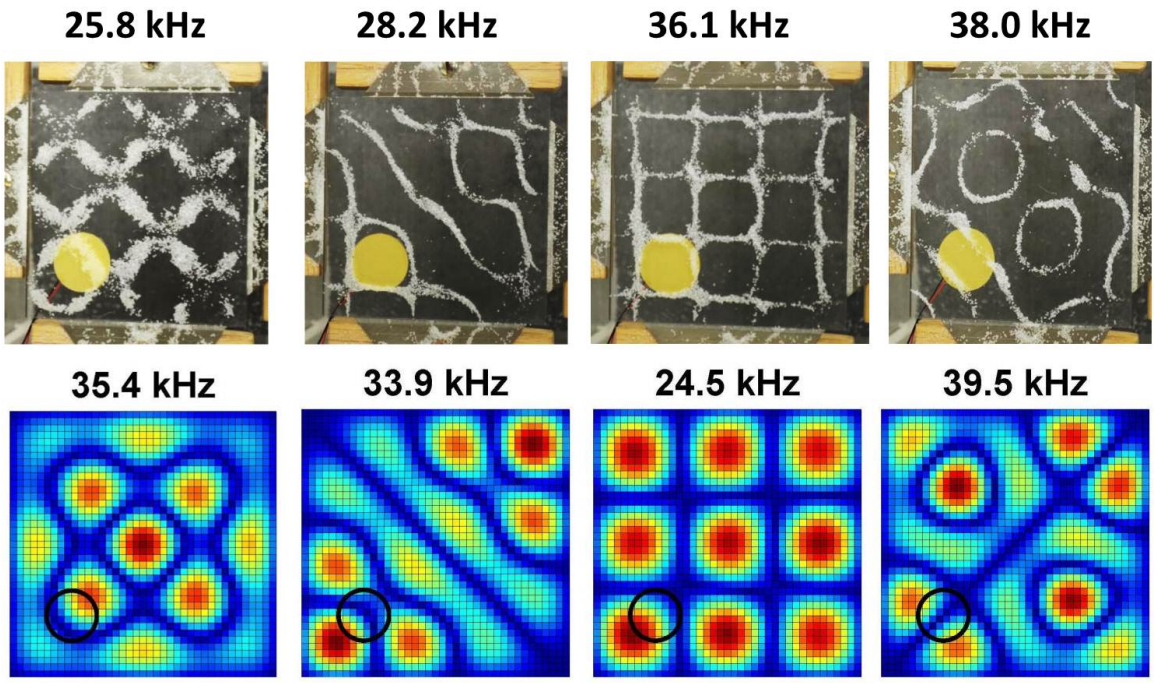

Figure 4.5: The experimentally observed resonant modes and their corresponding frequencies (top) compared with the predicted modal shapes of the coupled system and their corresponding frequencies (bottom), for one piezoelectric actuator placed in the corner. The piezoelectric is the gold circle in the experimental pictures and the black circle in the simulation pictures. In the simulation pictures, amplitude displacement ranges from smallest (blue) to largest (red). The nodal lines will occur at the blue locations.

pair 3,1, and thus, either of these modes could occur at the resonant frequency indicated in the bode plot. To choose which mode was appropriate, we looked at our electromechanical coupling matrix, which told us which mode the piezo was coupling to the most. We then created a 3D surface plot of this mode. The experimentally observed and predicted modal shapes and their corresponding frequencies are shown in Figure 4.5.

As predicted in simulation and measured experimentally, four resonant modes were ex-

perimentally observed. Comparing the experimental mode shapes with those predicted in simulation, we observe good qualitative agreement between the general shapes excited, for each of the four modes. Specifically, we note that our model is accounting for the coupling between multiple modes, as represented by the hard diagonal observed in the second experimental mode and predicted in the second simulated mode. We note, however, that the half waves observed experimentally on the edges of the plate (most easily seen in the third experimental mode) are not represented in our predicted modal shapes. This is likely due to the boundary conditions of the plate not perfectly being simply supported experimentally, and thus, some behavior representative of a free boundary condition is still exhibited. This is also probably the reason that we observe a mismatch in the frequency of each mode. We also note that the frequencies at which we experimentally observed resonant modes, differ slightly from the frequencies in the experimental Bode plot (Figure 4.4). This is likely due to the fact that though the accelerometer was small, it's additional mass may have caused some shift in the resonant frequencies themselves. This is not problematic, however, since we still observed the same number of modes as we experimentally measured. Despite these discrepancies, the simply supported model is successful at predicting the number of modes and their general shapes, which is useful in understanding what modes and shapes are generated within the desired frequency range of 20-40kHz.

4.5 Experiments Demonstrating Simulation Flexibility

The real benefit of a simulation such as the one presented in this paper is to provide a quick, effective design tool that can predict mode shapes in any given scenario without having to experimentally construct a prototype each time. Having validated the simulation

in predicting the number and shapes of the modes expected in the one piezo case, we now use the simulation to predict mode shapes for two different scenarios – a plate with 3 piezos equally spaced along one edge and a thicker plate with one piezo in the corner.

4.5.1 Case 1: Multiple Piezoelectric Actuators

The first case we explored was the case of a plate with 3 piezos equally spaced along one edge of the plate. A similar configuration with 4 piezos along the edge was used in user studies conducted with variable friction toucshcreens in [58], though it is unclear why this configuration was chosen. In the user studies conducted in [58], the piezos were actuated at 26kHz, which enabled a reduction in friction on the surface of glass plates from approximately 1.0 to 0.15. Results from the user studies show enhancements in both user performance and overall experience in using variable friction feedback in targeting tasks. Here, we seek to show the flexibility and the effectiveness of our simulation as a design tool by exploring its success in predicting modal shapes with a configuration of multiple piezos attached to the glass and to provide insight into the modal shape chosen for the user studies in [58].

To do this, we ran our simulation as before, changing only the number and the location of the piezo actuators, and obtained a Bode plot of the coupled system. From the predicted frequency response, we observed 5 resonant modes between 20-40kHz. Next, we plotted the coupled system's modal shapes at the frequencies observed in the Bode plot, as described in Section 4.4.2. The simulation results are shown in Figure 4.6 (Top). To verify our simulation predictions, we constructed a plate with 3 piezo actuators evenly spaced along one edge and placed it within our razor blade experimental setup. We then performed

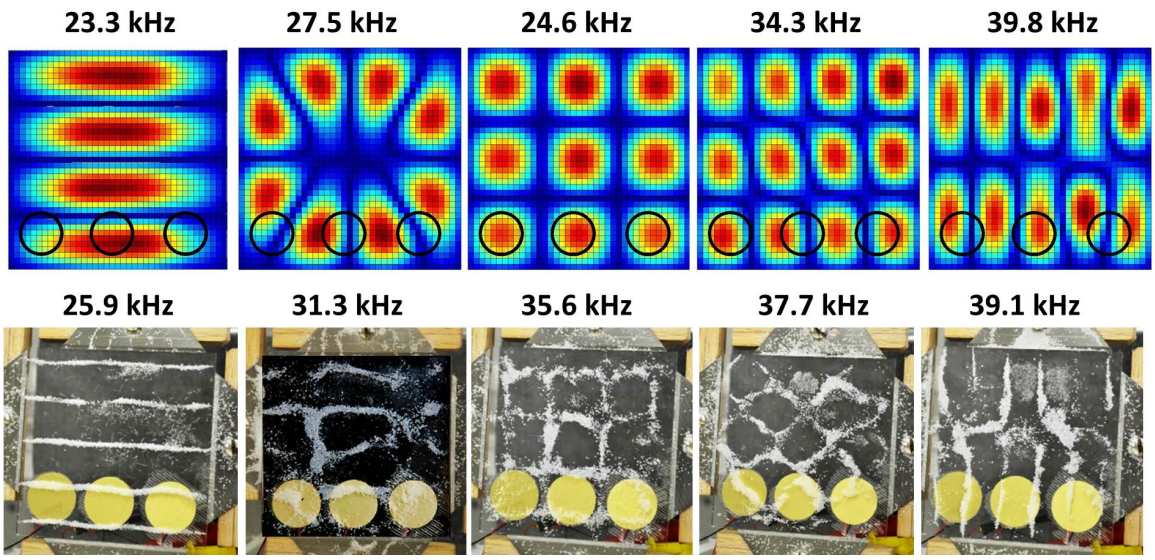

Figure 4.6: The predicted resonant modes and their corresponding frequencies (top) compared with the experimentally determined modal shapes of the coupled system and their corresponding frequencies (bottom), for three piezoelectric actuators placed along the plate edge. The piezoelectrics are the gold circles in the experimental pictures and the black circle in the simulation pictures. In the simulation pictures, amplitude displacement ranges from smallest (blue) to largest (red). The nodal lines will occur at the blue locations.

a frequency sweep over the plate between 20-40kHz (as done in the one piezo case), and recorded the resonant mode shapes and frequencies. The results are shown in Figure 4.6 (Bottom) and demonstrate the effectiveness of the simulation in the multiple piezo case.

We observe good alignment in predicting the number and the qualitative shape of experimentally observed modes. As in the one piezo case, we observe some mismatch in the frequencies at which the resonant modes occur, but we can confirm that our simultion predicts the correct number and shape of the modes within the interested frequency range. The mismatch in frequency is likely due to the plate not behaving completely like a simply

supported plate, but rather, having boundary conditions characterisitic of a free plate or a point-supported plate. This issue of boundary conditions will be discussed in more detail in Section 4.6. Despite this, however, this experiment demonstrates the effectiveness and flexibility of the simulation in predicting the modal shapes that are able to be excited in the case of multiple piezos.

Interestingly, we note that the mode shape generated at 26kHz (the mode used in the user studies in [58]), is a strong, but geometrically simple, mode. It is likely that this mode was chosen for the user studies in [58] because the straight nodal lines provide very defined regions of what the user perceives as "sticky" or "slippery." This pattern is ideal for the examples of user widgets that variable friction touchscreens might support, such as the alarm clock widget designed in [58] (see Figure 7 in this paper to see the interface). In this task, users were asked to set a specified time on an alarm clock by scrolling through number choices for the hour and the minute. Each choice had numbers that could be scrolled through vertically. These vertical columns were likely aligned with the nodal lines of the mode shape, such that friction could be cycled on and off by actuating and then turning off the piezos. Thus, users feel that they are switching between numbers due to this alternating friction sensation. This is just one example of many of the value a simulation provides in knowing a priori the modal shapes that will be generated from a specific design.

4.5.2 Case 2: Thicker Plates

In addition to varying the number and the location of the piezo actuators, one may also vary the properties of the plate itself. In order to show the effectiveness of the simulation in accomodating for this change, we performed a second experiment with a plate that was

0.25” thick, twice the thickness of the plate used in earlier experiments. To validate this scenario, we performed the same procedure as explained in Section 4.5.1. First, we ran our simulation, changing the thickness of the plate and locating the piezo one diameter from each plate edge in the corner of the plate. Our predicted results are shown in Figure 4.7 (Top). To validate these results, we constructed a thick plate with a piezo attached in the corner, and tested it experimentally. Our experimental results are shown in Figure 4.7 (Bottom).

We again observe qualitatively good alignment in terms of the modal shapes predicted compared with the ones we observed experimentally. We note, however, that the simulation predicted one extra mode that we did not experimentally observe (the lowest mode at 21.6kHz, shown in Figure 4.7 (Top)). This mismatch could be due to the fact that this plate is on the border of qualifying as a “thin plate” as its ratio of length to thickness is just less than 12 (see assumptions in Section 4.2.1). To address this, we decreased the thickness of the plate by 0.5mm in our simulation (which is within a 10% change in the thickness), to a total thickness of 0.23.” In this case, we observe that the simulation no longer predicts that lower mode, and instead, it predicts only the two modes we observe experimentally. Becuase this change in parameters is within a reasonable bound, this experiment demonstrates the effectiveness of the simulation in predicting modal shapes of plates with varying thickness.

4.6 Discussion

The above experiments demonstrate that a simply supported model of the coupled system (including both the plate and the piezoelectric actuators) is sufficient for predicting the

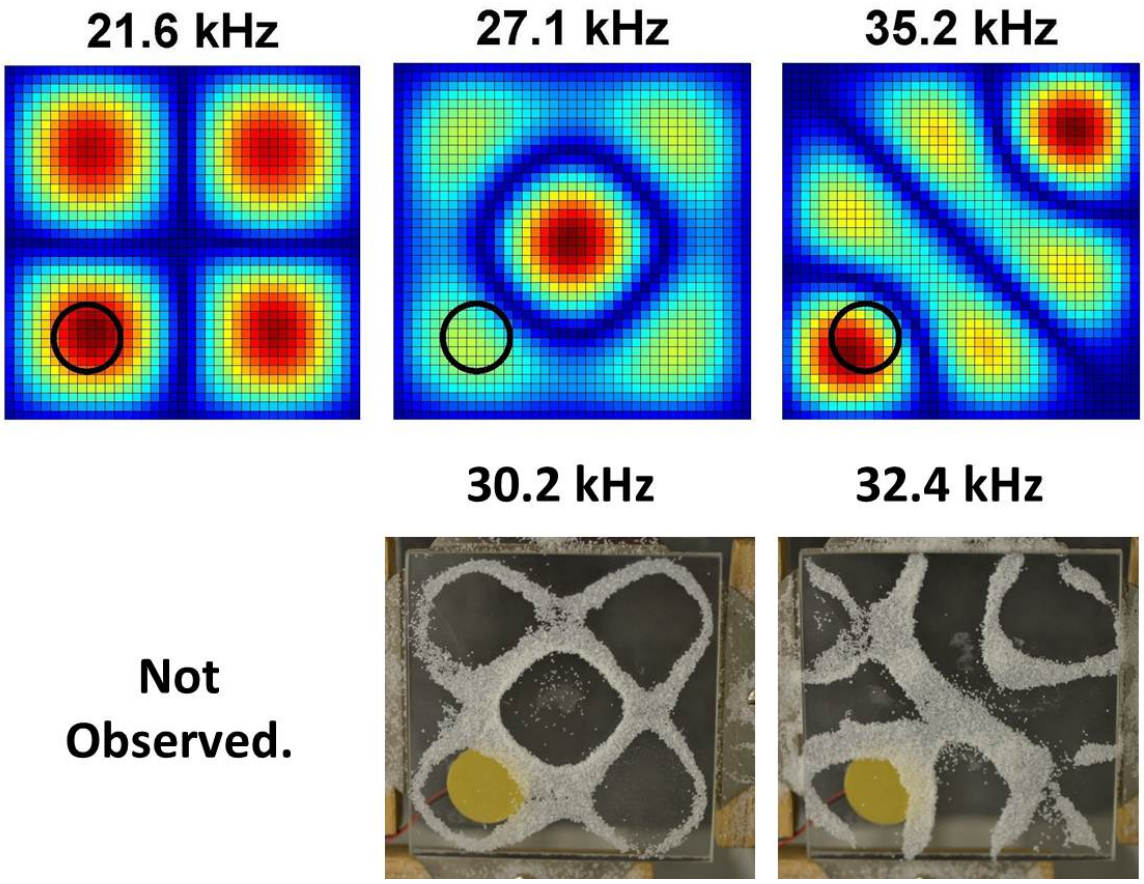

Figure 4.7: The predicted resonant modes and their corresponding frequencies (top) compared with the experimentally determined modal shapes of the coupled system and their corresponding frequencies (bottom), for the thicker plate (0.25") and one piezoelectric actuator placed in the corner. The piezoelectrics are the gold circles in the experimental pictures and the black circle in the simulation pictures. In the simulation pictures, amplitude displacement ranges from smallest (blue) to largest (red). The nodal lines will occur at the blue locations.

number and modal shapes of variable friction touchscreens with varying properties of plate thickness, number of actuators, and location of actuators. The benefits of a simulation such as this is its ability to provide designers with a tool that they can use to quickly observe

the shapes that can be generate on the surface of the plates without having to physically construct a prototype for each case. For example, in the case of the user studies conducted in [58], the modal shape generating only a few straight lines was ideal for enhancing the tasks that users were performing, and this mode is not observed using only one piezo. A simulation such as the one presented in this paper, will be useful in serving as a design aid for future user widgets on variable friction touchscreens.

Further, this simulation becomes extremely powerful in cases where users want to convey complex geometries on the screen, and perhaps switch in between modes to do so. In this case, this simulation can be used to explore what configuation of piezo actuators should be used to provide a class of shapes which can be actuated in constructive or destructive manners to generate other shapes. For example, if the user wants to display a circle in the middle of the screen, they may switch in between several modes, taking advantage of nodal line placement within each mode, to generate this shape. The exploration of modal superposition by applying different input signals to multiple piezos would be an interesting area of future research in variable friction touchscreens.

In addition, our results indicate that though general shape representation is sufficient from this simply supported model, the geometry at the edges of the plate are not completely captured. This is likely due to the fact that these plates are demonstrating behavior similar to that of a free plate or a point-supported plate instead of a purely simply supported plate. This is characterized by the half wavelengths displayed on the plate edges, which is a typical characterisitic of free plates. Further, as mentioned in our above experiments, this boundary condition mismatch is also likely the contributor for the discrepancies in frequencies between the predicted and experimentally observed mode shapes.

Thus, future work will involve expanding this simulation to model the free boundary condition case. Our initial efforts in doing this have enabled us to capture uncoupled mode shapes (mode shapes that appear as horizontal or vertical lines or a combination of both in the form of a grid). The challenge with this, however, is that the free case is mathematically more complex and computationally more expensive, particularly in the case of including the piezoelectrics within the model as we did in our simply supported model. Including the piezo actuators, however, is likely necessary. This is particularly true in cases where mutliple piezos are used, which may increase the stiffness of the system enough that a plate only model is not sufficient, or in the case of exploring modal superposition, where the peizos are being actuated with different input signals. Thus, we intend to explore this extension in our future work toward achieving better frequency alignments. It is arguable, however, whether the simply supported model is sufficient from a design perspective, as it correctly predicts the number and the shapes of resonant modes within the 20-40kHz range.

4.7 Conclusion and Future Work

In this chapter, we have addressed two key design issues impeding variable friction touchscreens from entering the commercial market. The first is the practical constraint of the plate itself, which was addressed through the exploration of two physical prototypes which reliably constrain the plate using nails and razor blades, respectively. The second design issue was addressed by developing a simulation which successfully predicts the number and shapes of the modes that can be achieved with varying plate and piezo parameters. This simulation is a valuable tool that enables designers to explore the appropriate number and location of piezo actuators, as well as how the plate responses change with varying plate

thickness. A tool such as this allows designers to quickly iterate through design scenarios, mitigating the need to physically construct prototypes in each case.

Complementing user studies that having shown the effectiveness of variable friction touchscreens in enhancing user engagement, perception, and performance on a variety of tasks performed on a touchscreen [58, 60], this work expands upon the foundation in surface haptics for realizing the potential of this new class of touchscreens. The modeling presented in this work provides a design tool that can be generalized to variable friction touchscreens of larger sizes and rectangular shapes. Future work using this simulation will explore quantitative analyses in plate displacements toward exploring its effectiveness in predicting what shapes users can actually perceive, design optimization of variable friction touchscreens, and geometry creation via modal superposition. The exploration of each of these will help realize the potential that variable friction touchscreens have in providing a more realistic user experience from touchscreen platforms and will likely propel this new class of touchscreens into commercial use.

Chapter 5

Conclusion and Future Work

This dissertation has bridged the fields of haptics, engineering, and education to explore some of the potential benefits of tactile and force feedback devices in educational settings. The challenges that motivated this work include (1) developing a better understanding of novel techniques for generating realistic tactile feedback, (2) exploring new haptic technologies to enhance the educational experience of students, particularly those who are visually impaired, (3) designing low-cost haptic interfaces that could easily be implemented within a classroom setting, (4) assessing the effectiveness of haptic devices in enhancing student learning, and (5) making adoption of haptic interfaces more feasible in challenging, dynamic educational settings where time and resources are limited and robustness, ease of use, and educational value are critical.

5.1 Haptic Paddles

Toward these ends, Chapter 2 presented design, hardware, and software enhancements to a one DOF force feedback device, called the haptic paddle and presented the first formal assessment of the learning benefits associated with the haptic paddle laboratories. The main results of the enhancements were a more robust, easy-to-use interface, including a friction drive design that relies on USB communication using low-cost Arduino microcontrollers, and a more engaging, interactive software program that runs in Matlab and Simulink, enabling students to independently program their haptic paddle. These improvements have reduced the cost of the haptic paddle to less than $100 including all components and elec-

tronics except for a laptop. The main results of the formal assessment were that the haptic paddle laboratories enhanced student learning and retention of majority of the course concepts in System Dynamics and that students did significantly better on quizzes after having completed the lab exercises than after only having had the in-class lecture.

A comprehensive website (see [6]) was developed containing all of the files needed to build the haptic paddle, run the simulations, conduct the laboratories, and perform the assessments. Further, in collaboration with MathWorks, Inc. a webinar was created that includes an introduction to the haptic paddle, its associated laboratories, and using Arduinos and Simulink, which is freely available for anyone who is interested in learning more. Our version of the haptic paddle has been successfully used in an Introduction to Engineering course and in a graduate course on haptics and teleoperation at California State University Long Beach. We have also received several emails from both individual students and educators expressing interest in building a haptic paddle or using it in their System Dynamics course, respectively.

Future goals in the haptic paddle research includes three facets. The first is on enhancing and improving the laboratory exercises, particularly Lab 1, which consistently showed up in our assessments as having material that was difficult for students to grasp (see Chapter 2). Second, one of the greatest advantages of the haptic paddle is that it can be used to simulate several dynamic systems. Currently, however, it is only used to explore a multi-DOF mass, spring, damper system. We plan to develop more simulations of different dynamic systems, perhaps including those outside of the mechanical domain, for students to explore and interact with in lab exercises. Similarly, we plan to expand upon the simulations associated with the haptic paddle to include those that may be used outside of system dynamics,

and perhaps even used in teaching physics concepts at the K-12 level. Finally, we plan to use the System Dynamics concept inventory (CI) we developed for our initial assessment of the haptic paddle as a starting point for the development of a more broadly-agreed upon Dynamics and Controls CI. While there exists several CIs for use in STEM education, there is currently not one in these two areas. This will require establishing a team of researchers at a subset of diverse universities who will work together to develop this CI and then use it in their classroom. This CI will be submitted to CI Hub [10], a widely accepted and used online community for concept inventory developers, educators, and students. Multi-site evaluations of this CI and corresponding teaching techniques in System Dynamics, will also enable us to compare the haptic paddle laboratories to learning opportunities provided at other universities. This type of multi-site formal assessment will be beneficial for broadly validating the learning benefits of haptic interfaces such as the haptic paddle and for encouraging wide adoption of such a device.

5.2 Vibratory Touchscreens in Math Education for the Blind

Toward illustrating the potential of tactile touchscreens in education, Chapter 3 introduced a new teaching paradigm in math education for the visually impaired using *commercially* available tactile touchscreens. Vibratory touchscreens are designed for portability, robustness, and are already commercially available, providing a unique opportunity for quick adoption of them into mathematics education for the visually impaired. We developed a software program, running on a commercially available vibratory touchscreen, that enables users to feel and/or hear graphical content being displayed on the screen, and also enables users to sketch their own graphs or images on the screen. The main results of

this work demonstrated that both sighted and blind users could perceive some of the basic mathematical concepts (including grids, points, and lines) using auditory feedback and vibrations from a touchscreen. We also report our intial experiences using the touchscreen with blind students and their educators, both of whom expressed excitement at the potential of this technology. Finally, to demonstrate the portability of this technology as well as its potential for rapid, widespread adoption, we developed an Android application with the same capabilities mentioned above that runs on the Samsung Galaxy Tab. We note, however, that the ideas and the software developed in this work could be generalized to a number of other tablets with different operating systems. Several companies, including Apps4Android, have expressed interest in the software developed in this work, and these collaborations will be sought out for further development and dissemination of software applications.

Future goals in this work are two-fold. The first includes further validation of tactile touchscreens as teaching tools in math education, both through psychophysical evaluations determining how to best represent graphical concepts through touch on a flat surface and through further user studies such as the ones presented in Chapter 3. Exploring how to enable edge detection using superimposed vibrations or a combination of vibratory and auditory feedback will be interesting challenges to explore in future work. Similarly, to date, tactile feedback has been provided at only a single point of contact. As technology advances and multi-point contact becomes possible, it will be interesting to explore how this will be harnessed haptically. The second area of future work focuses on the educational benefits of tactile touchscreens. As mentioned in Chapter 1, a haptic device alone is inadequate if it lacks associated curriculum. Thus, we plan to work with educators of the visually

impaired to develop lessons and eventually, curriculum, incorporating tactile toucshcreens. We then plan to formally assess the learning benefits of using a tactile touchscreen and compare it with current methods of teaching visually impaired students. Beyond math education, tactile touchscreens have the potential to enhance many other areas of study including chemistry, physics, history, and statistics, to name a few, and could one day become a primary educational tool for many types of learners.

5.3 Variable Friction Touchscreens

While Chapter 3 focused on the capabilities of current commercial tactile touchscreen, Chapter 4 explored variable friction touchscreens, a new class of tactile touchscreens that have the potential to provide more realistic interactions with flat touch surfaces. Such touchscreens have already been shown to engage users and enhance their ability to perform targeting tasks on a touchscreen [58], yet optimal design of these touchscreens has not yet been realized. Toward understanding how these touchscreens should be designed to achieve optimal performance, we developed a comprehensive model of variable friction touchscreens. The model presented in this work accounts for the coupled system of the plate and the piezoelectric actuators, and can be generalized to a number of other plate and piezo shapes and configurations. The model accounts for a simply supported plate, but could be extended to include other boundary conditions, such as the free-free case, as deemed necessary. The main results of this work lay a theoretical and design foundation for realizing the potential benefits of variable friction touchscreens by enabling us to quickly and optimially choose both the number and location of the piezoelectric actuators that oscillate the plate to achieve maximum performance. This work also resulted in a list

of design guidelines for the future development of variable friction touchscreens.

Future goals in this work involve investigating how we can use the various resonant modes of the plate to create new textures and complex geometries on the surface. Variable friction touchscreens have the potential to provide more realistic and rich feedback to the user by enabling them to perceive frictional changes on the plate surface. By combining these areas of low and high friction in unique combinations, we may be able to provide users with more engaging types of feedback than what are currently available. While some of these sensations have already been investigated [26,96], there is likely many more sensations that can be simulated via these variable friction touchscreens. An equally promising direction is to use combinations of resonant modes to explore how we can create complex geometries on a plate surface. For example, through constructive or destructive interference of resonant modes or by actuating one piezo at a given frequency and actuating another piezo at a different frequency, we may be able to create lines, polynomials, or even shapes on the plate surface. This would open up an entirely new realm of surface haptic features that could be explored from a psychophysical, design, and application perspective. From an educational perspective, it would be interesting to explore if the realistic feedback provided by these touchscreens could enhance students' ability to perceive graphical content displayed from a touchscreen platform. Several studies focusing on creating these geometries, accompanied with user studies evaluating them, could follow from this work.

5.4 The Future of Haptics in Education

It is likely that a combination of force feedback devices and tactile devices, some of which may not yet be discovered, will play an important role in education (and in human-machine

interfaces) moving forward. Though it is still unclear which devices and feedback types may prove to be successful and become widely adopted, it is clear that haptics has the potential to tremendously impact education in several ways. Much like the three chapters presented in this dissertation, realizing these impacts will require design, curriculum development, and formal assessments of haptic devices with an emphasis on in-classroom use (e.g. Chapter 2), integration of new hardware and software and feasibility studies supporting their functionality (e.g. Chapter 3), and cross-disciplinary research investigating the design of new devices that provide enhanced haptic feedback (e.g. Chapter 4). While it may be several years before haptic devices become mainstream within a classroom (whether it be in a classroom of sighted or blind students, or both), this dissertation has addressed many of the key pieces required in realizing the potential of haptic devices in STEM education. In addition, the methods and devices presented in this dissertation are broadly applicable in other domains where force feedback or surface haptics may facilitate enhanced human-machine interfaces.

Appendix A

Supplementary Material to Chapter 2

This appendix contains the 25-question multiple choice quiz and the 5 lab quizzes (taken directly from the 25-question quiz) used to assess student learning in the haptic paddle laboratories discussed in Chapter 2. It also contains the data presented in Chapter 2, Figures 2.7 - 2.12, in tabular form, showing the exact values of appropriate quiz scores and their corresponding statistical metrics.

Note that in all tables presented, significance at the 95% confidence level ($\alpha = 0.05$) and 90% confidence level ($\alpha = 0.10$) were determined from the paired t-test analyses, and the effect sizes were based upon the Cohen's d computation (as discussed in Section 2.3.1. We note that these two statistical analyses are complementary to one another, with the t-tests providing insight on whether or not quiz means were significantly different from one another, and the effect sizes providing insight on the magnitude of this difference. In our discussions of effect size, we follow the standard interpretation that $d = 0.2$ is a small effect, $d = 0.5$ is a medium effect, and $d = 0.8$ is a large effect, where the value of d indicates the difference between two means as a fraction of the pooled standard deviation. A positive value of d suggests an increase in student performance on the quiz at the specified time compared to the pre-test, and a negative value of d indicates a decrease in student performance on the quiz at the specified time compared to the pre-test.

Name: _____ Section: _____

ME 234: System Dynamics
Fall 2011

Conceptual Assessment

1. Consider a spinning motor with a mass attached to the rotor. You got the motor to spin up to a constant speed using a power supply, then you removed the power. If the quantity of interest is ω, the motor speed in rad/s, what is the order of this system?

   A. First order

   B. Second order

   C. Third order

   D. Fourth order

2. Which of the followig graphs best represents the time response of the motor, $\omega(t)$ versus t from the instant you cut the power to the motor?

   A.

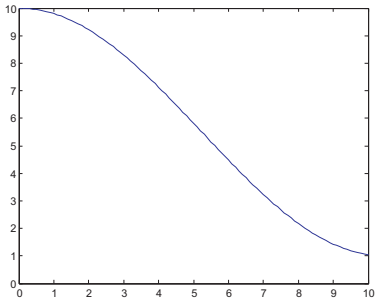

   B.

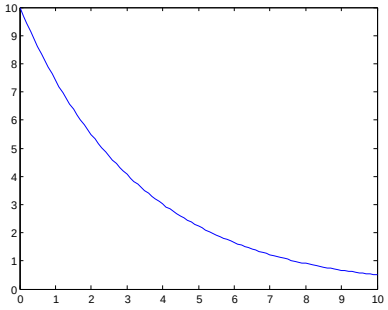

C.

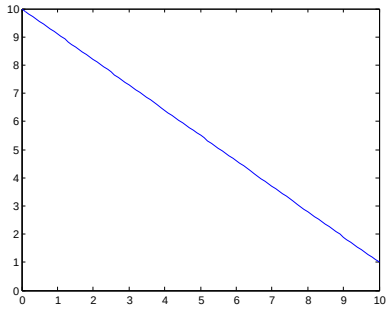

D.

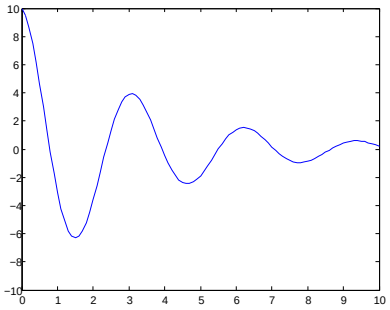

3. Which of the following elements would be present in the dynamic equation for ω? (Choose all that apply)

   A. Stiffness

   B. Inertia

   C. Damping

   D. Heat

4. Which of the following is the most important factor which causes ω to decrease following the cutoff ?

   A. Motor inertia

   B. Back EMF

   C. Bearing friction

   D. Air resistance

5. The Back EMF (electromotive force) has

    A. a linear

    B. an inverse

    C. an exponential

    D. no

    relationship to ω.

6. You make measurements a, b, and c with some amount of uncertainty in each measurement. If you use these measurements to calculate x = a + b + c and y = abc your percentage error in x will be,

    A. The same as the percentage error in y

    B. Greater than the percentage error in y

    C. Less than the percentage error in y

    D. Not enough information is given to determine the answer

7. Consider the following. You are powering a spinning motor, and slowly turn down the applied current until the motor just stops. After the motor stops, you notice that there is still a non-zero current applied. Which of the following phenomena is this due to?

    A. Motor inertia

    B. Static Bearing Friction

    C. Back EMF

    D. Air Resistance

8. The torque constant for a motor represents the relationship between

    A. Current and Torque

    B. Voltage and Torque

    C. Speed and Torque

    D. Position and Torque

9. Which of the following is the primary reason for the fact that a bifilar pendulum (torsional pendulum held by two strings) oscillates (i.e. which of the following provides the restorative force)

    A. Friction between the string and the other components

    B. Air Resistance

    C. Gravity

    D. Spring-like behavior of the string

10. To measure the natural frequency of an oscillatory system you would

    A. Divide the total time by the total number of oscillations

    B. Divide the total number of oscillations by the total time

    C. Divide the average amplitude by the length of one cycle

    D. Divide the stiffness by the mass

11. An object's rotational inertia is

    A. Dependent on only the mass of the object

    B. Dependant on only the mass and shape of the object

    C. Dependant on the mass and shape of the object, and the axis of rotation

    D. Dependant on the mass and shape of the object, and frictional coefficients between the object and it's surroundings

12. A system is guaranteed to be "stable" if

    A. The output approaches the same fixed value under any initial condition

    B. The output oscillates randomly

    C. The output increases without bound

    D. The output approaches the same fixed value under certain specific initial conditions

13. Which of the following characteristics necessarily implies that a system is inherently unstable?

    A. A pole with a negative real part

    B. A pole with a positive real part

    C. A pole with a zero real part

    D. A pole with an imaginary part

14. Which of the following is an example of a stable system?

    A. A spring mass damper with negative damping

    B. A simple inverted pendulum

    C. A ball balanced on the roof of a house

    D. A typical spring mass damper

15. The period of an undamped pendulum (assuming a small amplitude) is

    A. Dependent on only the length of the pendulum

    B. Dependent on only the length of the pendulum and the acceleration of gravity

    C. Dependent on only the length and rotational inertia of the pendulum

    D. Dependent on the length and rotational inertia of the pendulum, and the acceleration of gravity

16. Critical damping means a system

A. Is on the edge of instability
B. Will reach its set point as fast as possible without overshoot
C. Will oscillate about its set point with an increasing amplitude
D. Will not move at all due to such damping

The following four plots are the choices for the next three questions:

A.

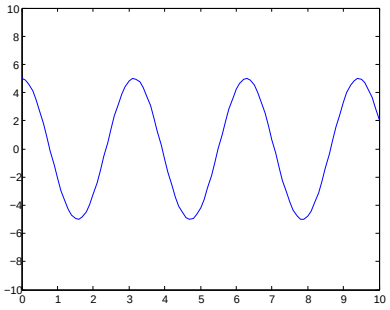

B.

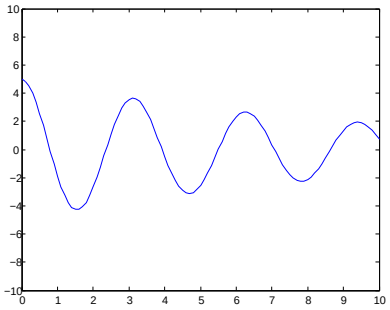

C.

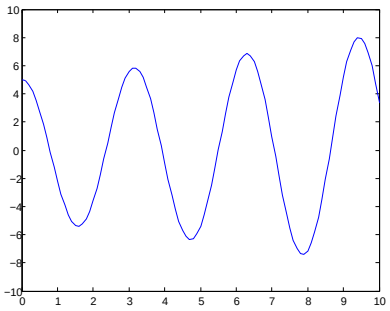

D.

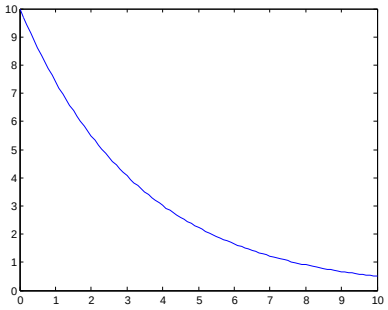

17. What would be the system response to an initial condition $x = x_0$, $f(t) = 0$ if the dynamic system model is $m\ddot{x} + kx = f(t)$?

    A.

    B.

    C.

    D.

18. What would the physical effect of the feedback $f(t) = -c_1\dot{x}$ if the dynamic system model is $m\ddot{x} + kx = f(t)$ and $c_1 > 0$?

    A.

    B.

    C.

    D.

19. What about if $c_1 < 0$?

    A.

    B.

    C.

    D.

20. What type of feedback can potentially stabilize an inverted pendulum with a motor providing a torque τ at the base?

    A. $\tau = -k\theta$

    B. $\tau = -k\dot{\theta}$

    C. $\tau = -k\ddot{\theta}$

    D. $\tau = -k\int \theta dt$

Consider the following system:

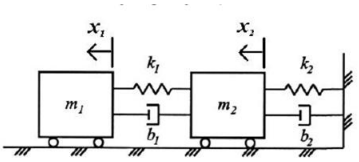

21. What is the appropriate Free Body Diagram for the two masses shown above?

A.

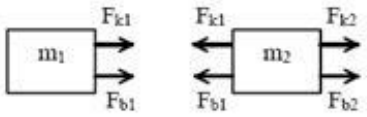

B.

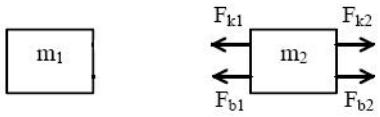

C.

D.

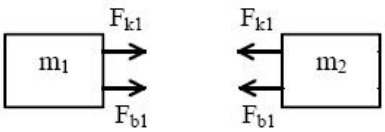

22. Consider a harmonic driving force $f(t)$ applied to m_1. In order to excite mode 2, the frequency of $f(t)$ must be

    A. Higher than the frequency needed to excite mode 1.

    B. Lower than the frequency needed to excite mode 1.

    C. Equal to the frequency needed to excite mode 1.

    D. The frequency does not matter.

23. In order to excite mode 2 at some amplitude, the magnitude of the driving force should be:

    A. Higher than the magnitude needed to excite mode 1 at the same amplitude.

    B. Lower than the magnitude needed to excite mode 1 at the same amplitude.

    C. Equal to the magnitude needed to excite mode 1 at the same amplitude.

    D. Any magnitude will excite mode 2 at the same amplitude as mode 1

24. How many modes of vibration are possible for the above system?

    A. 1

    B. 2

    C. 3

    D. 4

25. What will be the effect on the observed modal frequencies if damping is introduced?

    A. Increased

    B. Decreased

    C. No change

    D. One will increase and the other will decrease

Name: _____ Section: _____

ME 234: System Dynamics
Fall 2011

Lab 1 Quiz

This quiz will not be graded, but you must answer the questions below to the best of your ability to receive full credit for your lab assignment. You have a maximum of 5 minutes to answer the following questions. Write your answers in the space provided. Turn in to the Lab TA as soon as you are finished.

1. Consider a spinning motor with a mass attached to the rotor. You got the motor to spin up to a constant speed using a power supply, then you removed the power. If the quantity of interest is ω, the motor speed in rad/s, what is the order of this system?

   A. First order

   B. Second order

   C. Third order

   D. Fourth order

2. Which of the followig graphs best represents the time response of the motor, $\omega(t)$ versus t from the instant you cut the power to the motor?

   A.

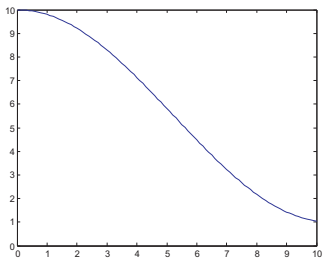

   B.

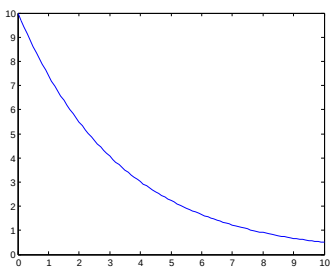

C.

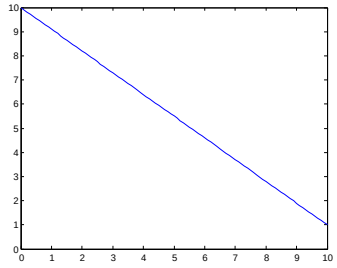

D.

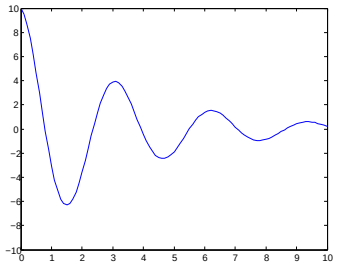

3. Which of the following elements would be present in the dynamic equation for ω? (Choose all that apply)

   A. Stiffness
   B. Inertia
   C. Damping
   D. Heat

4. Which of the following is the most important factor which causes ω to decrease following the cutoff ?

   A. Motor inertia
   B. Back EMF
   C. Bearing friction
   D. Air resistance

5. The Back EMF (electromotive force) has

   A. a linear
   B. an inverse
   C. an exponential
   D. no

   relationship to ω.

Name: _____ Section: _____

ME 234: System Dynamics
Fall 2011

Lab 2 Quiz

5 points

This quiz will not be graded, but you must answer the questions below to the best of your ability to receive full credit for your lab assignment. You have a maximum of 5 minutes to answer the following questions. Write your answers in the space provided. Turn in to the Lab TA as soon as you are finished.

1. You make measurements a, b, and c with some amount of uncertainty in each measurement. If you use these measurements to calculate x = a + b + c and y = abc your percentage error in x will be,

    A. The same as the percentage error in y

    B. Greater than the percentage error in y

    C. Less than the percentage error in y

    D. Not enough information is given to determine the answer

2. Consider the following. You are powering a spinning motor, and slowly turn down the applied current until the motor just stops. After the motor stops, you notice that there is still a non-zero current applied. Which of the following phenomena is this due to?

    A. Motor inertia

    B. Static Bearing Friction

    C. Back EMF

    D. Air Resistance

3. The torque constant for a motor represents the relationship between

    A. Current and Torque

    B. Voltage and Torque

    C. Speed and Torque

    D. Position and Torque

4. Which of the following is the primary reason for the fact that a bifilar pendulum (torsional pendulum held by two strings) oscillates (i.e. which of the following provides the restorative force)

    A. Friction between the string and the other components
    B. Air Resistance
    C. Gravity
    D. Spring-like behavior of the string

5. To measure the natural frequency of an oscillatory system you would

    A. Divide the total time by the total number of oscillations
    B. Divide the total number of oscillations by the total time
    C. Divide the average amplitude by the length of one cycle
    D. Divide the stiffness by the mass

Name: _____ Section: _____

ME 234: System Dynamics
Fall 2011

Lab 3 Quiz

5 points

This quiz will not be graded, but you must answer the questions below to the best of your ability to receive full credit for your lab assignment. You have a maximum of 5 minutes to answer the following questions. Write your answers in the space provided. Turn in to the Lab TA when you are finished.

1. An object's rotational inertia is

   A. Dependent on only the mass of the object

   B. Dependant on only the mass and shape of the object

   C. Dependant on the mass and shape of the object, and the axis of rotation

   D. Dependant on the mass and shape of the object, and frictional coefficients between the object and it's surroundings

2. A system is guaranteed to be "stable" if

   A. The output approaches the same fixed value under any initial condition

   B. The output oscillates randomly

   C. The output increases without bound

   D. The output approaches the same fixed value under certain specific initial conditions

3. Which of the following characteristics necessarily implies that a system is inherently unstable?

   A. A pole with a negative real part

   B. A pole with a positive real part

   C. A pole with a zero real part

   D. A pole with an imaginary part

4. Which of the following is an example of a stable system?

   A. A spring mass damper with negative damping

   B. A simple inverted pendulum

   C. A ball balanced on the roof of a house

   D. A typical spring mass damper

5. The period of an undamped pendulum (assuming a small amplitude) is

   A. Dependent on only the length of the pendulum

   B. Dependent on only the length of the pendulum and the acceleration of gravity

   C. Dependent on only the length and rotational inertia of the pendulum

   D. Dependent on the length and rotational inertia of the pendulum, and the acceleration of gravity

Name: _____ Section: _____

ME 234: System Dynamics
Fall 2011

Lab 4 Quiz

5 points

This quiz will not be graded, but you must answer the questions below to the best of your ability to receive full credit for your lab assignment. You have a maximum of 5 minutes to answer the following questions. Write your answers in the space provided. Turn in to the Lab TA as soon as you are finished.

1. Critical damping means a system

   A. Is on the edge of instability
   B. Will reach its set point as fast as possible without overshoot
   C. Will oscillate about its set point with an increasing amplitude
   D. Will not move at all due to such damping

The following four plots are the choices for the next three questions:

A.

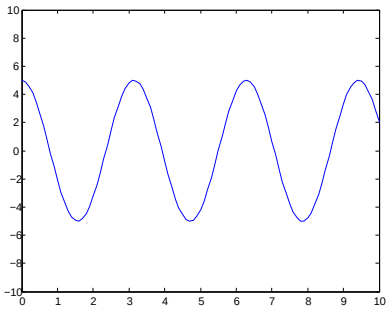

B.

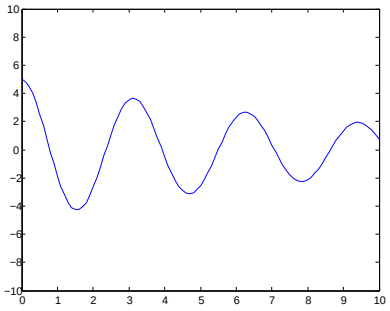

C.

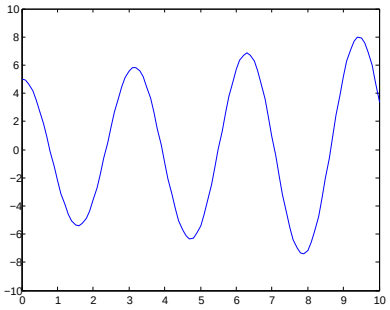

D.

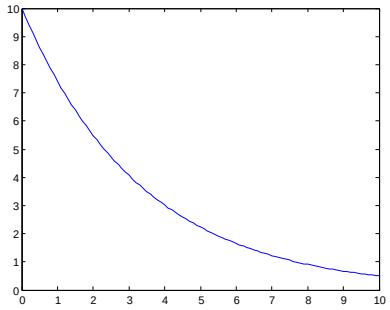

2. What would be the system response to an initial condition $x = x_0$, $f(t) = 0$ if the dynamic system model is $m\ddot{x} + kx = f(t)$?

   A.

   B.

   C.

   D.

3. What would the physical effect of the feedback $f(t) = -c_1\dot{x}$ if the dynamic system model is $m\ddot{x} + kx = f(t)$ and $c_1 > 0$?

   A.

   B.

   C.

   D.

4. What about if $c_1 < 0$?

   A.
   B.
   C.
   D.

5. What type of feedback can potentially stabilize an inverted pendulum with a motor providing a torque τ at the base?

   A. $\tau = -k\theta$
   B. $\tau = -k\dot{\theta}$
   C. $\tau = -k\ddot{\theta}$
   D. $\tau = -k \int \theta dt$

Name: _____ Section: _____

ME 234: System Dynamics
Fall 2011

Lab 5 Quiz

5 points

This quiz will not be graded, but you must answer the questions below to the best of your ability to receive full credit for your lab assignment. You have a maximum of 5 minutes to answer the following questions. Write your answers in the space provided. Turn in to the Lab TA as soon as you are finished.

Consider the following system:

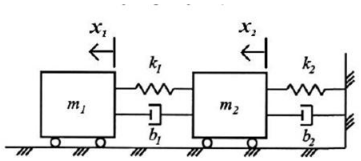

1. What is the appropriate Free Body Diagram for the two masses shown above?

A.

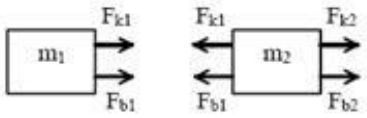

B.

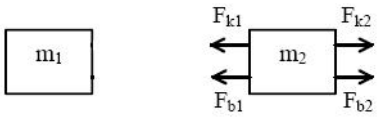

C.

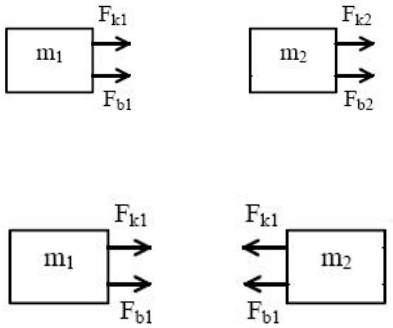

D.

2. Consider a harmonic driving force $f(t)$ applied to m_1. In order to excite mode 2, the frequency of $f(t)$ must be

   A. Higher than the frequency needed to excite mode 1.

   B. Lower than the frequency needed to excite mode 1.

   C. Equal to the frequency needed to excite mode 1.

   D. The frequency does not matter.

3. In order to excite mode 2 at some amplitude, the magnitude of the driving force should be:

   A. Higher than the magnitude needed to excite mode 1 at the same amplitude.

   B. Lower than the magnitude needed to excite mode 1 at the same amplitude.

   C. Equal to the magnitude needed to excite mode 1 at the same amplitude.

   D. Any magnitude will excite mode 2 at the same amplitude as mode 1

4. How many modes of vibration are possible for the above system?

   A. 1

   B. 2

   C. 3

   D. 4

5. What will be the effect on the observed modal frequencies if damping is introduced?

   A. Increased

   B. Decreased

   C. No change

   D. One will increase and the other will decrease

Table A.1: The means (standard deviations) of all students' pre-test score compared with their post-test score for years 2 and 3. The corresponding p-value from the paired t-test is shown, denoting significance at $\alpha = 0.05$ with a ** and at $\alpha = 0.1$ with a *. The effect size, d, is also presented, and the sample size for each test, N, is shown in the last column. This table corresponds to Figures 2.7 and 2.8.

	Pre-Test	**Post-Test**	**p-value**	**Cohen's d**	**N**
Lab 1 (Y2)	2.49 (1.14)	2.87 (1.06)	0.1212	0.32	39
Lab 1 (Y3)	2.14 (1.26)	2.39 (1.04)	0.1324	0.22	56
Lab 2 (Y2)	2.90 (1.07)	3.08 (1.20)	0.4132	0.16	39
Lab 2 (Y3)	2.30 (1.11)	3.07 (1.19)	0.0004**	0.67	44
Lab 3 (Y2)	2.05 (1.00)	3.64 (1.01)	1.393e-10**	1.58	39
Lab 3 (Y3)	1.98 (1.05)	3.20 (1.42)	1.955e-8**	0.97	56
Lab 4 (Y2)	2.13 (1.30)	3.72 (1.32)	9.138e-7**	1.21	39
Lab 4 (Y3)	1.80 (1.30)	3.45 (1.44)	2.822e-8**	1.20	56
Lab 5 (Y2)	2.48 (1.09)	3.34 (0.77)	0.0004**	0.91	29
Lab 5 (Y3)	2.875 (1.32)	3.36 (1.09)	0.0187**	0.40	56
Cumulative (Y2)	12.26 (2.94)	16.64 (3.27)	1.913e-11**	1.41	39
Cumulative (Y3)	11.27 (2.96)	15.46 (4.22)	4.552e-10**	1.15	56

Table A.2: The means (standard deviations) of the appropriate student section's quiz score on the pre-test compared with the quiz score taken after completing the lab for year 1 (Y1), year 2 (Y2), and year 3 (Y3). The corresponding p-value from the paired t-test is shown, denoting significance at $\alpha = 0.05$ with a ** and at $\alpha = 0.1$ with a *. The effect size, d, is also presented, and the sample size for each test, N, is shown in the last column. This table corresponds to Figure 2.9.

	Pre-Test	**After Lab**	**p-value**	**Cohen's d**	**N**
Lab 1 (Y1)	2.39 (1.04)	2.72 (1.02)	0.3808	0.32	18
Lab 1 (Y2)	2.72 (1.02)	3.5 (0.79)	0.0116**	0.86	18
Lab 1 (Y3)	2.13 (1.31)	2.06 (0.85)	0.8425	-0.06	16
Lab 2 (Y1)	1.86 (1.61)	4.64 (0.63)	1.223e-5**	2.28	14
Lab 2 (Y2)	3.06 (0.93)	3.50 (0.89)	0.1862	0.48	16
Lab 2 (Y3)	2.28 (1.32)	3.44 (1.04)	0.0007**	0.98	18
Lab 3 (Y1)	2.07 (1.14)	4.00 (0.78)	0.0011**	1.97	14
Lab 3 (Y2)	2.17 (0.94)	3.83 (0.94)	6.603e-4**	1.78	12
Lab 3 (Y3)	1.73 (0.88)	2.87 (0.99)	0.0006**	1.21	15
Lab 4 (Y1)	3.00 (1.30)	4.07 (0.92)	0.0295**	0.95	14
Lab 4 (Y2)	2.00 (1.32)	2.67 (1.73)	0.3856	0.43	9
Lab 4 (Y3)	1.44 (1.04)	3.17 (1.25)	0.0010**	1.50	18
Lab 5 (Y1)	2.94 (1.64)	4.06 (0.75)	0.02302**	0.88	17
Lab 5 (Y2)	2.53 (0.94)	3.18 (0.95)	0.0686*	0.68	17
Lab 5 (Y3)	2.56 (1.63)	3.81 (0.75)	0.0161**	0.98	16

Table A.3: The means (standard deviations) of the appropriate student section's quiz score on the pre-test compared with the quiz score taken at the beginning of lab for year 1 (Y1), year 2 (Y2), and year 3 (Y3). The corresponding p-value from the paired t-test is shown, denoting significance at $\alpha = 0.05$ with a ** and at $\alpha = 0.1$ with a *. The effect size, d, is also presented, and the sample size for each test, N, is shown in the last column. This table corresponds to Figure 2.10.

	Pre-Test	**Beginning of Lab**	**p-value**	**Cohen's d**	**N**
Lab 1 (Y1)	2.33 (1.29)	2.73 (0.96)	0.3200	0.35	15
Lab 1 (Y2)	2.06 (1.16)	2.00 (0.93)	0.7921	-0.06	15
Lab 1 (Y3)	2.27 (1.16)	2.8 (0.86)	0.0878*	0.52	15
Lab 2 (Y1)	2.92 (1.49)	2.21 (1.31)	0.0354**	- 0.51	14
Lab 2 (Y2)	2.79 (1.19)	3.0 (1.47)	0.6198	0.16	14
Lab 2 (Y3)	2.39 (1.04)	2.72 (0.83)	0.2307	0.36	18
Lab 3 (Y1)	2.28 (1.02)	3.17 (1.25)	0.0054**	0.78	18
Lab 3 (Y2)	1.67 (0.97)	3.17 (1.29)	0.0013**	1.31	18
Lab 3 (Y3)	2.06 (0.93)	3.31 (1.30)	0.0042**	1.11	16
Lab 4 (Y1)	2.63 (1.15)	3.94 (1.00)	0.0031**	1.22	16
Lab 4 (Y2)	1.73 (1.33)	3.67 (0.82)	1.815e-4**	1.75	15
Lab 4 (Y3)	2.00 (1.28)	3.17 (1.15)	0.0018**	0.92	18
Lab 5 (Y1)	3.00 (1.00)	3.47 (1.06)	0.1689	0.45	15
Lab 5 (Y2)	3.31 (1.11)	3.62 (0.77)	0.3925	0.32	13
Lab 5 (Y3)	2.79 (1.37)	3.36 (0.93)	0.1788	0.49	14

Table A.4: The means (standard deviations) of the appropriate student section's quiz score on the pre-test compared with the quiz score taken after the pre-lab lecture for year 1 (Y1), year 2 (Y2), year 3 (Y3). The corresponding p-value from the paired t-test is shown, denoting significance at $\alpha = 0.05$ with a ** and at $\alpha = 0.1$ with a *. The effect size, d, is also presented, and the sample size for each test, N, is shown in the last column. This table corresponds to Figure 2.11.

	Pre-Test	**After Pre-Lab Lecture**	**p-value**	**Cohen's d**	**N**
Lab 1 (Y1)	1.75 (1.18)	2.38 (1.09)	0.0859*	0.55	16
Lab 1 (Y2)	2.75 (0.86)	2.81 (1.05)	0.8489	0.07	16
Lab 1 (Y3)	2.00 (1.28)	2.11 (0.96)	0.7492	0.10	18
Lab 2 (Y1)	2.53 (0.74)	4.33 (1.29)	1.688e-4**	1.71	15
Lab 2 (Y2)	2.79 (1.19)	3.43 (1.16)	0.0445**	0.55	14
Lab 2 (Y3)	2.86 (0.86)	3.29 (1.27)	0.1386	0.40	14
Lab 3 (Y1)	2.07 (1.00)	3.71 (1.20)	3.395e-4**	1.49	14
Lab 3 (Y2)	2.00 (1.18)	3.07 (1.39)	7.552e-4**	0.83	14
Lab 3 (Y3)	2.11 (1.18)	2.72 (1.23)	0.0855*	0.51	18
Lab 4 (Y1)	2.50 (1.62)	4.11 (0.90)	0.0024**	1.23	18
Lab 4 (Y2)	2.31 (1.35)	3.13 (1.31)	0.0431**	0.61	16
Lab 4 (Y3)	1.75 (1.18)	3.88 (1.26)	0.0001**	1.74	16
Lab 5 (Y1)	2.5 (1.03)	4.63 (0.62)	1.149e-6**	2.50	16
Lab 5 (Y2)	2.64 (1.34)	3.79 (0.70)	0.0041**	1.07	14
Lab 5 (Y3)	3.22 (1.40)	3.72 (0.75)	0.2168	0.45	18

Table A.5: The means (standard deviations) of the appropriate student section's quiz score on the pre-test compared with the quiz score taken after completing the lab report for year 1 (Y1), year 2 (Y2), and year 3 (Y3). The corresponding p-value from the paired t-test is shown, denoting significance at $\alpha = 0.05$ with a ** and at $\alpha = 0.1$ with a *. The effect size, d, is also presented, and the sample size for each test, N, is shown in the last column. This table corresponds to Figure 2.12.

	Pre-Test	**After Lab Report**	**p-value**	**Cohen's d**	**N**
Lab 1 (Y1)	2.36 (1.28)	2.07 (0.92)	0.4533	-0.26	14
Lab 1 (Y2)	2.14 (1.03)	2.57 (0.94)	0.2896	0.44	14
Lab 1 (Y3)	2.56 (1.42)	2.22 (1.11)	0.2687	-0.26	18
Lab 2 (Y1)	2.61 (0.92)	3.94 (0.87)	1.812e-4**	1.49	18
Lab 2 (Y2)	2.56 (1.25)	3.44 (0.92)	0.0311**	0.81	18
Lab 2 (Y3)	2.25 (1.06)	3.17 (0.83)	0.0501*	0.96	12
Lab 3 (Y1)	2.25 (1.12)	3.81 (1.26)	1.754e-4**	1.30	16
Lab 3 (Y2)	1.93 (1.03)	3.60 (0.83)	2.443e-5**	1.78	15
Lab 3 (Y3)	2.00 (1.14)	3.56 (1.04)	1.384e-05**	1.43	18
Lab 4 (Y1)	3.00 (1.20)	3.73 (0.80)	0.0853*	0.72	15
Lab 4 (Y2)	2.54 (1.45)	3.62 (1.26)	7.230e-4**	0.79	13
Lab 4 (Y3)	2.14 (1.79)	3.5 (1.22)	0.0261**	0.88	14
Lab 5 (Y1)	2.71 (1.27)	4.07 (0.73)	0.0073**	1.31	14
Lab 5 (Y2)	2.33 (1.50)	3.00 (0.71)	0.1950	0.59	9
Lab 5 (Y3)	2.57 (0.94)	3.14 (1.17)	0.1352	0.54	14

Bibliography

[1] Surround Haptics. Disney Research. http://www.disneyresearch.com/research/projects/hci_surround_haptics_drp.htm. Accessed July 2012.

[2] T. Hodgson, Math Description Engine. http://prime.jsc.nasa.gov/mde/. Accessed June 2012.

[3] R. Shelton, MathTrax. http://prime.jsc.nasa.gov/mathtrax/. Accessed June 2012.

[4] The HyperBraille Project. http://www.hyperbraille.de/. Accessed July 2012.

[5] VT Player. VirTouch. http://vtplayer.sourceforge.net/. Accessed July 2012.

[6] Vanderbilt University Haptic Paddle Webpage. http://research.vuse.vanderbilt.edu/MEDLab/haptic _ paddle.html.

[7] EduHaptics. http://eduhaptics.org/index.php/HapticDevices/HapticPaddles.

[8] SensAble Technologies, Inc. http://www.sensable.com/documents/documents/STI_Jan2009_DesktopOmniComparison_print.pdf. Accessed February 2013.

[9] Arduino Development Environment. http://arduino.cc/en/Guide/Environment. Accessed May 2012.

[10] CI Hub. http://cihub.org/. Accessed June 2012.

[11] J. J. Abbott. Virtual fixtures for bilateral telemanipulation. *Ph.D. Dissertation submitted to The Johns Hopkins University*, pages 195–199, 2005.

[12] Mahmoud Abdulwahed and Z.K. Nagy. Applying Kolb's experiential learning cycle for laboratory education. *Journal of Engineering Education*, 98:283–294, 2009.

[13] M. Akamatsu and I. S. MacKenzie. Movement characteristics using a mouse with tactile and force feedback. *International Journal of Human-Computer Studies*, 45:483–493, 1996.

[14] M. E. Altinsoy and S. Merchel. Audiotactile feedback design for touch screens. *HAID Lecture notes in Computer Science*, 5763:136–144, 2009.

[15] Artificial Muscle Inc. Artificial Muscle Inc. ViviTouch Technology. *http://www.artificialmuscle.com.*, 2012. Accessed March 2012.

[16] B. Banter. Touch screens and touch surfaces are enriched by haptic force-feedback. *Information Display*, 26:26–30, 2010.

[17] O. Bau, I. Poupyrev, A. Israr, and C. Harrison. Teslatouch: Electrovibration for touch surfaces. *In Proc. of User Interface Software and Technology (UIST)*, pages 283–292, 2010.

[18] J. C. Bean. *Engaging Ideas: The Professor's Guide to Integrating Writing, Critical Thinking, and Active Learning in the Classroom*. John Wiley & Sons, Inc., 2011.

[19] M. Benali-Khoudja, M. Hafez, J.-M. Alexandre, and A. Kheddar. Tactile interfaces: a state-of-the-art survey. *International Symposium on Robotics*, 2004.

[20] C. Bernareggi, P. Mussio, and L. P. Provenza. Toward multimodal notation for math-

ematics: Why and how. *Journal of Visual Languages and Computing*, pages 326–340, 2009.

[21] M. Bialeschki. The three rs for experiental education researchers. *Journal of Experiential Education*, 29:366–368, 2007.

[22] S. J. Biggs and M. A. Srinivasan. *Haptic Interfaces in Handbook of Virtual Environments*. Lawrence Erlbaum, Inc., 2002.

[23] K. Bowen and M. K. O'Malley. Adaptation of haptic interfaces for a labview-based system dynamics course. *Proceedings of the 14th Symposium on Haptic Interfaces for Virtual Environment and Teleoperator Systems (HAPTICS 06)*, pages 147–152, 2006.

[24] L. Bussel. Touch tiles: Elementary geometry software with a haptic and auditory interface for visually impaired children. *EuroHaptics*, pages 512–515, 2003.

[25] X.Q. Chen, J. G. Chase, W. Wang, P. Gaynor, and A. McInnes. Embedding design projects into multidisplinary engineering education. *International Conference on Educational and Information Technology*, 3:398–402, 2010.

[26] E. C. Chubb, J. E. Colgate, and M. A. Peshkin. Shiverpad: A glass haptic surface that produces shear force on a bare finger. *IEEE Transactions on Haptics*, 3:189–198, 2010.

[27] A. Cockburn and S. Brewster. Multimodal feedback for acquisition of small targets. *Ergonomics*, 48(9):1129–1150, 2005.

[28] R. D. Cook. *Concepts and Applications of Finite Element Analysis, 2nd Edition*. John Wiley & Sons, 1981.

[29] D.J. Cox. Hands-on experiments in dynamic systems and control for applied education in robotics and automation. *World Automation Congress*, pages 1–6, 2008.

[30] A. Crossan and S. Brewster. Multimodal trajectory playback for teaching shape information and trajectories to visually impaired computer users. *ACM Transactions on Accessible Computing (TACCESS)*, 1(2):Article 12 (34 pages)., 2008.

[31] M. M. Dewoolkar, L. George, N. J. Hayden, and M. Neumann. Hands-on undergraduate geotechnical engineering modules in the context of effective learning pedagogies, ABET outcomes, and our curricular reform. *Journal of Professional Issues in Engineering Education and Practice*, 135:161–175, 2009.

[32] P. K. Edman. *Tactile graphics*. American Foundation for the Blind, 1992.

[33] L.D. Feisel and A.J. Rosa. The role of the laboratory in undergraduate engineering education. *Journal of Engineering Education*, 94 (1):121–130, 2005.

[34] R. M. Felder and L. K. Silverman. Learning and teaching styles in engineering education. *Engineering Education*, 78(7):674–681, 1988.

[35] D.M. Fraser, R. Pillay, L. Tjatindi, and J.M. Case. Enhancing the learning of fluid mechanics using computer simulations. *Journal of Engineering Education*, No.4:381–388, 2007.

[36] B. Frey, C. Southern, and M. Romero. Brailletouch: Mobile texting for the visually

impaired. *Proceedings of Human-Computer Interaction International*, pages 19–25, July 2011.

[37] R. Gassert, J.-C. Megzger, K. Leuenberger, Popp. W. L., M. R. Tucker, B. Vigaru, R. Zimmermann, and O. Lambercy. Physical student-robot interaction with the ethz haptic paddle. *IEEE Transactions on Education*, 56:9–17, 2013.

[38] R. B. Gillespie, M. B. Hoffman, and J. Freudenberg. Haptic interface for hands-on instruction in system dynamics and embedded control. *Proceedings of the 11th Symposium on Haptic Interfaces for Virtual Environment and Teleoperator Systems (HAPTICS 03)*, pages 410–415, 2003.

[39] P.T. Goeser, W. M. Johnson, F. G. Hamza-Lup, and D. Schaefer. VIEW - a virtual interactive web-based learning environment for engineers. *Advances in Engineering Education*, 2011.

[40] J. L. Gorlewicz, J. Burgner, T. J. Withrow, and R. J. Webster III. Initial experiences using vibratory touchscreens to display graphical math concepts to students with visual impairments. *Journal of Special Education and Technology*, 2013. [Submitted].

[41] J. L. Gorlewicz, L. B. Kratchman, and R. J. Webster III. The vanderbilt haptic paddle: Educational haptics using simulink. *The MathWorks, Inc. Virtual Conference*, March, 2012. (Webinar available online at The MathWorks, Inc.).

[42] J. L. Gorlewicz, L. B. Kratchman, and R. J. Webster III. Haptic paddle enhancements and a formal assessment of student learning in system dynamics. *Journal of Science Education and Technology*, 2013. [Submitted].

[43] J. L. Gorlewicz and R. J. Webster III. A formal assessment of the haptic paddle laboratories in teaching system dynamics. *American Society of Engineering Education Conference*, 2012. **Best Paper Award**.

[44] D. Grow, L. N. Verner, and A. M. Okamura. Educational haptics. *AAAI Spring Symposia - Robots and Robot Venues: Resources for AI Education*, 2007.

[45] N. W. Hagwood, W. H. Chung, and A. von Flotow. Modelling of piezoelectric actuator dynamics for active structural control. *Journal of Intelligent Material Systems and Structures*, 1:327–354, 1990.

[46] M. Hamblin. Taking touch to new frontiers: Why it makes sense and how to make it happen. *Information Display*, 26:36–39, 2010.

[47] F. G. Hamza-Lup and I. A. Stanescu. The haptic paradigm in education: Challenges and case studies. *Internet and Higher Education*, 13:78–81, 2010.

[48] I. Han and J. B. Black. Incorporating haptic feedback in simulation for learning physics. *Computers and Education*, 57:2281–2290, 2011.

[49] V. Hayward, O. R. Astley, M. Cruz-Hernandez, D. Grant, and G. Robles-De-La-Torre. Haptic interfaces and devices. *Sensor Review*, 24:16–29, 2004.

[50] E. Hoggan, S. A. Brewster, and J. Johnston. Investigating the effectiveness of tactile feedback for mobile touchscreens. *Proc. of the 26th annual SIGCHI conference on Human factors in computing systems*, pages 1573–1582, 2008.

[51] Winnie Hu. Math that moves: Schools embrace the ipad. The New York Times, January 4 2011. January 4, 2011.

[52] M. G. Jones, J. Minogue, T. R. Tretter, A. Negishi, and R. Taylor. Haptic augmentation of science instruction: Does touch matter? *Science Education*, 90:111–123, 2006.

[53] S. K. Kane, J. P Bigham, and J. O. Wobbrock. Slide rule: making mobile touch screens accessible to blind people using multi-touch interaction techniques. *ASSETS ACM SIGACCESS Conference on Computers and Accessibility*, pages 73–80, 2008.

[54] S. K. Kane, M. R. Morris, A. Z. Perkin, D. Wigdor, R. E. Ladner, and J. O. Wobbrock. Access overlays: Improving non-visual access to large touch screens for blind users. *UIST*, pages 273–282, 2011.

[55] J. Kang, J. Lee, H. Kim, K. Cho, S. Wang, and J. Ryu. Smooth vibrotactile flow generation using two piezoelectric actuators. *IEEE Transactions on Haptics*, 5(1):21–32, 2012.

[56] A. I. Karshmer and C. Bledsoe. Access to mathematics by blind students. *International Conference on Computers Helping People With Special Needs, Lecture Notes in Computer Science*, 2398:620–627, 2002.

[57] R. Leung, K. MacLean, M. B. Bertelsen, and M. Saubhasik. Evaluation of a haptically augmented touchscreen gui elements under congitive load. *International Conference on Multimodal Interfaces*, pages 374–381, 2007.

[58] V. Levesque, L. Oram, K. MacLean, A. Cockburn, N. D. Marchuk, D. Johnson, J. E. Colgate, and M. A. Peshkin. Enhancing physicality in touch interaction with programmable friction. *Computer and Human Interaction*, pages 2481–2490, 2011.

[59] J. G. Linvill and J. C. Bliss. A direct translation reading aid for the blind. *Proceedings of the IEEE*, 54:40–50, 1966.

[60] N. D. Marchuk, J. E. Colgate, and M. A. Peshkin. Friction measurements on a large area tpad. *IEEE Haptics Symposium*, pages 317–320, 2010.

[61] J. Minogue and M. G. Jones. Haptics in education: Exploring an untapped sensory modality. *Review of Educational Research*, 76:317–348, 2006.

[62] J. Minogue, M. G. Jones, B. Broadwell, and T. Oppewall. The impact of haptic augmentation on middle school students' conceptions of the animal cell. *Virtual Reality*, 10:293–305, 2006.

[63] S. Mitic. Development of a graphical tactile display based on electromagnetic actuators. *International Conference on Microelectronics*, 2004.

[64] G. R. Morrison, S. M. Ross, and D. L. Lowther. *"Technology as a Change Agent in the Classroom" in Learning and Instructional Technologies For the 21st Century*. Springer Science+Business Media, LLC, 2009.

[65] A.M. Okamura, C. Richard, and M.R. Cutkosky. Feeling is believing: Using a force-feedback joystick to teach dynamic systems. *Journal of Engineering Education*, pages 345–349, 2002.

[66] M. K. O'Malley and A. Gupta. *HCI: Beyond the GUI. Haptic Interfaces*. Morgan-Kaufman Publisher, 2008.

[67] M. J. Pitts, G. E. Burnett, L. Skrypchuk, T. Wellings, and M. A. Attridge, A. Williams. Visual-haptic feedback interaction in automotive touchscreens. *Displays*, 33:7–16, 2012.

[68] I. Poupyrev and S. Maruyama. Tactile interfaces for small touch screens. *Proceedings of the 16th Annual ACM Symposium on User Interface Software and Technology*, pages 217–220, 2003.

[69] M. Prince. Does active learning work? a review of the research. *Journal of Engineering Education*, 93:223–231, 2004.

[70] K. Rassmus-Grohn, C. Magnusson, and H. Eftring. User evaluations of a virtual haptic-audio line drawing prototype. *Haptics and Audio Interaction Design*, 4129:81–91, 2006.

[71] R. Rastogi, D. T. Pawluk, and J. M. Ketchum. Issues of using tactile mice by individuals who are blind and visually impaired. *IEEE Transactions on Neural Systems and Rehabilitation Engineering*, 18:311–318, 2010.

[72] M. Reiner. Conceptual construction of fields through tactile interface. *Interactive Learning Environments*, 7:31–55, 1999.

[73] J. Rosen and B. Hannaford. Doc at a distance. *IEEE Spectrum*, pages 34–39, 2006.

[74] P. Roth, H. Kamel, L. Petrucci, and T. Pun. A comparison of three nonvisual methods for presenting scientific graphs. *Journal of Visual Impairment and Blindness*, 96:420–428, 2002.

[75] A. E. Saddik. The potential of haptic technologies. *IEEE Instrumentation and Measurement Magazine*, pages 10–17, 2007.

[76] A. E. Saddik, M. Orozco, M. Eid, and J. Cha. *Haptics Technologies*. Springer-Verlag Berlin Heidelberg, 2011.

[77] J. P. San Diego, M. J. Cox, B. F. A. Quinn, J. T. Newton, A. Banerjee, and M. Woolford. Researching haptics in higher education: The complexity of developing haptics virtual learning systems and evaluating its impact on students' learning. *Computers and Education*, 59:156–166, 2012.

[78] K. Sathian. Perceptual learning. *Current Science*, 75:451–456, 1998.

[79] K. J. Schnborn, P. Bivall, and L. A. E. Tibell. Exploring relationships between students' interacting and learning with a haptic virtual biomolecular model. *Computers and Education*, 57:2095–2105, 2011.

[80] S. Sharmin, G. Evreinov, and R. Raisamo. Non-visual feedback cues for pen computing. *IEEE World Haptics Conference*, pages 625 – 628, 2005.

[81] M. Takasaki, H. Kotani, T. Mizuno, and T. Nara. Transparent surface acoustic wave tactile display. *International Conf. on Intelligent Robots and Systems*, pages 3354–3359, 2005.

[82] J.P. Terpenny and R.M. Goff. Utilizing assistive technology design projects and interdisplinary teams to foster inquiry and learning in engineering design. *International Journal of Engineering Education*, 22:609–616, 2006.

[83] TN Standards. Tennessee Department of Education Curriculum Standards. *http://www.tennessee.gov/education/ci/math/index.shtml*, 2012. Accessed March 2012.

[84] J. L. Toennies, J. Burgner, T. J. Withrow, and R. J. Webster III. Toward haptic/aural touchscreen display of graphical mathematics for the education of blind students. *IEEE World Haptics Conference*, pages 373–378, 2011.

[85] O. A. J. van der Meijden and M. P. Schiven. The value of haptic feedback in convential and robot-assisted minimal invasive surgery and virtual reality training: a current review. *Surgical Endoscopy*, 23:1180–1190, 2009.

[86] A. F. Van Scoy, D. McLaughlin, J. V. Odom, R. T. Walls, and M. E. Zuppuhaur. Touching mathematics: a prototype tool for teaching pre-calculus to visually impaired students. *Journal of Modern Optics*, 53:1287–1294, 2006.

[87] R. Velazquez, E. E. Pissaloux, M. Hafez, and J. Szewczyk. A low-cost highly-portable tactile display based on shape memory alloy micro-actuators. *IEEE International Conference on Virtual Environments, Human-Computer Interfaces and Measurement Systems*, 2005.

[88] E. Ventsel and T. Krauthammer. *Thin Plates and Shells*. Marcel Dekker, Inc., 2001.

[89] F. Vidal-Verdu and M. Hafez. Graphical tactile displays for visually-impaired people. *IEEE Transactions on Neural Systems and Rehabilitation Engineering*, 15:119–130, 2007.

[90] T. Watanabe and S. Fukui. A method for controlling tactile sensation of suface roughness using ultrasonic vibration. *IEEE International Conference on Robotics and Automation*, 1:1134–1139, 1995.

[91] T. Watanabe, M. Kobayashi, S. Ono, and K. Yokoyama. Practical use of interactive tactile graphic display system at a school for the blind. *Current Developments in Technology-Assisted Education*, pages 1111–1115, 2006.

[92] WHO. World Health Organization. *http://www.who.int/mediacentre/factsheets/fs282/en/*, 2012. Accessed March 2012.

[93] C. Wieman and K. Perkins. Transforming physics education. *Physics Today*, pages 36–41, November 2005.

[94] R. L. Williams II, M. Y. Chen, and J. M. Seaton. Haptics-augmented simple-machine educational tools. *Journal of Science Education and Technology*, 12:1–12, 2003.

[95] R. L. Williams II, X. He, T. Franklin, and S. Wang. Haptics-augmented undergraduate engineering education. *International Conference on Engineering Education*, 2004.

[96] L. Winfield, J. Glassmire, J. E. Colgate, and M. A. Peshkin. T-pad: Tactile pattern display through variable friction reduction. *World Haptics*, pages 421–426, 2007.

[97] J. Wood, M. Magennis, E. F. C. Arias, T. Gutierrez, H. Graupp, and M. Bergamasco. The design and evaluation of a computer game for the blind in the GRAB haptic audio virtual environment. *Proceedings of Eurohaptics Conference*, 2003.

[98] A. Yamamoto, T. Ishii, and T. Higuchi. Electrostatic tactile display for presenting surface roughness sensation. *IEEE Conf. on Industrial Technology*, pages 680–684, 2003.

[99] F. Yan, Z. Hou, D. Zhang, W. Kang, and J. Zheng. Research of haptic technologies for computer-based education. *International Conference on Computer Science and Education*, pages 1636–1640, 2009.

[100] W. Yu and S. A. Brewster. Evaluation of multimodal graphs for blind people. *Universal Access in the Information Society*, 2:105–124, 2003.

[101] W. Yu and K. Kangas. Web-based haptic applications for blind people to create virtual graphs. *11th Symposium on Haptic Interfaces for Virtual Environment and Teleoperator Systems*, pages 318–325, 2003.